uOttawa

L'Université canadienne
Canada's university

FACULTÉ DES ÉTUDES SUPÉRIEURES ET POSTOCTORALES

uOttawa

L'Université canadienne
Canada's university

FACULTY OF GRADUATE AND POSDOCTORAL STUDIES

Matthew Yorke
AUTEUR DE LA THÈSE / AUTHOR OF THESIS

M.Sc. (Chemistry)
GRADE / DEGREE

Department of Chemistry
FACULTÉ, ÉCOLE, DÉPARTEMENT / FACULTY, SCHOOL, DEPARTMENT

Photochemistry of Amido Xanthonate Photocages:
Potential Candidates for Polymer-Tethered Photorelease of Drugs

TITRE DE LA THÈSE / TITLE OF THESIS

J.C. Scaiano
DIRECTEUR (DIRECTRICE) DE LA THÈSE / THESIS SUPERVISOR

CO-DIRECTEUR (CO-DIRECTRICE) DE LA THÈSE / THESIS CO-SUPERVISOR

A. Beauchemin

M. Berezovski

Gary W. Slater
Le Doyen de la Faculté des études supérieures et postdoctorales / Dean of the Faculty of Graduate and Postdoctoral Studies

PHOTOCHEMISTRY OF AMIDO XANTHONATE PHOTOCAGES: POTENTIAL CANDIDATES FOR POLYMER-TETHERED PHOTORELEASE OF DRUGS

Matthew Yorke

Thesis submitted to the
Faculty of Graduate and Postdoctoral Studies
In partial fulfillment of the requirements of
Master of Science
Specialization in Chemistry

uOttawa

In the Ottawa-Carleton Chemistry Institute
Department of Chemistry, University of Ottawa

Your file Votre référence
ISBN: 978-0-494-73843-6
Our file Notre référence
ISBN: 978-0-494-73843-6

"I like the tone of your trumpet

Come on let's spill some paint

Let's raise a glass of milk

To the end of another day"

- Gordon Downie

Abstract

Recently, photocages capable of releasing biologically relevant molecules have been reported, which utilize the rapid and efficient photodecarboxylation of 2-xanthone acetic acid (XAA) with UVA irradiation. This thesis focuses on the development of functionalized xanthonate photocages to be used for surface-tethering applications.

Firstly, the preparation of amine and acetamide functionalized xanthonate (and thioxanthonate) photocage precursors will be described. Investigation into the photochemistry of the prepared derivatives led to the discovery of a solvent composition dependence on the photodecarboxylation quantum yield of acetamide derivatives. The photodecarboxylation of these derivatives occurs cleanly in the same way as XAA, but with lower efficiency.

The preparation and photochemical study of acetamide functionalized photocages will then be described. Photorelease of acetate and phenylalanine demonstrated the capability of amide functionalized photocages to release biologically relevant molecules.

Lastly, initial investigations into polymer tethering will be described. Attempted amide coupling through the aromatic amine led to the attachment of a short chain carboxylic acid terminated linker to modify the linking site.

Table of Contents

List of Figures.....v

List of Schemes.....vii

List of Tables and Charts.....x

List of Abbreviations.....xi

Acknowledgements.....xiv

Chapter 1
Introduction.....1

Chapter 2
Photochemistry of Nitro, Amine and Amide Functionalized Xanthone Acetic Acids.....21

Chapter 3
Toward Photorelease from Surface Tethered Xanthonate Photocages.....80

Chapter 4
Conclusions and Future Directions.....115

APPENDIX 1 - ^{1}H and ^{13}C NMR Spectra.....121

List of Figures

Figure 1 - 1: Cartoon representation of a general photocage. Following electronic excitation *via* absorption of a photon (h*v*) by the chromophore, the caged leaving group is released..... 2

Figure 1 - 2: Jablonski diagram summarizing excited state process. Solid lines indicate radiative processes, and dashed lines indicate non-radiative processes..... 4

Figure 1 - 3: UV/Vis Absorptivity spectra for ketoprofen (Kp, ■) and 2-xanthone acetic acid (XAA, ●) in PBS..... 9

Figure 1 - 4: Absorption spectrum before (thick) and after (thin) solar exposure for 20 hours. a) human cornea, b) collagen-MPC hydrogel.....15

Figure 2 - 1: Molar absorptivity of **6** (solid blue), **7** (solid red) and **XAA** (dashed black) in PBS. Spectra were measured by J.A. Blake..... 31

Figure 2 - 2: Molar absorptivity of **8** (solid blue), **9** (solid red) and XAA (dashed black) in 80:20 v/v PBS:ACN.....36

Figure 2 - 3: Fluorescence spectrum of **8** in PBS. Absorbance of 0.1 at the excitation wavelength (350 nm).....38

Figure 2 - 4: Molar absorptivity of **10** (solid blue) and **XAA** (dashed black) in 80:20 v/v PBS:ACN..... 40

Figure 2 - 5: UV/Vis Absorbance of **10** with UVB Irradiation (in 80:20 v/v PBS:ACN)..... 42

Figure 2 - 6: **10** Photodecarboxylation quantum yield dependence on acetonitrile concentration, using the decarboxylation of **Kp** as an actinometer..... 44

Figure 2 - 7: Cartoon representation of the energy barrier dependence on water concentration. This dependence can be used to explain the trend in which the photodecarboxylation quantum yield of 10 increases with acetonitrile concentration. The energy levels for reactant and product may also be subject to such solvent effects, this has been omitted for clarity..... 45

Figure 2 - 8: Fluorescence excitation (dashed) and emission (solid) spectra of 10 (0.01 mM in 80:20 v/v PBS:ACN). Spectra are shown non-normalized. Excitation spectrum was recorded by monitoring emission at 450 nm. Emission spectrum was recorded by exciting at 358 nm..... 46

Figure 2 - 9: Absorbance matched fluorescence spectra of **10**, varying solvent composition from 100:0 (black trace) to 40:60 (purple trace) v/v PBS:ACN.....47

Figure 2 - 10: Representative fluorescence decay trace of **10** (20 μM in PBS:ACN mixtures)..... 49

Figure 2 - 11: Representative laser flash photolysis spectrum for 10 in PBS under nitrogen. Spectra were recorded at 5.2 μs (●), 9.2 μs (■), 26.8 μs (◆), and 93.6 μs (▲) (A_{355} = 0.3).....51

Figure 2 - 12: Laser flash photolysis spectrum of 2-methylxanthone in 80:20 PBS:ACN under nitrogen. Spectra were recorded at 2.4 us (●), 8.0 us (■), 16.8 us (◆), and 40.8 μs (▲) (A_{355} = 0.3).....52

Figure 2 - 13: Molar absorptivity of **11** (blue solid) and **XAA** (black dashed) in 80:20 v/v PBS:ACN.....55

Figure 2 - 14: UV/Vis Absorbance spectra of **11** with UVB Irradiation (in 80:20 v/v PBS:ACN).....57

Figure 2 - 15: Photodecarboxylation quantum yield dependence of **11** on acetonitrile concentration..... 59

Figure 2 - 16: Fluorescence excitation (dashed) and emission (solid) spectra of **11** in 80:20 v/v PBS:ACN. Spectra are shown non-normalized.....60

Figure 3 - 1: ^{1}H NMR splitting pattern of diastereotopic protons (indicated in red) for **23**. The signal for each proton is observed as a doublet of doublets split first by the vicinal proton (J_2 = 10.6 Hz) and again by the geminal alcohol (J_1 = 5.2 Hz)..... 85

List of Schemes

Scheme 1 - 1: Photorelease mechanism from *o*-nitrobenzyl alcohol derivatives (oNB) based on the photochemical isomerization into *o*-nitrosobenzaldehyde. 5

Scheme 1 - 2: Photorelease of 'caged ATP' from *ortho*-nitrobenzyl (oNB) based photocage..... 6

Scheme 1 - 3: Photodegradation of ketoprofen (**Kp**) in basic aqueous solution *via* protonation of the carbanion intermediate to form 3-ethylbenzophenone..... 7

Scheme 1 - 4: Photorelease of anionic leaving groups from ketoprofenate photocages (**1**) by elimination *via* benzyl carbanion following photodecarboxylation..... 8

Scheme 1 - 5: Photodecarboxylation of 2-xanthone acetic acid (**XAA**) in basic aqueous media from the singlet excited state..... 10

Scheme 1 - 6: Photorelease of acetate leaving group from xanthonate photocage (**2**) in basic aqueous media..... 11

Scheme 1 - 7: Photorelease of aniline leaving group *via* its carbamate from xanthonate photocage in basic aqueous media.....11

Scheme 1 - 8: Photorelease of dithiane leaving group from **5** *via* homolytic bond cleavage and subsequent disproportionation of the generated radicals..... 12

Scheme 1 - 9: A potential way to attach xanthonate photocages to surfaces, such as collagen-MPC hydrogel (X = leaving group). Coupling of the aromatic amine to carboxylic acid terminated surfaces could ideally be achieved through the use of standard amide coupling chemistry.....16

Scheme 2 - 1: Conversion of primary amines to thiol and carboxylic acid linkers *via* amide coupling chemistry..... 23

Scheme 2 - 2: Original synthesis of 6. i) CuCl, dioxane, tris(2-(2-methoxyethoxy)ethyl)amine (TDA-1), Cs_2CO_3; ii) H_2SO_4, Δ; iii) KNO_3, H_2SO_4.....26

Scheme 2 - 3: New synthetic route for **6** (X = O) and 7 (X = S). i) KOH, DMSO; ii) H_2SO_4, Δ.....27

Scheme 2 - 4: Synthesis of **8** (X = O) and **9** (X = S). i) Pd/C, H_2, EtOAc.....29

Scheme 2 - 5: Synthetic Route for **10** (X = O) and **11** (X = S): i) EtOH, H_2SO_4, Δ; ii) H_2, Pd/C, EtOAc; iii) Ac_2O, pyridine, DCM; iv) NaOH, CH_3CN.....31

Scheme 2 - 6: Photoreaction of **6** and **7** in basic aqueous media (pH 7.4).....34

Scheme 2 - 7: Clean photodecarboxylation of **10** in basic aqueous media (pH 7.4) to afford **18**.....41

Scheme 2 - 8: Photodecarboxylation of **11** in basic aqueous media.....56

Scheme 3 - 1: Synthetic route for **20**: i) LDA, CH_3I, THF, -78°C; ii) K_2CO_3, $(CH_2O)_n$, DMSO; iii) Pd/C, H_2, EtOAc; iv) Ac_2O, pyridine, DCM, v) 0.1 M NaOH, ACN; vi) Ac_2O, pyridine, DCM.....84

Scheme 3 - 2: Photorelease of acetate leaving group from **20** in basic aqueous media *via* photodecarboxylation followed by elimination of the generated carbanion.....87

Scheme 3 - 3: Synthetic route for **21**: i) triphosgene, pyridine, DCM; ii) Phe-Me, pyridine, iii) Pd/C, H_2, EtOAc, iv) Ac_2O, pyridine, DCM; v) 0.1 M NaOH, ACN.....89

Scheme 3 - 4: Photorelease of phenylalanine leaving group from **21** in basic aqueous media *via* photodecarboxylation followed by elimination of the generated carbanion to produce the photoproduct **27**. Thermal decarboxylation from the released carbamate then affords phenylalanine.....91

Scheme 3 - 5: Proposed alternative coupling strategy through a short chain alkyl linker (Phe = phenylalanine).....94

Scheme 3 - 6: Synthetic route for the preparation of **33**. i) glutaric anhydride, DMF, Δ; ii) NaOH, ACN.....95

Scheme 3 - 7: Photorelease of phenylalanine leaving group from **33** in basic aqueous media to form the photoproduct **34**. The reaction proceeds by a mechanism analogous to that shown in Scheme 3 - 4.....95

List of Tables and Charts

Table 2 - 1: **10** photodecarboxylation dependence on solvent composition. a) estimated quantum yields based on that measured in 80:20 v/v acetonitrile:PBS.....43

Table 2 - 2: Fluorescence data of **10** with varying solvent composition.....48

Table 2 - 3: Summary of fluorescence lifetimes of **10** in varying solvent compositions. All lifetimes were recorded using a PTI Easylife with 350 nm diode excitation. The data was fit to first order kinetics using the PTI software.....49

Table 2 - 4: **11** decarboxylation dependence on solvent composition. a) estimated quantum yields based on that measured in 50:50 v/v PBS:ACN.....58

Table 2 - 5: Photochemical comparison of ketoprofen (**Kp**) in PBS, 2-xanthone acetic acid (**XAA**) in PBS, and new derivatives **8-11** in 80:20 v/v PBS:ACN.....61

Chart 2 - 1: Adopted nomenclature used for nitro, amine, and acetamide derivatives of xanthone acetic acid and thioxanthone acetic acid.....24

List of Abbreviations

Ac_2O	Acetic Anhydride
ACN	Acetonitrile
ATP	Adenosine Triphosphate
DCM	Dichloromethane
DCC	Dicyclohexylcarbodiimide
Δ	Delta, used to denote Heat
DMF	N,N-Dimethylformamide
DMSO	Dimethyl Sulfoxide
DMSO-d_6	Deuterated Dimethyl Sulfoxide
$CDCl_3$	Deuterated Chloroform
EEDQ	2-Ethoxy-1-ethoxycarbonyl-1,2-dihydroquinoline
EDC	1-Ethyl-3-(3-dimethylaminopropyl)carbodiimide
EI	Electron Impact Ionization
ESI	Electrospray Ionization
EtOAc	Ethyl Acetate
EtOH	Ethanol
HOMO	Highest Occupied Molecular Orbital
HPLC	High Performance Liquid Chromatography
HPLC-UV	High Performance Liquid Chromatography with UV Detection

HR-MS	High Resolution Mass Spectroscopy
HSV-1	Herpes Simplex Virus 1
Hz	Hertz (s^{-1}), Basic S.I. Unit for Frequency
IC	Internal Conversion
IPN	Interpenetrating Network
ISC	Intersystem Crossing
J	NMR Coupling Constant
Kp	Ketoprofen
LDA	Lithium Diisopropylamine
LFP	Laser Flash Photolysis
LUMO	Lowest Unoccupied Molecular Orbital
MS	Mass Spectroscopy
mg	Milligram (10^{-3} g)
mm	Millimeter (10^{-3} m)
M	Molar ($molL^{-1}$)
mM	Millimolar (10^{-3} M)
μM	Micromolar (10^{-6} M)
MPC	2-Methacryloyloxyethyl phosphorylcholine
Nd/YAG	Neodymium-Doped Yttrium Aluminium Garnet
nm	Nanometer (10^{-9} m)
ns	Nanosecond (10^{-9} s)
NMR	Nuclear Magnetic Resonance Spectroscopy
NpOH	1-Naphthalenemethanol
NSAID	Nonsteroidal Anti-inflammatory Drug

oNB	*ortho*-Nitrobenzyl Group
PBS	Phosphate Buffered Saline (pH 7.4)
Pd/C	Palladium on Activated Carbon (10% Loading)
Phe	Phenylalanine
PTI	Photon Technology International
R_f	Retention Factor
S_0	Ground State Singlet
S_1	First Singlet Excited State
TDA-1	Tris[2-(2-methoxyethoxy)-ethyl]amine
THF	Tetrahydrofuran
TLC	Thin Layer Chromatography
T_1	First Triplet Excited State
Φ_D	Quantum Yield of Photodecarboxylation
Φ_F	Quantum Yield of Fluorescence
UV	Ultraviolet Radiation
UVA	Ultraviolet radiation ranging from 315-400 nm
UVB	Ultraviolet radiation ranging from 280-315 nm
VR	Vibrational Relaxation
XAA	2-Xanthone Acetic Acid

Acknowledgements

My supervisor, Professor Tito Scaiano, has been an inspiration and great mentor throughout the past few years. You provide a truly unique and friendly research environment. Thank you so much for all of your patience, advice, guidance, entertaining stories and amazing BBQs.

I would like to express sincere thanks to the entire Scaiano research group, both past and present members, as they were my family away from home: Jessie Blake, Paul Billone, Kathy McGilvray, Matt Decan, Eve Heafey, Kevin Stamplecoskie, Andrea Pardoe, Laetitia René-Boisneuf, Mathieu Frenette, María González Béjar, Rob Godin, Mark Perry, Vasilisa Filipenko, Liliana Jimenez, Natalia Pacioni, Emilio Alarcon, Michel Grenier, José Carlos Ferreira, Carlos J Bueno Alejo, Chiara Fasciani, Marta Liras, Geniece Tapley, Alexis Apee, Kathy-Sarah Focsaneanu, Belinda Heyne, Luca Maretti, Carlos Gonzalez, and Erika Wee. Aside from being the helpful and dynamic unit that you are, you have made me feel so welcome and in place in a new city. Additional thanks to Betty Yakimenko for running a tight ship and keeping it all together for us. Thanks also to honorary group member Keith Ingold, for still caring about the "real chemistry" as well as the many fantastic times water-skiing.

I would like to specifically mention Jessie "J-Roc" Blake, my photocage teammate, for elbow high-fives and being a very cheerful and helpful source of advice through experimental trials since day 1.

Thanks to The Can (and his wife Nathalie) and Paully for many good times dans le Cuba, UFC watching (and demonstrating where necessary), video-gaming and general havoc raising.

Many thanks to my deskmates María González Béjar, Mathieu Frenette, José Carlos Ferreira, and Geniece Tapley for many helpful discussions and dealing with my inherent talkativeness and constant music listening habits (or propagating the habit, as was the case with José Carlos).

An additional thanks to the Scaiano group for introducing me to my "light at the end of the tunnel", Eve Heafey. You are a constant source of love and support. Many thanks for all of the encouragement, rationalization, and *meticulous spell chekking*.

The Accommodators were my source of musical output throughout my graduate school years. I would like to thank Joseph Moran, Mathieu Lemay, Roger Tam and Charles Russell for making some great memories jamming and playing shows. Apart from musical development, I would like to thank Joseph, Mathieu and Roger for being accommodating with several helpful discussions regarding organic synthesis.

Last but not least, my deepest thanks go out to my parents, Ethel and John, for remaining supportive and understanding through everything.

1. Introduction

1.1. Photocages 2
1.1.1. Excited State Processes 3
1.1.2. *ortho*-Nitrobenzyl Photocages 5
1.1.3. Ketoprofenate Photocages 7
1.1.4. Xanthonate Photocages 9
1.2. The Cornea Project 13
1.2.1. HSV-1 Problem 13
1.2.2. Replacement Corneas 13
1.3. Photocages for Antiviral Release 16
1.4. References 18

1.1. Photocages

Photocages, or photolabile protecting groups are, in the most general sense, molecules that are capable of releasing a desired activity following irradiation from a light source. Photocages are generally composed of two components, a chromophore and a leaving group. The chromophore is that part of the molecule that is capable of absorbing light and the leaving group is that which is released following absorption of a photon. The general concept of a photocage is depicted in Figure 1 - 1.

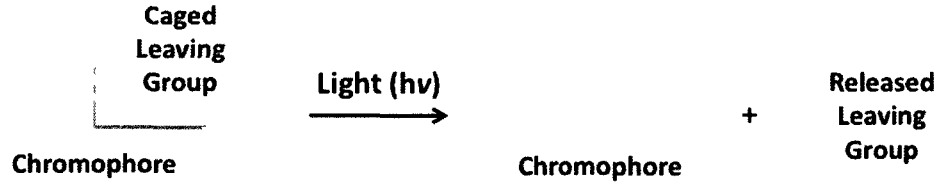

Figure 1 - 1: Cartoon representation of a general photocage. Following electronic excitation *via* absorption of a photon (h*v*) by the chromophore, the caged leaving group is released.

Photocages are commonly used for time-resolved studies of fast biological processes requiring rapid, clean and efficient release of signaling molecules. They have also been demonstrated useful for other applications such as photolithography and DNA synthesis.[1]

1.1.1. Excited State Processes

Before discussing the organic photochemistry of photocages it is first important to understand the principal pathways that are possible in a photochemical event. The excited state processes of an organic molecule are well summarized in the Jablonski diagram shown in Figure 1 - 2.[2, 3] In this diagram radiative transitions are represented as solid lines and non-radiative transitions are represented as dashed lines. After absorbing a photon the molecule is excited into the singlet manifold producing an electronic excited state (S_n). Through vibrational relaxation (VR) and internal conversion (IC), the lowest singlet excited state (S_1) is populated. From the singlet excited state, there are four main processes that can occur: 1) relaxation to the ground state (S_0) *via* the emission of a photon of lower energy, known as fluorescence, 2) non-radiative relaxation *via* vibrational relaxation, 3) intersystem crossing (ISC) to generate a triplet excited state (T_1) and 4) chemistry from the singlet excited state. Singlet excited states are generally very short lived (on the order of nanoseconds), thus any of the above processes must occur within that short time frame.

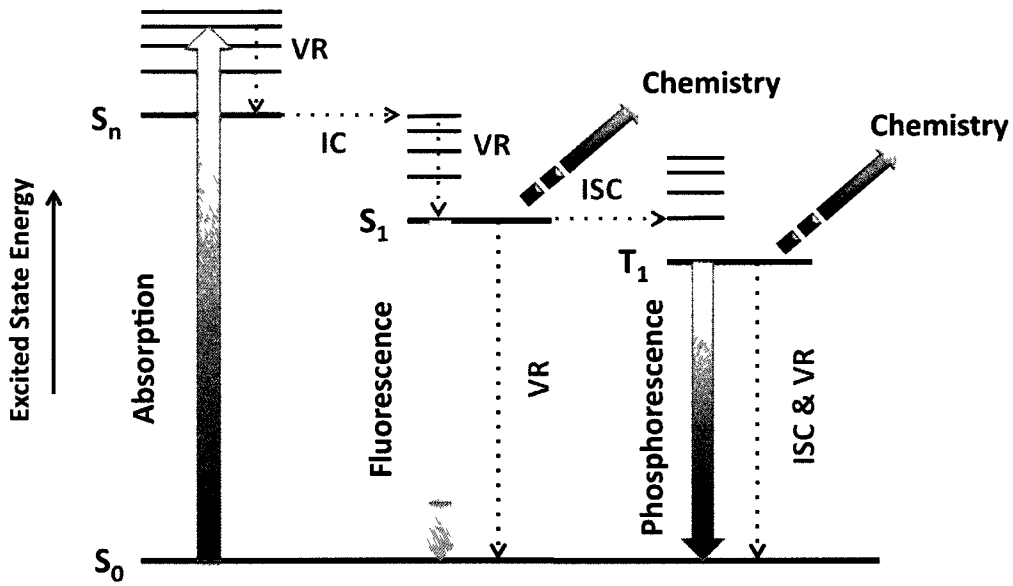

Figure 1 - 2: Jablonski diagram summarizing excited state process. Solid lines indicate radiative processes, and dashed lines indicate non-radiative processes.

It is important to note that in the context of photocages, the most desirable deactivation pathway is chemistry from the excited state (photochemistry). Radiative pathways, while they reduce the quantum efficiency of photorelease, are often very useful since they allow for spatial resolution *via* fluorescence imaging.

1.1.2. *ortho*-Nitrobenzyl Photocages

The most commonly used photocage is that based on *ortho*-nitrobenzyl (**oNB**) photochemistry. In 1970 Patchornik *et al.*[4] proposed the use of the **oNB** group as a photosensitive protecting group based on the photochemical isomerization of *ortho*-nitrobenzyl alcohol derivatives into *ortho*-nitrosobenzaldehyde, as shown in Scheme 1 - 1.

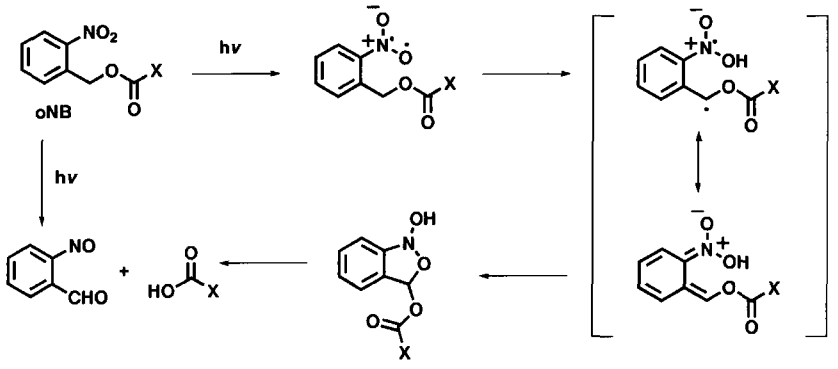

Scheme 1 - 1: Photorelease mechanism from *o*-nitrobenzyl alcohol derivatives (oNB) based on the photochemical isomerization into *o*-nitrosobenzaldehyde.[5]

This photochemistry was later harnessed to release several biologically relevant leaving groups, including the classic example of 'caged ATP'. The synthesis and release of adenosine triphosphate (ATP) from an oNB photocage was first reported in 1978 by Kaplan, as shown in Scheme 1 - 2.[6] This example clearly demonstrated the bioapplicability of photocages, as photoreleased ATP was able to reactivate the Na:K pump *in vitro*, while caged ATP was unable to do so.[6]

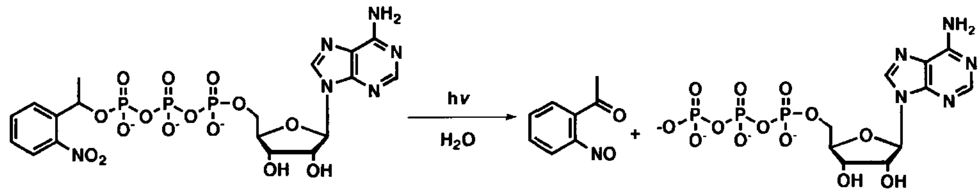

Scheme 1 - 2: Photorelease of 'caged ATP' from *ortho*-nitrobenzyl (oNB) based photocage.[6, 7]

A number of oNB caged derivatives are commercially available due to their ease of synthesis and their familiarity within biological researchers. Though these are commonly used for a variety of applications, they do have some disadvantages from a biological standpoint. In a 2002 review[8] Pellicciolli and Wirz outlined the six main criteria for the design of a good photolabile protecting group to be used for biological applications. The criteria listed included:

- 1) clean and efficient photochemistry,
- 2) high absorption coefficient (ε) above 300 nm,
- 3) production of inert and non-absorbing reaction byproducts,
- 4) high rate constant of photorelease,
- 5) good aqueous solubility and
- 6) absense of "dark" reactions such as release *via* thermal decomposition.

Photocages based on oNB chemistry fell short on a few of these criteria, namely the formation of reactive nitroso byproducts, slow release

following excitation (typically on the order of microseconds), and poor aqueous solubility.[9, 10] These shortcomings encouraged further development in the field of photocages better suited to biological applications requiring rapid release with spatial and temporal control.

1.1.3. Ketoprofenate Photocages

Ketoprofen (**Kp**), a potent nonsteroidal anti-inflammatory drug (NSAID), has received a lot of attention during the last two decades due to its reported phototoxicity. Following absorption of a photon *via* UV irradiation in basic aqueous solution, **Kp** undergoes decarboxylation from its singlet excited state, generating the corresponding benzyl carbanion, which is then protonated by the surrounding media to produce 3-ethylbenzophenone as shown in Scheme 1 - 3.[11-13]

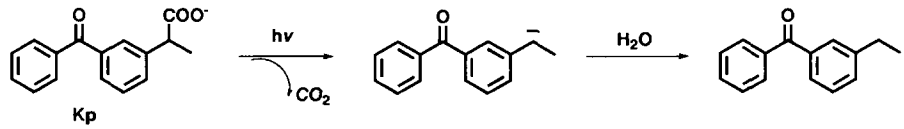

Scheme 1 - 3: Photodegradation of ketoprofen (Kp) in basic aqueous solution *via* protonation of the carbanion intermediate to form 3-ethylbenzophenone.

Shortly after the proposal of the singlet mechanism by Scaiano and coworkers, efforts were made toward harnessing the carbanion chemistry by substituting leaving groups on the β position relative to the generated

carbanion.[14] Following photodecarboxylation of the ketoprofenate photocage (**1**), the generated carbanion eliminates the anionic leaving group (X^-) as shown in Scheme 1 - 4. It should be noted that release proceeds by a mechanism most closely resembling E1cb rather than E2, as evidenced by the observation of the long-lived carbanion intermediate of **Kp** under extremely dry conditions.[15, 16]

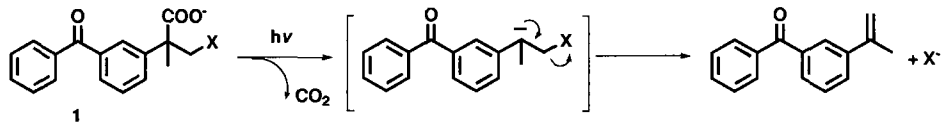

1

X = OAc, OCH_3, I, Br, Cl, Ibuprofen

Scheme 1 - 4: Photorelease of anionic leaving groups from ketoprofenate photocages (1) by elimination *via* benzyl carbanion following photodecarboxylation.[14]

The ketoprofenate photocages showed a marked improvement over the oNB predecessors in several respects including an increase of the release rate over 1000-fold, excellent aqueous solubility, the formation of stable and benign photoproducts, and a significant increase in the photorelease quantum yield.[14]

1.1.4. Xanthonate Photocages

Further insight into the photodecarboxylation mechanism was gained through the study of an analogous set of aryl acetic acids based on the xanthone chromophore which, as opposed to benzophenone, is fluorescent in aqueous solutions. This property makes detection possible in various environments *via* conventional fluorescence microscopy. An additional advantage of the xanthone chromophore, in terms of biological applicability, is the longer wavelength absorbance above 300 nm as shown in Figure 1 - 3.

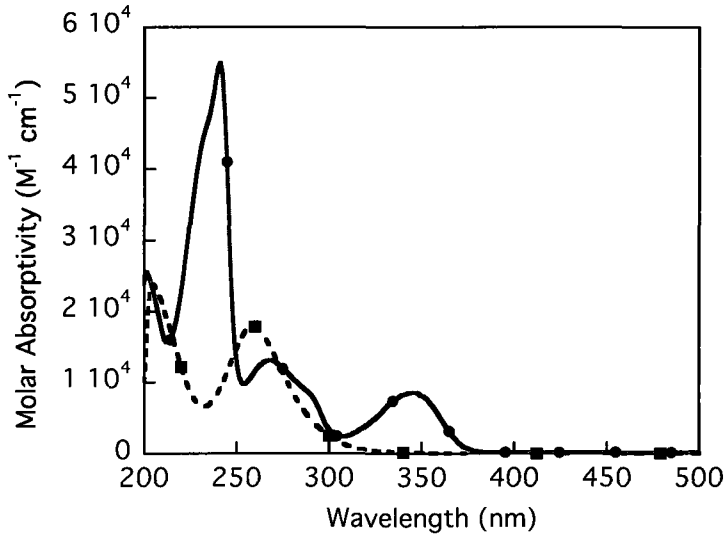

Figure 1 - 3: UV/Vis Absorptivity spectra for ketoprofen (Kp, ■) and 2-xanthone acetic acid (XAA, ●) in PBS.

In basic aqueous media 2-xanthone acetic acid (**XAA**) undergoes rapid and efficient photodecarboxylation upon irradiation (Φ_D = 0.67 in PBS)

generating a benzylic carbanion which is then protonated by the surrounding media to produce 2-methylxanthone as the sole photoproduct as shown in Scheme 1 - 5, consistent with the singlet mechanism proposed for ketoprofen.[17] Interestingly, unlike ketoprofen, which forms oxidation products following aerobic photolysis, **XAA** produced no photoproducts aside from 2-methylxanthone under the same conditions.

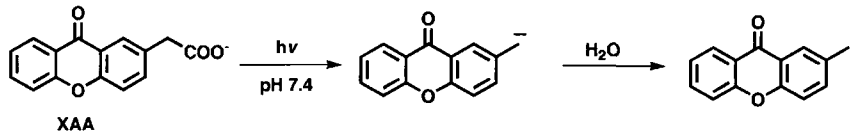

XAA

Scheme 1 - 5: Photodecarboxylation of 2-xanthone acetic acid (XAA) in basic aqueous media from the singlet excited state.[17]

Utilizing the clean and efficient photodecarboxylation chemistry of **XAA**, photolabile protecting groups were synthesized with anionic leaving groups β to the carbanion, as shown in Scheme 1 - 6 for acetate (**2**).[18] UV irradiation of **2** in PBS gave only acetate (observed as acetic acid following protonation) and 2-propenylxanthone (**3**), resulting from elimination of the benzyl carbanion.

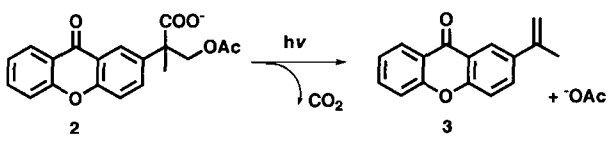

Scheme 1 - 6: Photorelease of acetate leaving group from xanthonate photocage (2) in basic aqueous media.[18]

The clean photorelease of acetate from **2** encouraged development of a wider range of leaving groups to improve biological applicability of the xanthonate photocage. By connecting through a carbamate linker, as shown for (**4**) in Scheme 1 - 7, the range was extended to aniline, a general model for primary amines. When releasing through a carbamate, photodecarboxylation generates the carbanion, which undergoes elimination to generate **3** and the aniline carbamate anion. Thermal elimination of a second molecule of carbon dioxide and subsequent protonation affords the aniline leaving group.[18]

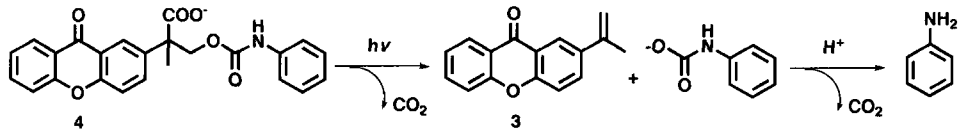

Scheme 1 - 7: Photorelease of aniline leaving group via its carbamate from xanthonate photocage in basic aqueous media.[18]

Aside from those based on **XAA**, the fluorescent nature of the xanthone (or thioxanthone) core has been taken advantage of by others, by

using the fluorescence as a reporting function to signal photorelease.[19] To do this, a dithiane leaving group is attached at the ketone position in such a way as to disrupt the conjugation of the thioxanthone chromophore. Electronic excitation of the resulting photocage, **5**, by absorption of a photon leads to homolytic cleavage, generating two radicals, which then undergo disproportionation to produce the dithiane leaving group and the substituted thioxanthone as shown in Scheme 1 - 8. The fluorescent thioxanthone is easily seen by conventional fluorescence microscopy, thus has potential to be used as a "release and report" photocage.[19]

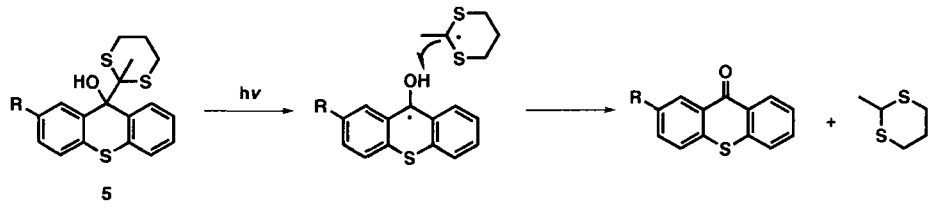

5

Scheme 1 - 8: Photorelease of dithiane leaving group from 5 *via* homolytic bond cleavage and subsequent disproportionation of the generated radicals.[19, 20]

While the reporting nature of photoreleasing thioxanthone from **5** is advantageous, some major drawbacks accompany this release strategy as compared to those based on **XAA**, namely the requirement of shorter wavelength excitation and the limited scope of leaving groups available. These points make photocages based on **XAA** much more appealing for biological applications.

1.2. The Cornea Project

1.2.1. HSV-1 Problem

The herpes simplex virus 1 (HSV-1) is the most common cause of corneal blindness in North America.[21] Primary infection by exposure generally leads to several damaging symptoms, which eventually leads to loss of corneal transparency and thus total loss of vision.[22]

An antiviral, acyclovir (ACV), is used to control symptoms of HSV-1, but the current drug delivery methods are quite inefficient. Oral dosage leads to only a small fraction of ACV reaching the infected area, and eye drops are washed away too rapidly for the antiviral to be absorbed into the cornea. The only widely accepted treatment to date is transplantation with human donors; however, in many countries the demand for donor corneas far outweighs the supply.[22]

1.2.2. Replacement Corneas

Recently, efforts have been made toward developing synthetic replacement corneas to aid the HSV-1 problem.[22-24] The material developed by the Griffith group is an interpenetrating network (IPN), combining recombinant human collagen and 2-methacryloyloxyethyl phosphorylcholine (MPC).[22] Collagen, the main component of the extracellular matrix of the

cornea, is incorporated into the synthetic material in order to promote corneal regeneration, which has been reported following transplantation in human subjects.[24] Polymeric MPC is used to mimic phospholipids found in cell plasma membranes, and has the added advantage of increasing the mechanical strength of the hydrogel, as well as increasing resistance to enzymatic degradation by collagenase.[25] It is also important to note here that the absorption properties of the synthetic cornea should be comparable to that of the human cornea if it is to be considered for implementation into human beings.

The collagen-MPC IPN hydrogels prepared showed encouraging results in many areas of interest including *in vitro* biodegradation, *in vivo* biocompatibility and UV/sunlight irradiation effects.[22] The resistance of the hydrogel to collagenase digestion was demonstrated by lower mass lost than that the human cornea when placed in concentrated collagenase for 26 days. *In vivo* pig implantation of the hydrogel into the cornea demonstrated a comparable re-epithelialization rate to that of normal wound healing in a human cornea. Exposure to solar irradiation for 20 hours showed minimal change in the absorption spectrum, as shown in Figure 1 - 4, suggesting that the hydrogels are stable and the patient's vision will not be affected by sunlight irradiation.

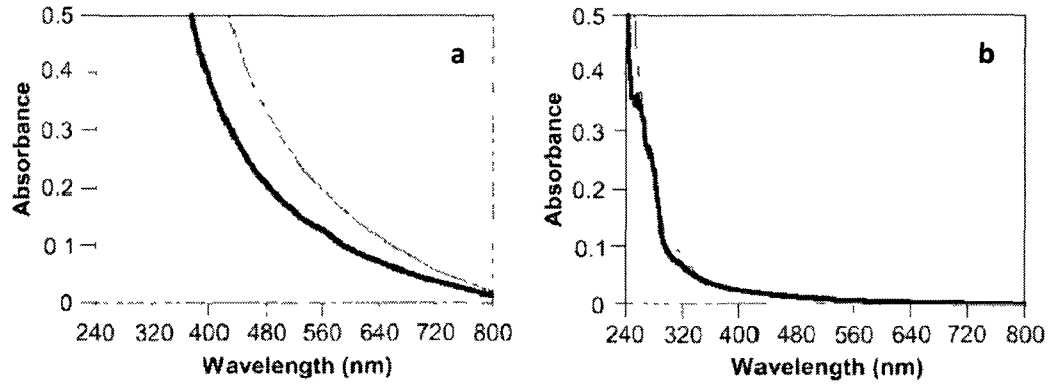

Figure 1 - 4: Absorption spectrum before (thick) and after (thin) solar exposure for 20 hours. a) human cornea, b) collagen-MPC hydrogel.[22]

The collagen-MPC IPN hydrogel demonstrated encouraging results when compared to natural human corneas, making it a potential candidate for use as future corneal substitutes.[22] However, an inherent problem still remains with HSV related transplants: the virus often remains latent in the ocular nerve,[21] leading to eventual reactivation of the virus following corneal transplant.

1.3. Photocages for Antiviral Release

Our research group is currently involved in a collaborative project with Dr. May Griffith at the Ottawa Eye Institute and Dr. James Harden the University of Ottawa Physics Department to develop a potential solution to the previously described HSV-1 problem.

One possible route is to tether xanthonate photocages equipped with an antiviral to the collagen-MPC hydrogel, as represented in Scheme 1 - 9. This would allow for controlled delivery of an antiviral (such as ACV) directly into the transplanted cornea following surgery.[26] This modification of the replacement corneas is expected to prevent reactivation of the virus, and thus improve the success rate of transplantation.

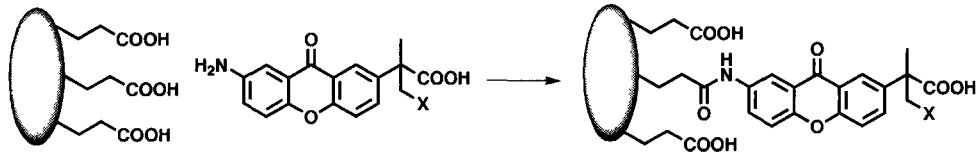

Scheme 1 - 9: A potential way to attach xanthonate photocages to surfaces, such as collagen-MPC hydrogel (X = leaving group). Coupling of the aromatic amine to carboxylic acid terminated surfaces could ideally be achieved through the use of standard amide coupling chemistry.

Prior to attachment of xanthonate photocages to the collagen-MPC hydrogel, it is first crucial that the photochemistry is investigated to ensure

that the same clean photorelease is achieved for the amide tethered photocage as is observed for the parent xanthonate photocages.

The following chapters describe the initial investigations toward surface/polymer-tethered photorelease of antivirals. Firstly, the amine and acetamide derivatives of **XAA** are synthesized and their photochemical properties assessed and compared with the clean photodecarboxylation chemistry of the parent **XAA**. Next, the feasibility of photorelease from amide-tethered photocages is probed by the synthesis and photochemical study of acetamide functionalized xanthonate photocages equipped with biologically relevant leaving groups. Lastly, initial work related to polymer tethering through amide coupling chemistry is investigated.

1.4. References

1. Flickinger, S. T.; Patel, M.; Binkowski, B. F.; Lowe, A. M.; Li, M.-H.; Kim, C.; Cerrina, F.; Belshaw, P. J., Spatial Photorelease of Oligonucleotides, Using a Safety-Catch Photolabile Linker. *Org. Lett.* **2006,** *8* (11), 2357-2360.

2. Turro, N. J.; Ramamurthy, V.; Scaiano, J. C., *Modern Molecular Photochemistry of Organic Molecules*. University Science Books: Sausalito, California, 2010.

3. Lakowicz, J. R., In *Principles of Fluorescence Spectroscopy*, Second ed.; Kluwer Academic/Plenum: New York, 1999; p 698.

4. Patchornik, A.; Amit, B.; Woodward, R. B., Photosensitive Protecting Groups. *J. Am. Chem. Soc.* **1970,** *92*, 6333-6335.

5. Bochet, C. G., Photolabile Protecting Groups and Linkers. *J. Chem. Soc., Perkin Trans.* **2002,** *1*, 125-142.

6. Kaplan, J. H.; Forbush, B.; Hoffman, J. F., Rapid Photolytic Release of Adenosine 5'-Triphosphate from a Protected Analogue: Utilization by the Na:K Pump of Human Red Blood Cell Ghosts. *Biochemistry* **1978,** *17*, 1929-1935.

7. Walker, J. W.; Reid, G. P.; McCray, J. A.; Trentham, D. R., Photolabile 1-(2-Nitrophenyl)ethyl Phosphate Esters of Adenine Nucleotide Analogues. Synthesis and Mechanism of Photolysis. *J. Am. Chem. Soc.* **1988,** *110*, 7170-7177.

8. Pelliccioli, A. P.; Wirz, J., Photoremovable Protecting Groups: Reaction Mechanisms and Applications. *Photochem. Photobiol. Sci* **2002,** *1*, 441-458.

9. Il'ichev, Y. V.; Schworer, M. A.; Wirz, J., Photochemical Reaction Mechanisms of 2-Nitrobenzyl Compounds: Methyl Esters and Caged ATP. *J. Am. Chem. Soc.* **2004,** *126*, 4581-4595.

10. Corrie, J. E. T.; Barth, A.; Munasinghe, V. R. N.; Trentham, D. R.; Hutter, M. C., Photolytic Cleavage of 1-(2-Nitrophenyl)ethyl Ethers Involves Two Pathways and Product Release is Rate-Limited by Decomposition of a Common Hemiacetal Intermediate. *J. Am. Chem. Soc.* **2003,** *125*, 8456-8554.

11. Martinez, L. J.; Scaiano, J. C., Transient Intermediates in the Laser Flash Photolysis of Ketoprofen in Aqueous Solutions: Unusual Photochemistry for the Benzophenone Chromophore. *J. Am. Chem. Soc.* **1997,** *119* (45), 11066-11070.

12. Cosa, G.; Martinez, L. J.; Scaiano, J. C., Influence of Solvent Polarity and Base Concentration on the Photochemistry of Ketoprofen: Independent Singlet and Triplet Pathways. *Phys. Chem. Chem. Phys.* **1999,** *1*, 3533-3537.

13. Cosa, G.; Llauger, L.; Scaiano, J. C.; Miranda, M. A., Absolute Rate Constants for Water Protonation of 1-(3-Benzoylphenyl)alkyl Carbanion. *Org. Lett.* **2002,** *4*, 3083-3085.

14. Lukeman, M.; Scaiano, J. C., Carbanion-Mediated Photocages: Rapid and Efficient Photorelease with Aqueous Compatibility. *J. Am. Chem. Soc.* **2005,** *127*, 7698-7699.

15. Chretien, M. N.; Cosa, G.; Garcia, H.; Scaiano, J. C., Increasing the Life Expectancy of Carbanions by Zeolite Inclusion. *Chem. Comm.* **2002,** (18), 2154-2155.

16. Laferriere, M.; Sanrame, C. N.; Scaiano, J. C., A Remarkably Long-Lived Benzyl Carbanion. *Org. Lett.* **2004,** *6*, 873-875.

17. Blake, J. A.; Gagnon, E.; Lukeman, M.; Scaiano, J. C., Photodecarboxylation of Xanthone Acetic Acids: C-C Bond Heterolysis from the Singlet Excited State. *Org. Lett.* **2006,** *8*, 1057-1060.

18. Blake, J. A.; Lukeman, M.; Scaiano, J. C., Photolabile Protecting Groups Based on the Singlet State Photodecarboxylation of Xanthone Acetic Acid. *J. Am. Chem. Soc.* **2009,** *131*, 4127-4135.

19. Majjigapu, J. R. R.; Kurchan, A. N.; Kottani, R.; Gustafson, T. P.; Kutateladze, A. G., Release and Report: A New Photolabile Caging System with a Two-Photon Fluorescence Reporting Function. *J. Am. Chem. Soc.* **2005,** *127*, 12458-12459.

20. Ezhov, R. N.; Rozhkov, V. V.; Majjigapu, J. R. R.; Kutateladze, A. G., Photolabile Amphiphiles with Fluorogenic Thioxanthone-Dithiane Functionality: Synthesis and Photoinduced Fragmentation in Micelles. *J. Sulf. Chem.* **2008,** *29*, 389-400.

21. Toma, H. S.; Murina, A. T.; Areaux, R. G. J.; Neumann, D. M.; Bhattacharjee, P. S.; Foster, T. P.; Kaufman, H. E.; Hill, J. M., Ocular HSV-1 Latency, Reactivation and Recurrent Disease. *Semin. Ophthalmol.* **2008,** *23* (4), 249-273.

22. Liu, W.; Deng, C.; McLaughlin, C. R.; Fagerholm, P.; Lagali, N. S.; Heyne, B.; Scaiano, J. C.; Watsky, M. A.; Kato, Y.; Munger, R.; Shinozaki, N.; Li, F.; Griffith, M., Collagen-Phosphorylcholine Interpenetrating Network Hydrogels as Corneal Substitutes. *Biomaterials* **2009,** *30*, 1551-1559.

23. Merrett, K.; Liu, W.; Mitra, D.; Camm, K. D.; McLaughlin, C. R.; Liu, Y.; Watsky, M. A.; Li, F.; Griffith, M.; Fogg, D. E., Synthetic Neoglycopolymer-Recombinant Human Collagen Hybrids as Biomimetic Crosslinking Agents in Corneal Tissue Engineering. *Biomaterials* **2009,** *30*, 5403-5408.

24. Fagerholm, P.; Lagali, N. S.; Carlson, D. J.; Merrett, K.; Griffith, M., Corneal Regeneration Following Implantation of a Biomimetic Tissue-Engineered Substitute. *CTS* **2009,** *2*, 162-164.

25. Nam, K.; Kimura, T.; Kishida, A., Physical and Biological Properties of Collagen-Phospholipid Polymer Hybrid Gels. *Biomaterials* **2007,** *28*, 3153-3162.

26. Scaiano, J. C.; Blake, J. A.; Griffith, M., Use of Ketoprofenate and Xanthonate Photocages for Antiviral Release. In *Extreme Photonics & Applications*, Springer Netherlands: Dordrecht, 2010.

2. Photochemistry of Nitro, Amine and Amide Functionalized Xanthone Acetic Acids

2.1. Introduction 22
2.2. Synthesis 26
2.2.1. Synthesis of Nitro Derivatives 6-7 26
2.2.2. Synthesis of Amine Derivatives 8-9 28
2.2.3. Synthesis of Acetamide Derivatives 10-11 30
2.3. Photochemistry of Nitro Derivatives 6-7 33
2.4. Photochemistry of Amine Derivatives 8-9 35
2.5. Photochemistry of Acetamide Derivative 10 39
2.5.1. Steady State Photochemistry 39
2.5.2. Fluorescence Spectroscopy 46
2.5.4. Laser Flash Photolysis Studies 50
2.6. Photochemistry of Acetamide Derivative 11 55
2.7. Summary 61
2.8. Experimental Details 64
2.8.1. Synthetic Procedures 64
2.8.2. Photodecarboxylation Quantum Yield 74
2.8.2. Fluorescence 75
2.8.2. Nanosecond Laser Flash Photolysis 76
2.9. References 77

2.1. Introduction

As described previously in Chapter 1, rapid and efficient photodecarboxylation from the singlet excited state following UV irradiation in basic aqueous media has been reported for both ketoprofen (**Kp**, $\Phi_D = 0.75$)[1] and 2-xanthone acetic acid (**XAA**, $\Phi_D = 0.67$).[2] Though both systems demonstrate high photodecarboxylation quantum yields, they differ in their absorption profiles: **XAA** has an absorption maximum at 347 nm, whereas **Kp**'s absorption tails off at wavelengths above 300 nm. From the perspective of designing photocages for antiviral release within biological systems, xanthonate photocages are more suited to the application than their ketoprofenate analogs since significant absorption above 300 nm is desired for biological applications.[3]

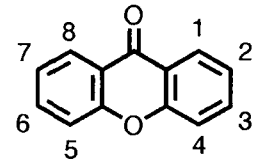

Xanthone

To achieve photorelease of antivirals from tethered photocages, a linker or handle is required to allow for direct attachment of the photocage to a polymer or surface of choice. Due to relative ease of synthesis, the proposed route to incorporate a linker into the system was functionalization of

a xanthonate photocage with a nitro group at the 7 position of the xanthone moiety. In this way, attachment would be distal to the carboxylate. Subsequent reduction of the nitro moiety will afford an amine. This added amino group would potentially allow for direct attachment to carboxylic acid terminated surfaces *via* amide coupling chemistry. Similar coupling methods could also be employed to modify the terminal amine with a variety of end groups, which has been reported for various common linkers such as thiols and carboxylic acids shown in Scheme 2 - 1.[4]

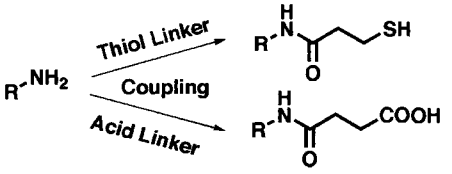

Scheme 2 - 1: Conversion of primary amines to thiol and carboxylic acid linkers *via* amide coupling chemistry.

Prior to attachment and photorelease of leaving groups, the potential substituent effect on photodecarboxylation required detailed investigation. The chosen route of attachment described above would place the amine/amide directly on the xanthone chromophore without aliphatic spacers. Such a direct modification of the chromophore could significantly change the resulting photochemical properties of the photocage, making this initial study necessary.

As discussed earlier, longer wavelength absorption is advantageous for photocages aimed at biological applications. Considering this point, an analogous series of molecules based on the thioxanthone chromophore could prove useful by further extending the absorbance band into the visible region. Replacement of the ether bridge in xanthone with the more electron rich thioether bridge present in thioxanthone causes a characteristically longer wavelength absorption.[5] The same behavior was expected for derivatives **7**, **9** and **11** when compared to their xanthone analogues (**6**, **8**, and **10**).

This chapter deals with the synthesis and photochemical study of **6** - **11** (all shown in Chart 2 - 1). Finally, the studied derivatives will be assessed with respect to their potential use as precursors for photocages for biological applications.

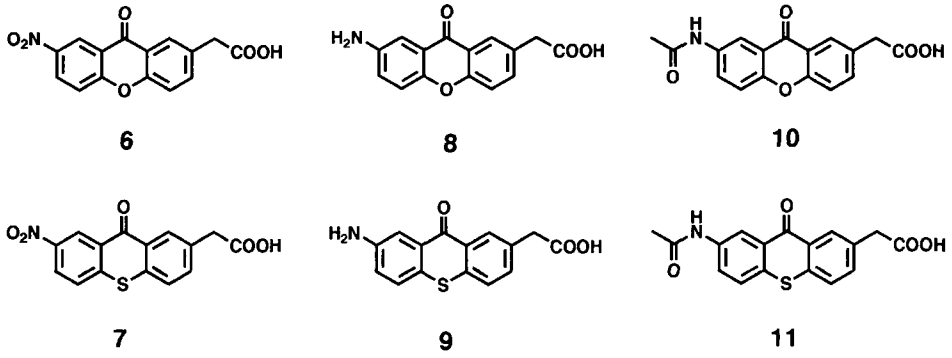

Chart 2 - 1: Adopted nomenclature used for nitro, amine, and acetamide derivatives of xanthone acetic acid and thioxanthone acetic acid.

This work has been in collaboration with J.A. Blake, a fellow graduate student in our research group. Further details regarding the in-depth photochemistry of nitro derivatives **6** and **7** can be found in her Ph.D. thesis.[6] My contribution to this work is focused on the synthesis and photochemistry of amine and amide derivatives **8-11**.

2.2. Synthesis

2.2.1. Synthesis of Nitro Derivatives 6-7

Derivatives **6-11** are not commercially available, thus they had to be synthesized prior to their photochemical study. The primary building block of these molecules is **6**, which was originally synthesized by J.A. Blake *via* **XAA** nitration.[6] **XAA** was synthesized according to a modification of a reported synthesis,[7] by using copper (I) catalyzed Ullmann coupling of *o*-iodobenzoic acid and *p*-hydroxyphenylacetic acid followed by acid-catalyzed intramolecular acylation to close the xanthone ring (Scheme 2 - 1). Literature xanthone nitration[8, 9] following ring closure afforded **6**.

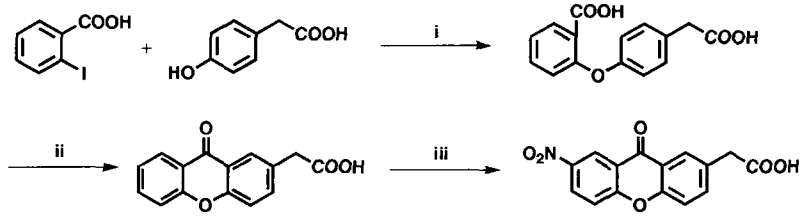

XAA (30% from start) **6**

Scheme 2 - 2: Original synthesis of 6. i) CuCl, dioxane, tris(2-(2-methoxyethoxy)ethyl)amine (TDA-1), Cs_2CO_3; ii) H_2SO_4, Δ; iii) KNO_3, H_2SO_4.

It is important to note here that the Ullmann coupling described above requires very dry, oxygen free conditions and recrystallization of copper (I)

chloride prior to use, making the reaction very tedious. On top of the sensitive nature of the reaction conditions, **XAA** was produced in relatively low yields (30%) even before nitration, making further synthesis difficult due to low quantities of **6** available.

Rather than performing the same Ullmann coupling using *o*-iodobenzoic acid and *p*-hydroxyphenylacetic acid, I took advantage of the electron withdrawing nature of the desired nitro group. To do this, 2-fluoro-5-nitrobenzoic acid and *p*-hydroxyphenylacetic acid were used to perform a nitro assisted S_NAr, as shown in Scheme 2 - 3.[10, 11] Stirring the starting materials in dimethyl sulfoxide (DMSO) with crushed sodium hydroxide (NaOH) at room temperature overnight afforded the desired product in significantly higher yields than the previous method described above. Following coupling, acid-catalyzed intramolecular ring closure produced **6** with an overall 91% yield of the crude product. The product was easily purified by ethanol recrystallization. This procedure provided a significant improvement in the synthesis of **6**.

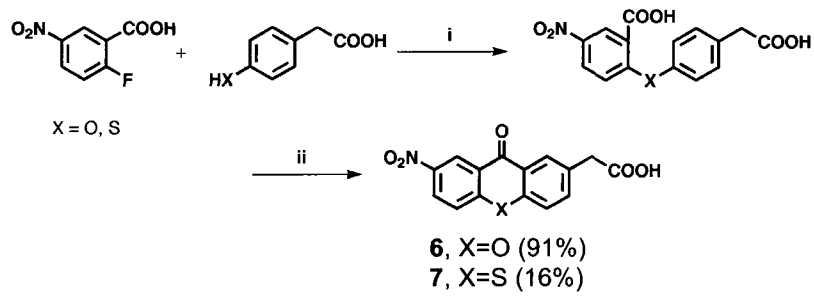

6, X=O (91%)
7, X=S (16%)

Scheme 2 - 3: New synthetic route for 6 (X = O) and 7 (X = S).
i) KOH, DMSO; ii) H_2SO_4, Δ.

With the improvement in the synthesis of **6**, the procedure was utilized in the same manner to make the thioxanthone analog, **7**, as shown in Scheme 2 - 3. The procedure afforded **7** as a pure yellow solid following organic extraction and ethanol recrystallization in 16% yield. With **6** and **7** on hand, it was possible to press forward with subsequent synthesis of other nitrogen containing derivatives, which require the nitro group as a building block starting material.

2.2.2. Synthesis of Amine Derivatives 8-9

The next task to be undertaken was the synthesis of amino derivatives by reduction of the nitro group. Attempts to reduce the nitro group using tin and hydrochloric acid following literature procedure[12] were successful at making the desired compound, but added significant difficulty in separation of the product from the aqueous environment due to their inherent pH sensitivity brought upon by having both carboxylic acid and amine functional groups present in the molecule.

After several frustrated attempts at separating **8** from the Sn/HCl mixture produced from the reaction, attention was turned to the use of palladium-catalyzed hydrogenation.[13] Using ethyl acetate (EtOAc) as the solvent and solid palladium on activated carbon (Pd/C) as the heterogeneous catalyst, one atmosphere of hydrogen gas reduced the nitro to the amine in near quantitative yield in just a few hours, as shown in Scheme 2 - 4. The

progress of the reaction was observable by thin layer chromatography showing the product as a yellow spot at lower retention factor (R_f). The workup required only removal of the catalyst by suction filtration through celite, followed by removal of the solvent by rotary evaporation. The product was easily verified by ^1H NMR in DMSO-d_6, with the appearance of a new amine singlet at 5.45 ppm as well as greater shielding of the aromatic protons nearest the amino group. ^{13}C NMR and HRMS further verified the identity of the amine, **8**.

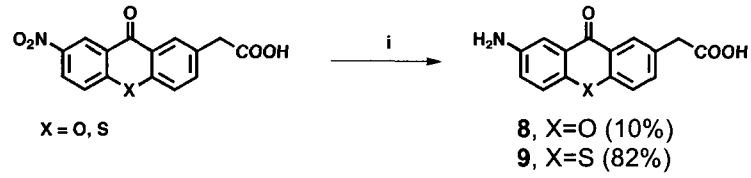

Scheme 2 - 4: Synthesis of 8 (X = O) and 9 (X = S). i) Pd/C, H_2, EtOAc.

To make the thioxanthone analog (**9**), the same reaction conditions were used as shown in Scheme 2 - 4. Again the reaction proceeded within 2 hours to afford pure **9** in near quantitative yield following catalyst and solvent removal. HRMS, ^1H and ^{13}C NMR verified the identity of the product.

2.2.3. Synthesis of Acetamide Derivatives 10-11

Following the successful preparation of **8** and **9** described above, the next step was to prepare a simple amide functionalized **XAA** to be able to study the photochemistry prior to tethering to complex systems such as polymers or particles. To study the effects caused by direct modification of the chromophore while keeping the model simple and easy to prepare, acetamide was chosen (as in **10** and **11**) to represent a generic amide.

The first synthetic step was to convert the carboxylic acid to an ethyl ester *via* acid catalyzed esterification of **6** (Scheme 2 - 5, i).[14] This was done to enhance the solubility in organic solvents as well as to protect the carboxylic acid functionality from potential reactions in the nitro reduction or amide formation steps. Following 2 hours of refluxing ethanol (EtOH) with a catalytic amount of H_2SO_4, **6** was converted to **12** quantitatively. The produced ester was then easily purified by ethanol recrystallization. ^{1}H NMR analysis in DMSO-d_6 showed the appearance of the ethyl ester signals (a quartet at 4.12 ppm and a triplet at 1.21 ppm), thus confirming the success of the reaction. ^{13}C NMR and HRMS further verified the identity of **12**.

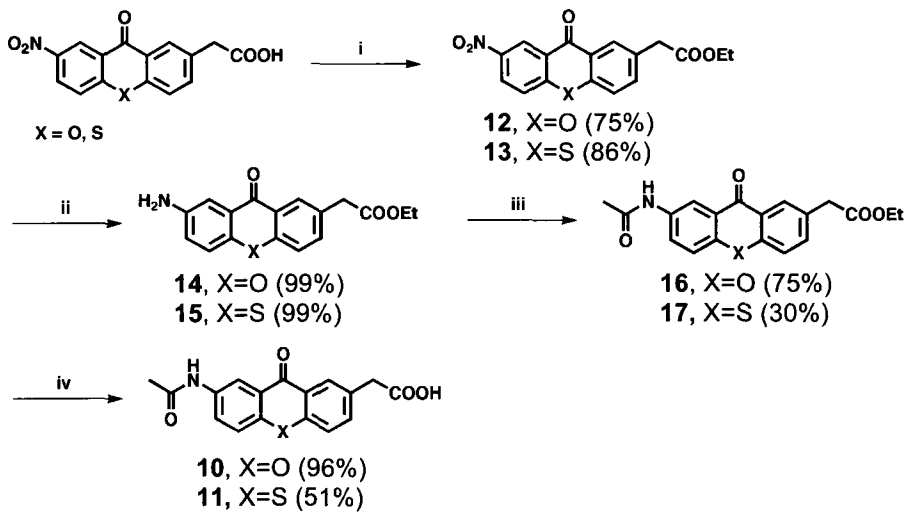

Scheme 2 - 5: Synthetic Route for 10 (X = O) and 11 (X = S): i) EtOH, H_2SO_4, Δ; ii) H_2, Pd/C, EtOAc; iii) Ac_2O, pyridine, DCM; iv) NaOH, CH_3CN.

Following esterification, the nitro group was reduced to an amine using palladium catalyzed hydrogenation (Scheme 2 - 5, ii).[13] Stirring **12** in EtOAc with Pd/C under one atmosphere of hydrogen gas, the reaction proceeded at room temperature within a few hours as observed by TLC. The product was isolated by filtration of the solid catalyst through celite followed by removal of the solvent by rotary evaporation. ^{1}H NMR in DMSO-d_6 verified the identity of **14** with the observable characteristic shift of the aromatic protons near the amino group along with the new amino singlet at 5.45 ppm. ^{13}C and HRMS were in agreement, confirming the structure of **14**.

Following nitro reduction, the acetamide was formed by conversion of the amine. **14** was stirred under nitrogen in dry dichloromethane (DCM) with excess acetic anhydride (Ac_2O) and pyridine for 2.5 hours to produce **16** (Scheme 2 - 5, iii).[14] The progress of the reaction was monitored by TLC in

1:1 EtOAc:hexanes, with the product appearing as a blue fluorescent spot at lower Rf than the starting material. **16** was isolated by organic extraction and purified by column chromatography (in 1:1 EtOAc:hexanes). The change in structure is easily observed using ^{1}H NMR in DMSO-d_6 by the appearance of the amide singlet at 10.3 ppm accompanied by the disappearance of the amine singlet at 5.45 ppm. ^{13}C NMR and HRMS further verified the identity of **16**.

Finally the carboxylic acid needed to be deprotected by ester hydrolysis in base to produce **10**. Stirring **16** in 1:1 v/v 0.1 M NaOH:acetonitrile (ACN) overnight gave **10** following organic extraction (Scheme 2 - 5, iv).[15] Recrystallization from boiling ethanol gave pure **10** as pale yellow solid. The disappearance of the ethyl ester peaks in the ^{1}H NMR spectrum verified the successful conversion to **10**, along with ^{13}C NMR and HRMS agreement.

Once the synthetic scheme was outlined for the production of **10**, the same route was utilized to synthesize the thioxanthone analog, **11**. Though the method afforded **11**, the synthetic yields were lower than that obtained for **10**. The quantities produced, however, were sufficient to perform the desired photochemical studies discussed later.

2.3. Photochemistry of Nitro Derivatives 6-7

As clearly seen in Figure 2 - 1, the absorbance profile of nitro derivative **6** is red-shifted with respect to the parent **XAA**. The thioxanthone analog, **7**, shows a further spectral shift into the red. The photochemistry of the nitro precursors, **6** and **7**, described in this section was carried out by J.A. Blake and are presented here to allow for complete comparison of photochemical reactivity.

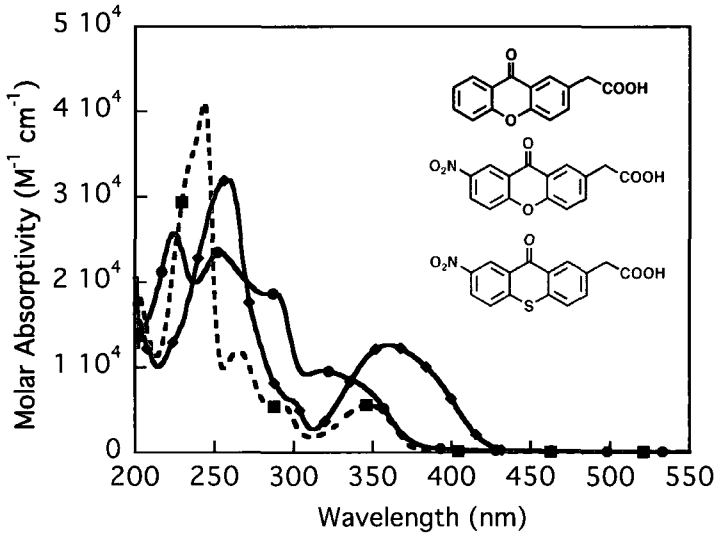

Figure 2 - 1: Molar absorptivity of 6 (solid blue), 7 (solid red) and XAA (dashed black) in PBS. Spectra were measured by J.A. Blake.

UVB irradiation of **6** and **7** in PBS under air gave a mixture of products, which were separated by preparative TLC and analyzed by ^1H

NMR and GC-MS. The expected photoproduct resulting from decarboxylation and subsequent protonation of the carbanion was observed as the main product, but was among a mixture of other photoproducts as shown in Scheme 2 - 6. Among these products were the aldehyde and alcohol resulting from reaction of the generated carbanion with oxygen. This is supported by reduced aldehyde and alcohol production when **6** is irradiated after purging with nitrogen. It should be noted the irradiation of **7** under the same conditions gave the same product distribution as observed for **6**. The photochemical behavior of **6** and **7** is not surprising, as the electron withdrawing nitro group further stabilizes the negative charge of the benzyl carbanion, causing the lifetime of the carbanion intermediate to increase. This lengthening of the carbanion lifetime brings about a competition between solvent protonation and other reactions, accounting for the variety of products formed from nitrobenzyl-like carbanions.[16]

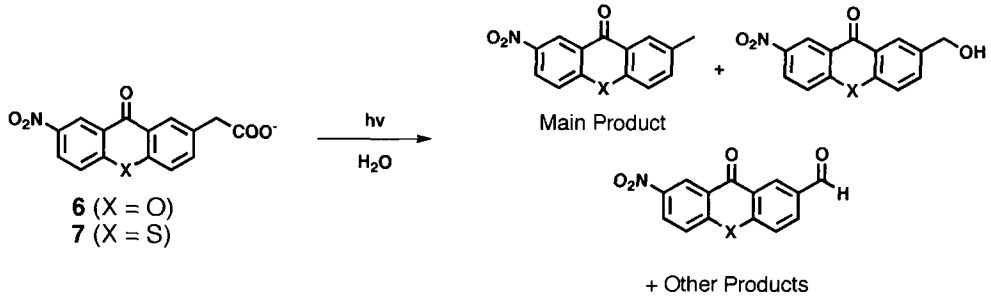

6 (X = O)
7 (X = S)

Scheme 2 - 6: Photoreaction of 6 and 7 in basic aqueous media (pH 7.4).

2.4. Photochemistry of Amine Derivatives 8-9

After having successfully prepared the amine functionalized xanthone acetic acid (**8**), the photochemistry was probed to test our assumption that the free amine would quench the singlet excited state. This assumption is based on reports in the literature that show aromatic amines undergo charge transfer quenching of a variety of singlet and triplet excited states.[17-19] It has also been recently reported that the presence of an amine moiety significantly reduces the fluorescence quantum yield in water from $\Phi_F = 0.17$ for xanthone to $\Phi_F = 0.009$ for 2-aminoxanthone.[9]

As can be seen from the UV/Vis absorbance spectra shown for **8** and **9** in Figure 2 - 2, the absorption is shifted to longer wavelengths (or red-shifted) compared to the parent **XAA**. The first absorption red-shift arises from the addition of the electron rich amino group, which raises the level of HOMO, and thus shortens the HOMO-LUMO gap of **8** with respect to **XAA**. Likewise, when modifying the ether hetero-atom from oxygen (in **8**) to the more electron rich sulfur (in **9**), the absorption band is further red-shifted.

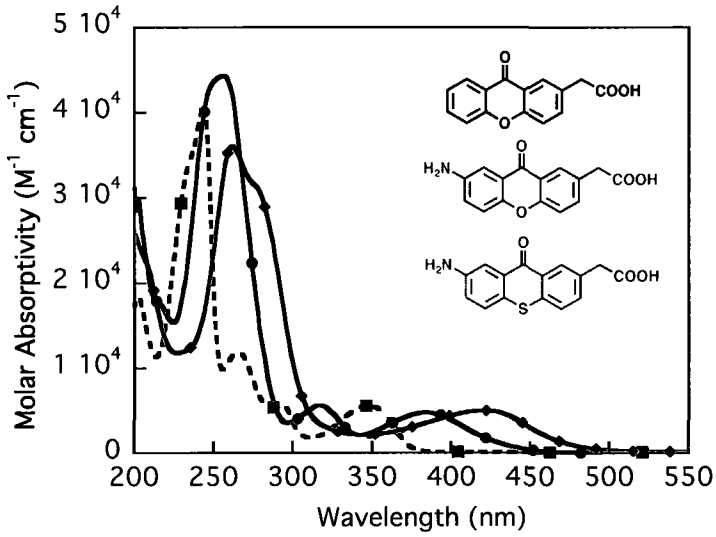

Figure 2 - 2: Molar absorptivity of 8 (solid blue), 9 (solid red) and XAA (dashed black) in 80:20 v/v PBS:ACN.

Product studies were used to determine the potential photoproducts produced upon irradiation. Following one hour of UVB irradiation, several solutions of **8** (5 mM in 90:10 v/v PBS:ACN) were analyzed by HPLC-UV. The irradiated samples showed the same single peak in the chromatograph indicating no change in the starting material. Samples acidified and extracted with ethyl acetate showed no change in the ^{1}H NMR spectrum, further verifying the lack of photochemical activity. These results are consistent with the assumption that the amine moiety would quench the generated excited states, thus turning off photodecarboxylation.

To assess the photochemical behavior of the thioxanthone analog, **9**, steady state photochemistry was used in the same manner as described above. HPLC-UV and ^{1}H NMR analysis following extensive UVB irradiation of

9 (5 mM in 90:10 v/v PBS:ACN) yielded only starting material. This shows that **9**, much like **8**, is photochemically inert under basic aqueous conditions, as expected.

The singlet photochemistry of **8** and **9** was further investigated using fluorescence spectroscopy. Figure 2 - 3 shows that the fluorescence intensity of **8** is very low, owing to a low fluorescent quantum yield. It should be noted here that the sharp peak observed at 400 nm arises from the Raman scattering of water, its observation is indicative of weak fluorescence emission. The quantum yield of fluorescence of **8** was determined to be 0.03 in PBS, as measured against quinine bisulfate (Φ_F = 0.58 in 1 N H_2SO_4).[20] This result is not surprising, as it was clearly demonstrated above that the amine effectively quenches all photochemical product formation for **8**. Likewise, it would be expected that the fluorescence would be quenched significantly, if not completely. Consistent with amine quenching, **9** showed no observable fluorescence signal under the same experimental conditions.

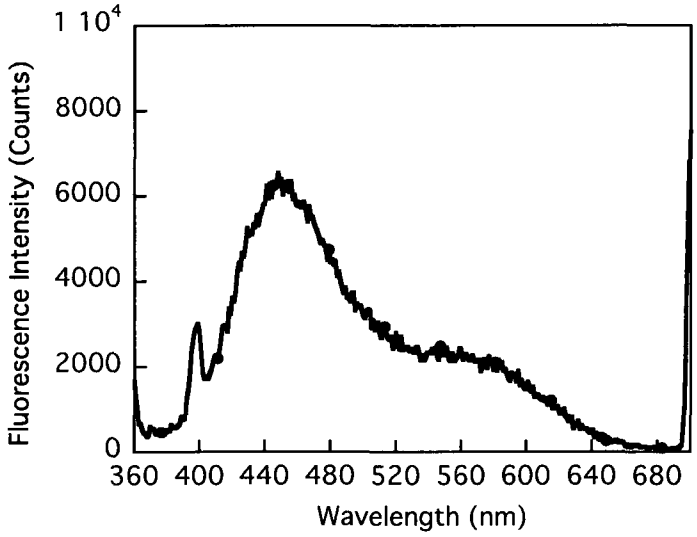

Figure 2 - 3: Fluorescence spectrum of 8 in PBS. Absorbance of 0.1 at the excitation wavelength (350 nm).

The low quantum yields of fluorescence and photodecarboxylation measured for **8** and **9** are consistent with the proposed mechanism whereby the excited state is quenched by the amine moiety. This quenching competes favorably with both the photoreaction and fluorescence deactivation pathways.

2.5. Photochemistry of Acetamide Derivative 10

2.5.1. Steady State Photochemistry

Following the preparation of **10**, the photochemistry was probed to assess its behavior and efficiency with respect to the parent **XAA**. This section describes the steady state techniques employed to probe the photochemical behavior of **10**. As shown in Figure 2 - 4, the absorption spectrum of **10** is red-shifted with respect to **XAA**, but to a lesser degree than that of **8**. The difference in **10** absorbance is caused by the electron rich acetamide moiety, which causes the red-shift by lowering the HOMO-LUMO energy gap.[21]

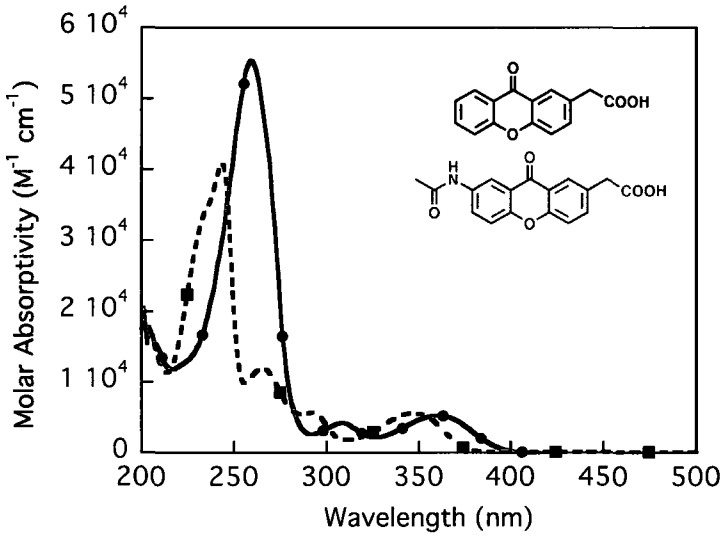

Figure 2 - 4: Molar absorptivity of 10 (solid blue) and XAA (dashed black) in 80:20 v/v PBS:ACN.

To identify the products resulting from irradiation of **10**, solutions (5 mM in 80:20 v/v PBS:ACN) were irradiated in quartz test tubes. Following acidification and extraction, the samples were analyzed by MS, ^{1}H and ^{13}C NMR. UVB Irradiation of **10** for 30 minutes gave **18** as the exclusive photoproduct (Scheme 2 - 7). This clean photochemistry is consistent with that of the parent **XAA**. Extensive irradiation (several hours UVB) of **10** led to precipitation of **18**, and gave no other photoproducts as confirmed by HPLC-UV and ^{1}H NMR. The same photoproduct was observed both under aerobic and anaerobic (nitrogen purged) conditions.

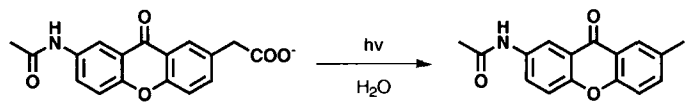

10 **18**

Scheme 2 - 7: Clean photodecarboxylation of 10 in basic aqueous media (pH 7.4) to afford 18.

The photochemical reaction was also studied by UV/Vis absorption spectroscopy. UV/Vis spectra of **10** following UVB irradiation are shown in Figure 2 - 5. As can be seen from this figure, the (π,π^*) band at 256 nm drastically decreases with irradiation. Consistent with the clean photochemistry, there were several clean isospestic points at 230, 274, 342, and 372 nm. It is not certain, however, why such a decrease in absorbance would occur, as the chromophore remains unchanged following photodecarboxylation. This result is in contrast to the results for **XAA** whose absorbance spectrum remains largely unchanged with photochemical conversion to 2-methylxanthone.[2]

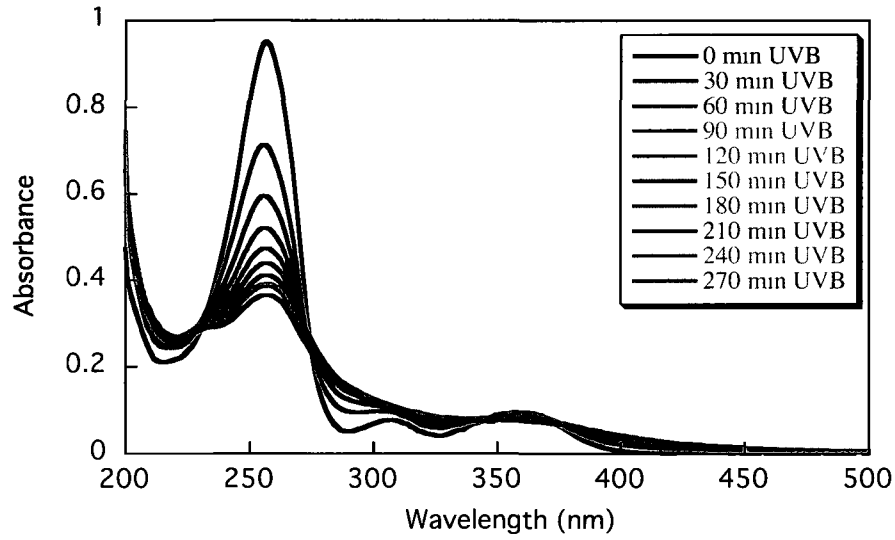

Figure 2 - 5: UV/Vis Absorbance of 10 with UVB Irradiation (in 80:20 v/v PBS:ACN).

To measure the efficiency of photodecarboxylation, several solutions of **10** and **Kp** (both 4 mM in PBS) were irradiated simultaneously in a merry-go-round apparatus. Surprisingly, the quantum yield of photodecarboxylation was determined to be quite low (Φ_D = 0.01 in PBS against **Kp**: Φ_D = 0.75 in PBS).[1, 22]

Upon further investigation, an interesting solvent effect on the photodecarboxylation quantum yield was discovered. When several solutions of **10** (4 mM in 80:20 v/v PBS:ACN) and **Kp** (4 mM in PBS) were irradiated simultaneously in a merry-go-round apparatus, the quantum yield of photodecarboxylation was determined to be 0.05 for **10**, five times higher than in pure PBS.

This promising result led to a more in-depth exploration of the solvent composition effect on the decarboxylation of **10**. Several 3 mM solutions in solvent systems ranging from 90:10 to 30:70 v/v PBS:ACN were irradiated simultaneously using a merry-go-round apparatus. The extent of photochemical conversion was obtained by HPLC-UV analysis, which is summarized in Table 2 - 1 and represented graphically in Figure 2 - 6 for the irradiated samples. It should be noted here that in solvents containing greater than 70% ACN, **10** was mostly insoluble, thus measurements of decarboxylation at higher acetonitrile proportions could not be obtained.

Solvent Composition (v/v PBS:ACN)	Conversion (%)	$\Phi_{Decarboxylation}$
100:0	-	0.01
90:10	2	0.023 [a]
80:20	5	0.055
70:30	8	0.086 [a]
60:40	11	0.12 [a]
50:50	16	0.17 [a]
40:60	19	0.19 [a]
30:70	23	0.24 [a]

Table 2 - 1: 10 photodecarboxylation dependence on solvent composition. a) estimated quantum yields based on that measured in 80:20 v/v acetonitrile:PBS.

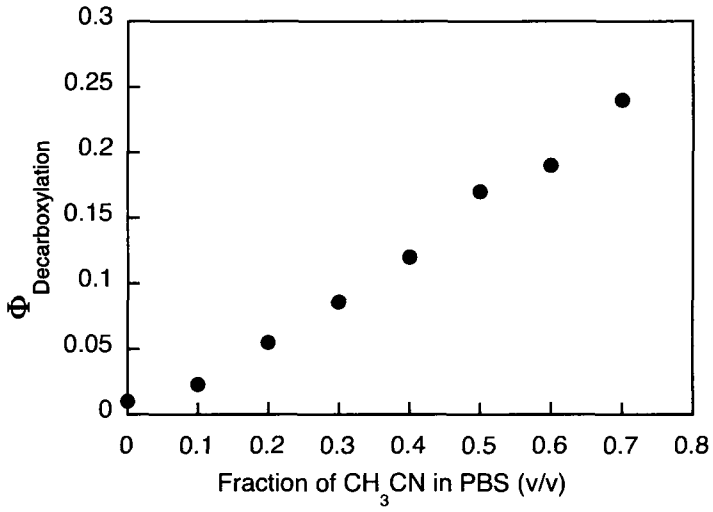

Figure 2 - 6: 10 Photodecarboxylation quantum yield dependence on acetonitrile concentration, using the decarboxylation of Kp as an actinometer.

The trend observed in Figure 2 - 6 shows that the quantum yield of decarboxylation of **10** is strongly dependent on solvent composition, increasing drastically with increasing acetonitrile proportions. This result is in contrast to that of **Kp**, in which the quantum yield of photodecarboxylation decreases from 0.75 to 0.65 in changing from pure PBS to 1:1 v/v PBS:ACN.[23] Recent results within our group show that, within experimental error, this trend is not observed for the photodecarboxylation of the parent **XAA**.[6]

This effect is easily rationalized in terms of the energy barrier associated with decarboxylation. For photodecarboxylation to occur the starting carboxylate of **10** is first promoted into the singlet excited state by absorption of a photon. In order to form the carbanion intermediate from the

excited carboxylate an energy barrier must be crossed. The trend in photodecarboxylation quantum yield suggests that the energy barrier itself may be strongly dependent on the solvent composition, as generally represented in Figure 2 - 7. In water (or PBS), a polar protic medium, the starting carboxylate may be stabilized by hydrogen bonding interactions, making the energy barrier higher. Likewise, as acetonitrile proportions are increased hydrogen bonding interactions are minimized, thus lowering the energy barrier of reaction. It should be mentioned that, while it was not investigated specifically, the pKa value of the carboxylic acid is subject to such solvent composition effects, thus may also provide an additional explanation for the observed behavior.

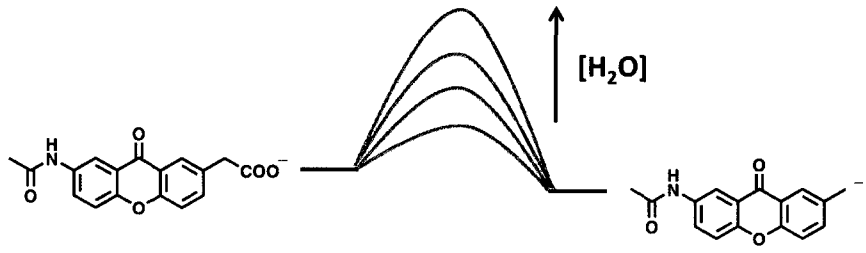

Figure 2 - 7: Cartoon representation of the energy barrier dependence on water concentration. This dependence can be used to explain the trend in which the photodecarboxylation quantum yield of 10 increases with acetonitrile concentration. The energy levels for reactant and product may also be subject to such solvent effects, this has been omitted for clarity.

As is observed in their absorbance spectra (Figure 2 - 4), **10** is red-shifted with respect to **XAA**, suggesting that the singlet excited state of **10** is

lower in energy. Due to **XAA**'s higher energy singlet excited state, transition to the carbanion intermediate from the excited carboxylate is more energetically favorable than its acetamide analog (**10**), thus such a solvent dependence is not observed.

2.5.2. Fluorescence Spectroscopy

To further investigate the singlet photochemistry of **10**, fluorescence spectroscopy was employed. Figure 2 - 8 shows the excitation (dashed) and emission (solid) spectra of **10** (20 μM in PBS solution).

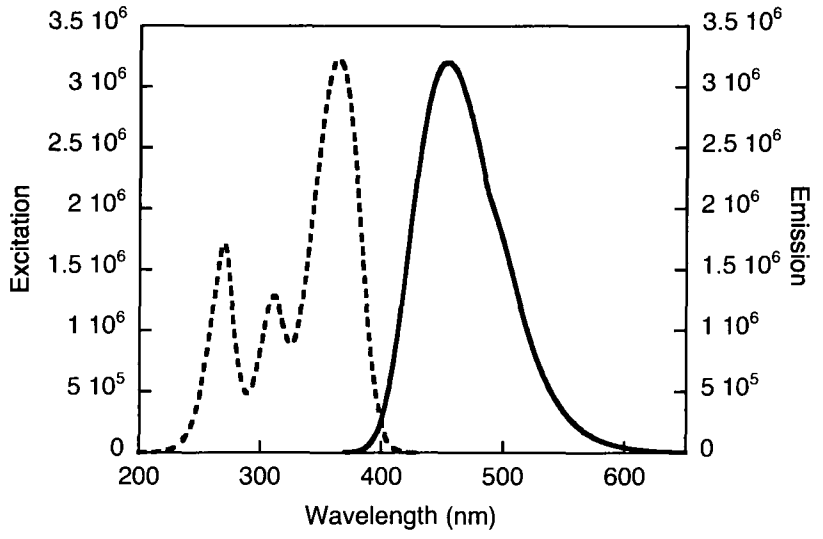

Figure 2 - 8: Fluorescence excitation (dashed) and emission (solid) spectra of 10 (0.01 mM in 80:20 v/v PBS:ACN). Spectra are shown non-normalized. Excitation spectrum was recorded by monitoring emission at 450 nm. Emission spectrum was recorded by exciting at 358 nm.

In PBS, the quantum yield of fluorescence of **10** was determined to be 0.31 as compared to quinine bisulfate (Φ_F = 0.58 in 0.1 N H_2SO_4).[20] This quantum yield is very high with respect to the parent **XAA** (Φ_F = 0.0077 in PBS).[2] This fluorescence enhancement is brought upon by the addition of electron donating substituents, which causes a separation of the $n\pi^*$ and $\pi\pi^*$ excited states.[24]

To test the potential solvent composition effect on the fluorescence emission maximum and quantum yield, several samples were prepared in solvents ranging from 100:0 to 40:60 v/v PBS:ACN. Each sample was absorbance matched (A = 0.1 at 350 nm) and all spectra were recorded under the same operating conditions, as shown in Figure 2 - 9.

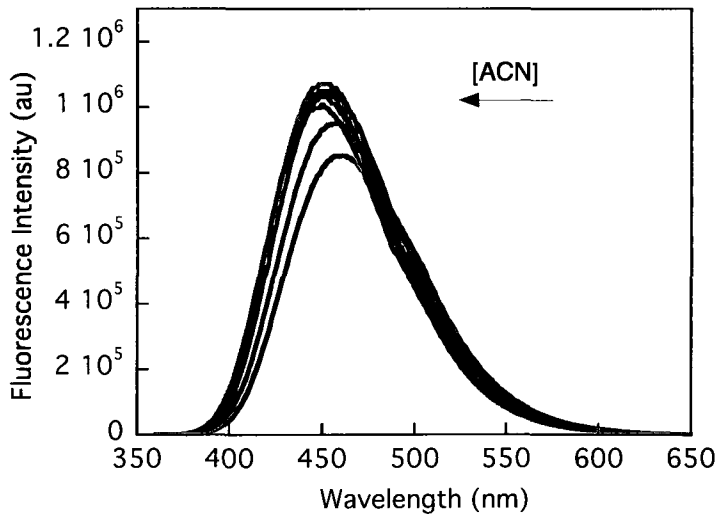

Figure 2 - 9: Absorbance matched fluorescence spectra of 10, varying solvent composition from 100:0 (black trace) to 40:60 (purple trace) v/v PBS:ACN.

It is clear from Figure 2 - 9 and Table 2 - 2 that solvent compositions containing higher proportions of acetonitrile cause a red-shift in the maximum emission of 10. It is interesting to note that there is minimal difference in the fluorescent quantum yields measured in solvents containing PBS; all quantum yields from 100:0 to 40:60 v/v PBS:ACN are in the range of 0.31 to 0.38.

Solvent Composition (v/v PBS:ACN)	λ_{max} (nm)	$\Phi_{Fluorescence}$
100:0	459	0.31
90:10	456	0.34
80:20	453	0.37
70:30	451	0.38
60:40	450	0.37
50:50	450	0.36
40:60	450	0.34

Table 2 - 2: Fluorescence data of 10 with varying solvent composition.

To further investigate the singlet excited state, the lifetimes of fluorescence were measured on a PTI Easylife with 350 nm diode excitation in various solvent compositions. All of the samples were absorbance matched at the excitation wavelength. A representative trace is shown for **10** (20 μM in PBS) in Figure 2 - 10, and the data is summarized in Table 2 - 3.

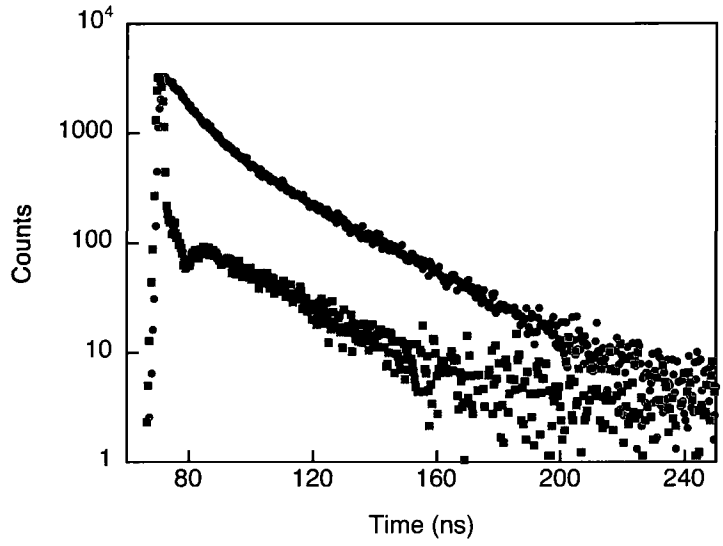

Figure 2 - 10: Representative fluorescence decay trace of 10 (black, 20 μM in PBS:ACN mixtures). The instrument response function is shown in red.

Solvent Composition (v/v PBS:ACN)	$\tau_{Fluorescence}$ (ns)
100:0	9.9
90:10	10.5
80:20	10.7
70:30	10.2
60:40	9.8
50:50	9.6
40:60	8.7

Table 2 - 3: Summary of fluorescence lifetimes of 10 in varying solvent compositions. All lifetimes were recorded using a PTI Easylife with 350 nm diode excitation. The data was fit to first order kinetics using the PTI software.

All fluorescence lifetimes measured for **10** in PBS:ACN mixtures (Table 2 - 3) were in the range of 8-10 ns. These measurements show

negligible solvent composition effect on the fluorescence lifetime. Since both fluorescence quantum yield and lifetime are mostly unchanged with varying solvent compositions, it follows that the combined quantum yields of photochemical and radiationless decay pathways must remain constant. This is consistent with the energy barrier explanation proposed earlier regarding the solvent composition dependence on the photodecarboxylation quantum yield, as the energy barrier is raised with higher water concentrations, radiationless deactivation competes more favorably with photodecarboxylation.

2.5.4. Laser Flash Photolysis Studies

The photochemistry of **10** was further investigated with laser flash photolysis to characterize potential transients or carbanion intermediates produced from the photodecarboxylation.

The xanthone triplet transient is one of the most well characterized signals in laser flash photolysis.[25, 26] The triplet-triplet absorption band is observed around 600 nm and is generally quite intense due to xanthone's high quantum yield of intersystem crossing. The triplet signal has been observed in the laser flash photolysis of **XAA** at 580 nm in basic aqueous media;[2] it is important to note here that although the triplet has been observed for **XAA**, the photodecarboxylation proceeds *via* a singlet-mediated

mechanism as it still occurs in the presence of high concentrations of triplet quenchers such as sorbate.[2]

Figure 2 - 11 shows a representative spectrum recorded for **10**. This particular experiment was performed using Nd/YAG laser (355 nm excitation) in PBS, with absorbance of 0.3 at the excitation wavelength. Interestingly, the recorded spectrum lacked the expected xanthone triplet signal. It is noteworthy that the absorbance does not exceed 0.0025, very low for an LFP signal.

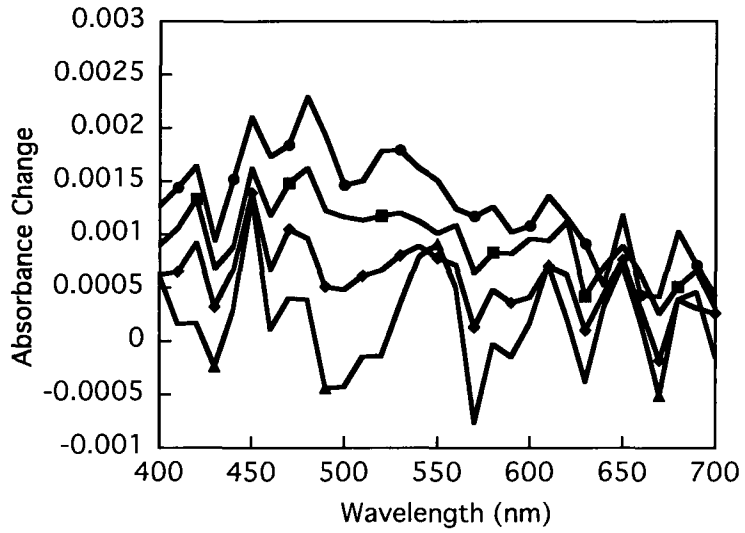

Figure 2 - 11: Representative laser flash photolysis spectrum for 10 in PBS under nitrogen. Spectra were recorded at 5.2 μs (●), 9.2 μs (■), 26.8 μs (◆), and 93.6 μs (▲) (A_{355} = 0.3).

To verify that the system was working properly, a sample of 2-methylxanthone (absorbance matched at 355 nm) was used as a

comparison. Using the same experimental conditions as **10** described above, the spectrum shown in Figure 2 - 12 was recorded. This spectrum clearly shows the xanthone triplet-triplet absorbance centered at 600 nm. Again it is important to note here that the signal observed is two orders of magnitude greater than that shown in Figure 2 - 11.

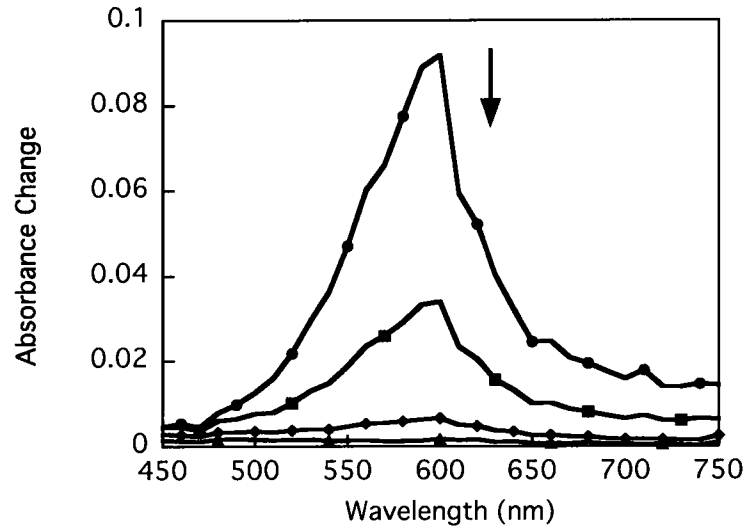

Figure 2 - 12: Laser flash photolysis spectrum of 2-methylxanthone in 80:20 PBS:ACN under nitrogen. Spectra were recorded at 2.4 us (●), 8.0 us (■), 16.8 us (◆), and 40.8 μs (▲) (A_{355} = 0.3).

Several laser flash photolysis experiments were carried out with the intention to characterize a potential transient signal. Using a flow system (*ca.* 1 drop/second) under nitrogen atmosphere, several solvent compositions ranging from 100:0 to 40:60 v/v PBS:ACN were prepared. Using the same

conditions described above yielded spectra that were comparable to that shown in Figure 2 - 11, with no significant observable signal.

Triplet energy transfer was used in a final attempt to observe a potential triplet signal from **10**. Naphthalene is a commonly used triplet quencher for aromatic ketones such as benzophenone and xanthone due to its lower triplet energy.[21] 1-Naphthalenemethanol (NpOH), a water soluble analog of naphthalene, is often used In the case of studies performed in aqueous media.[27] The triplet signal of NpOH has been reported at 420 nm in water/ACN mixtures.[28] To ensure that all, if any, potential **10** triplets formed undergo energy transfer to produce the NpOH triplet, it is important to use a high concentration of the quencher (NpOH).[21] One other consideration that must be made is that when studying triplet energy transfer processes, the excitation source must be chosen such that it does not directly excite the quencher. Conveniently, my previous laser flash photolysis experiments were carried out using an Nd/YAG laser, exciting at 355 nm where NpOH does not absorb.

A solution of **10** (60 μM) and NpOH (3 mM) was prepared in 80:20 v/v PBS:ACN. Using the 355 nm excitation source as before and under the same conditions as the experiments described above produced spectra that were comparable to that shown in Figure 2 - 11, with no observable NpOH triplet signal at 420 nm. The lack of NpOH triplet suggests either that the triplet energy is lower for **10** than for NpOH (which is unlikely) or that intersystem crossing is so inefficient for **10** that the triplet is not formed. The latter

explanation would not be entirely surprising as the **10** singlet state is both reactive and fluorescent.

2.6. Photochemistry of Acetamide Derivative 11

As is observed from the UV/Vis spectrum shown in Figure 2 - 13, **11** is significantly red-shifted with respect to **XAA**. This shift is caused by the added electron rich thioether and acetamide moieties.

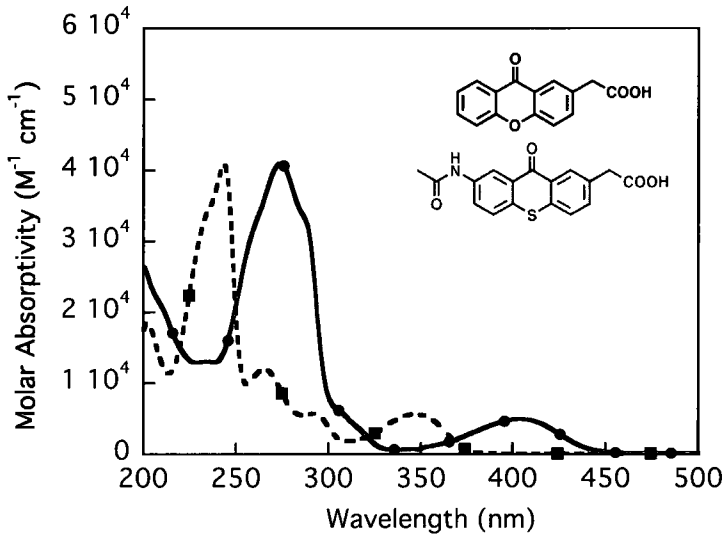

Figure 2 - 13: Molar absorptivity of 11 (blue solid) and XAA (black dashed) in 80:20 v/v PBS:ACN.

To test the photoreactivity of **11**, samples were prepared in 80:20 v/v PBS:ACN and irradiated in quartz cuvettes with 8 UVB lamps. Following acidification and extraction the samples were analyzed by HPLC-UV, HRMS, ^{1}H and ^{13}C NMR in the same manner as was done for **10**. The photochemistry proceeded cleanly, giving only the photoproduct resulting

from decarboxylation and subsequent protonation of the benzylic carbanion as shown in Scheme 2 - 8. It should be noted that extensive irradiation (48 hours under 8 UVB lamps) in basic aqueous media afforded only **19**.

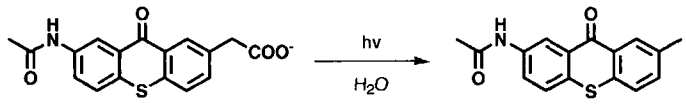

11 **19**

Scheme 2 - 8: Photodecarboxylation of 11 in basic aqueous media.

Like **10**, the photoreaction of **11** is easily monitored by UV/Vis spectroscopy, as shown in Figure 2 - 14. As was the case for **10**, the (π, π^*) band at 274 nm decreases significantly with UVB irradiation, showing a distinct change in the extinction coefficient from starting material to photoproduct. Consistent with the clean photochemistry observed, there is the appearance of clean isospestic points at 297, 380, and 419 nm.

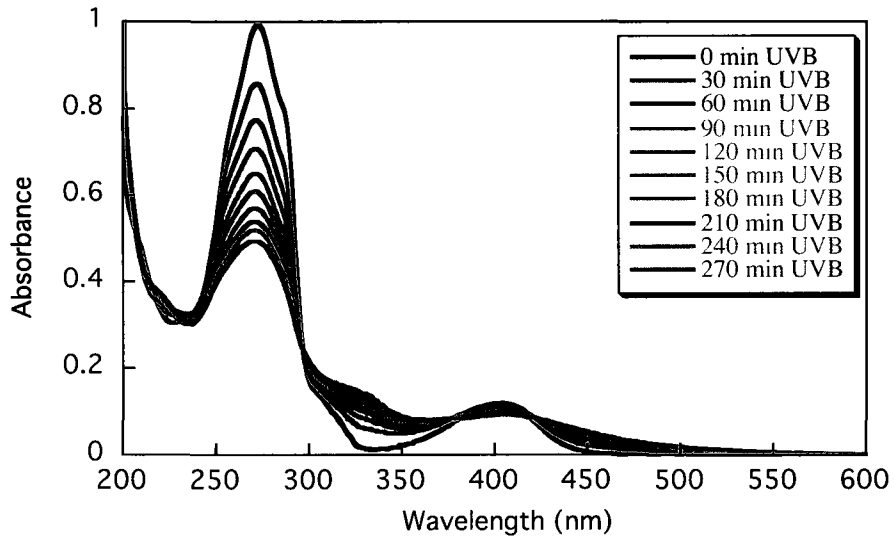

Figure 2 - 14: UV/Vis Absorbance spectra of 11 with UVB Irradiation (in 80:20 v/v PBS:ACN).

To measure the efficiency of photodecarboxylation, several solutions of **11** (0.8 mM in 50:50 v/v PBS:ACN, under air) and **Kp** (8 mM in PBS, nitrogen purged) were simultaneously irradiated with 8 UVB lamps for 5 minutes in a merry-go-round apparatus. Surprisingly, the quantum yield of decarboxylation was determined to be 4×10^{-3} in 1:1 PBS:ACN against **Kp**, significantly lower than that of **XAA** or even **10**.

Due to the results described above, there was interest in probing a potential solvent composition dependence on the photodecarboxylation of **11**. Several 0.8 mM solutions in solvent compositions ranging from 90:10 to 40:60 v/v PBS:ACN were irradiated with 8 UVB lamps simultaneously for 10 minutes in a merry-go-round apparatus. Following irradiation, each sample was diluted to match that of the HPLC eluent (20:80 v/v water:ACN) and

analyzed by HPLC-UV. The results of the experiment are summarized in Table 2 - 4, and are represented graphically in Figure 2 - 15. It should be noted here that the quantum yields marked with an 'a' superscript are estimated based on the conversion of the sample in 50:50 v/v PBS:ACN, for which the quantum yield was determined against **Kp**. Measurements in PBS and in solvents containing higher concentrations than 40:60 v/v PBS:ACN could not be obtained due to insolubility of **11**.

Solvent Composition (v/v PBS:Acetonitrile)	Conversion (%)	$\Phi_{Decarboxylation}$
90:10	1.3	3.9×10^{-4} a
80:20	2.5	7.6×10^{-4} a
70:30	4.8	1.5×10^{-3} a
60:40	7.9	2.4×10^{-3} a
50:50	11.9	3.6×10^{-3}
40:60	18.6	5.5×10^{-3} a

Table 2 - 4: 11 decarboxylation dependence on solvent composition. a) estimated quantum yields based on that measured in 50:50 v/v PBS:ACN.

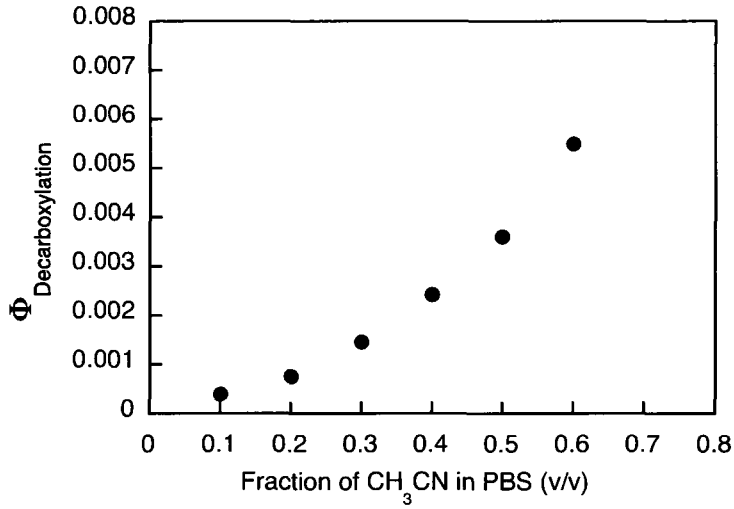

Figure 2 - 15: Photodecarboxylation quantum yield dependence of 11 on acetonitrile concentration.

The photodecarboxylation quantum yield dependence on the solvent composition for **11** follows the same trend as that measured for **10** but with overall lower efficiencies, by approximately two orders of magnitude.

To gain more insight into the deactivation pathways of **11**, fluorescence spectroscopy was used. The non-normalized excitation and emission spectra in 80:20 v/v PBS:ACN are shown in Figure 2 - 16. It should be noted that the excitation spectrum measured matches the absorbance spectrum shown in Figure 2 - 13, which indicates that the species emitting from the singlet excited state is **11**. In this solvent mixture the quantum yield of fluorescence of **11** was determined to be 0.25 as compared to quinine bisulfate (Φ_F = 0.58 in 0.1 N H_2SO_4).[20] This quantum is slightly lower than that measured for **10**, but still very high when compared to **XAA** (Φ_F = 0.0077

in PBS)[2] or thioxanthone (Φ_F = 0.006).[24] This fluorescence enhancement has been previously reported, owing to a separation of the $n\pi^*$ and $\pi\pi^*$ excited states introduced with the addition of electron donating substituents at the 2 or 7 positions of the ring.[24]

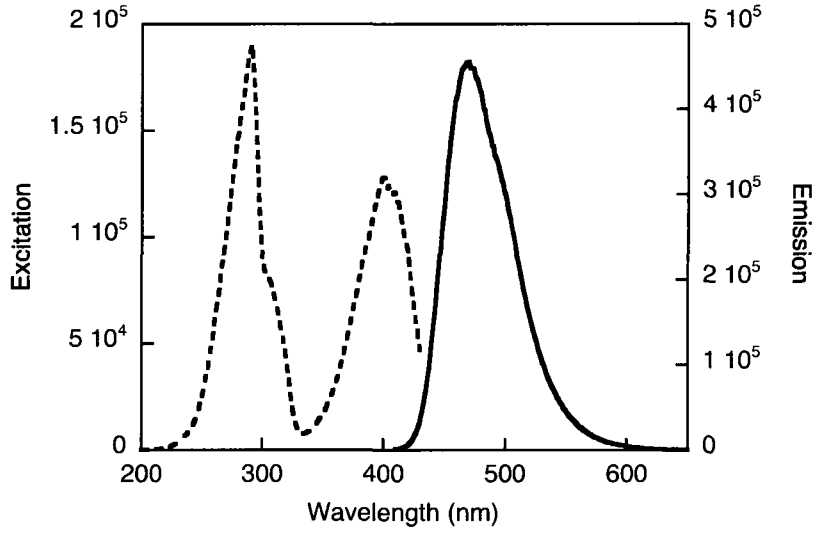

Figure 2 - 16: Fluorescence excitation (dashed) and emission (solid) spectra of 11 in 80:20 v/v PBS:ACN. Spectra are shown non-normalized. Excitation spectrum was recorded by monitoring emission at 440 nm. Emission spectrum was recorded by exciting at 400 nm.

Though the photochemistry of **11** is very interesting it was not pursued further due to its low photodecarboxylation quantum yield. To suit the current photocaging application described previously, this quantum yield needs to be significantly higher.

2.7. Summary

Given the results described above, it is clear that the nitro, amine, and acetamide substituents on the xanthone ring have a significant contribution to the photochemistry of xanthone acetic acids and thioxanthone acetic acids. Some of the photochemical properties are summarized in Table 2 - 5 for **Kp**, **XAA**, along with derivatives **8-11**.

	$\Phi_{Decarboxylation}$	$\lambda_{Absorption}$ (nm)	$\Phi_{Fluorescence}$	$\lambda_{Emission}$ (nm)
Kp	0.75	259	0	-
XAA	0.67	241, 268, 345	0.0077	410
8	0	256, 316, 384	0.03	448
9	0	261, 421	0	-
10	0.055 ± 0.02	259, 309, 360	0.37	453
11	7.6×10^{-4} ± 5×10^{-5}	274, 404	0.25	471

Table 2 - 5: Photochemical comparison of ketoprofen (Kp) in PBS, 2-xanthone acetic acid (XAA) in PBS, and new derivatives 8-11 in 80:20 v/v PBS:ACN.

It was Initially expected that the nitro derivatives would maintain efficient decarboxylation to produce the benzylic carbanion intermediate, though this intermediate may be longer-lived due to carbanion stabilization brought upon by the electron withdrawing nature of the aromatic nitro group. In nitro substituted xanthone acetic acids **6** and **7**, the electron withdrawing nature of the nitro group proved disadvantageous for a photocaging

application. The stabilization of the generated carbanion caused a lengthening of the lifetime, allowing other reactions, such as oxidation or dimerization, to occur follow following decarboxylation. To be a useful photocage for biological applications the release photochemistry needs to proceed without producing reactive byproducts,[3] thus making nitro derivatives **6** and **7** far less than ideal.

As was initially predicted, the primary amine was an efficient quencher of the photochemistry. Both **8** and **9** showed no change with extensive UVB irradiation. Likewise, both of these derivatives have zero or negligible quantum yields of fluorescence. These results are not at all surprising, as amine quenching has been frequently reported in the literature.[17] It is clear from these studies that amine derivatives **8** and **9** are not useful from a biological standpoint as they are photoinert, thus do not provide the desired carbanion chemistry needed to undergo photorelease.

Although the amino derivatives suffer from quenching, transformation into an amide through coupling restores some of the desired photochemistry found in **XAA**. Acetamide derivative **10** behaves similarly to **XAA** in that it undergoes clean decarboxylation following UVB irradiation, yielding only the protonated product, but a key difference arises in the effect of solvent composition on its photochemistry. As discussed previously, acetamide derivatives **10** and **11** show strong photodecarboxylation dependence on the acetonitrile proportion in the solvent system.

Of the acetamide derivatives, **10** showed greater promise than **11** in terms of photodecarboxylation quantum yield. From the perspective of

photocaging for biological applications **11** is simply too inefficient (Φ_D = 7.6 x 10^{-4} in 80:20 v/v PBS:ACN). **10**, on the other hand, photodecarboxylates with significantly higher quantum yield (Φ_D = 0.055 in 80:20 v/v PBS:ACN).

This investigation into the substituent effect on the photochemistry of xanthone acetic acid decarboxylation verified the hypothesis that the same clean photochemistry occurs with the acetamide linker in place. Though the photodecarboxylation quantum yield is lower in **10**, owing to a higher fluorescence quantum yield, it is still within a reasonable range to be potentially useful as a photocage for biological applications.

2.8. Experimental Details

All chemicals and solvents were purchased from Aldrich unless otherwise specified. Water was purified through a Millipore MilliQ system. 2-Fluoro-5-nitrobenzoic acid was purchased from Oakwood Laboratories and used without prior purification. ^{1}H and ^{13}C NMR spectra were recorded on a Bruker-Avance-400 at 400 and 100 MHz, respectively. All NMR shifts are reported relative to internal TMS. HR-MS (EI) spectra were recorded on a Kratos Concept 1S. All column chromatography used Merck silica gel 230-400 mesh.

2.8.1. Synthetic Procedures

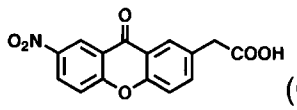

(6)

(7-nitro-9-oxo-9H-xanthen-2-yl)acetic acid

To a clean, flame dried, 2-neck 100 mL round bottom flask was added 1.92 g of crushed potassium hydride (KOH) and 50 mL dimethyl sulfoxide (DMSO). The solution was purged with nitrogen gas for ~20 minutes. To this solution was added 1.00 g (5.4 mmol) of 2-fluoro-5-nitrobenzoic acid and 0.82 g (5.5 mmol) 4-hydroxylphenylacetic acid. The solution was allowed to stir for 4 hours under nitrogen. Following this, the mixture was acidified with 10% HCl and extracted with 200 mL ethyl acetate, washing thoroughly with 1% HCl to

remove the remaining DMSO. The organics were dried over $MgSO_4$, filtered, and the solvent was removed by rotary evaporation yielding an orange-brown solid. The solid was then dissolved in 20 mL concentrated sulfuric acid and fit with a reflux condenser. The mixture was heated to 85°C in a controlled temperature oil bath and stirred for 2 hours. The mixture was then cooled to room temperature. Once at room temperature, the mixture was poured over ice, and the round bottom flask was rinsed with cold water. The solid product, **6**, (1.47 g, 4.9 mmol, 91%) was then collected by suction filtration and purified by recrystallization from boiling ethanol. R_f = 0.66 in 1:1:0.02 v/v/v DCM:diethyl ether:acetic acid. ^{1}H NMR (400 MHz, DMSO-d_6) δ 8.86 (d, 1H, J = 2.8 Hz), 8.62 (dd, 1H, J_1 = 2.8 Hz, J_2 = 9.4 Hz), 8.11 (d, 1H, J = 2.1 Hz), 7.90 (d, 1H, J = 9.2 Hz), 7.84 (dd, 1H, J_1 = 2.5 Hz, J_2 = 8.6 Hz) 7.69 (d, 1H, J = 8.6 Hz), 3.81 (s, 2H). ^{13}C NMR (100 MHz, DMSO-d_6) δ 175.1, 172.3, 158.7, 154.2, 143.3, 137.8, 132.6, 129.3, 126.3, 122.0, 120.9, 120.3, 118.2, 39.5 (CH_2 is under DMSO peak). HRMS (EI): Exact mass calculated for $C_{15}H_9NO_6[M]^+$: 299.0430. Found: 299.04135.

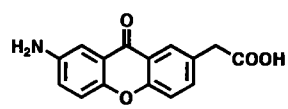

(**8**)

(7-amino-9-oxo-9H-xanthen-2-yl)acetic acid

In a clean dry 500 mL round bottom flask, **6** (0.38 g, 1.5 mmol) was dissolved in 200 mL ethyl acetate. 10% Pd/C (0.10 g, catalytic) was added and the solution was nitrogen purged while stirring for 15 minutes. Using hydrogen filled balloons, the solution was then purged for 20 minutes and left stirring

under hydrogen atmosphere. After 2 hours of stirring, celite was added to aid filtration of the Pd/C. After suction filtration, the organic solution was dried over $MgSO_4$ and the solvent was removed by rotary evaporation, yielding a yellow solid. Recrystallization from boiling ethanol gave pure yellow solid **8** (0.04 g, 0.15 mmol, 10%). R_f = 0.27 in 1:1:0.02 v/v/v DCM:diethyl ether:acetic acid. ^{1}H NMR (400 MHz, DMSO-d_6) δ 8.04 (d, 1H, J = 2.1 Hz), 7.70 (dd, 1H, J_1 = 2.5 Hz, J_2 = 8.8 Hz), 7.55 (d, 1H, J = 8.6 Hz), 7.41 (d, 1H, J = 8.9 Hz), 7.27 (d, 1H, J = 2.8 Hz), 7.13 (dd, 1H, J_1 = 3.0 Hz, J_2 = 8.8 Hz), 5.44 (s, 2H), 3.73 (s, 2H). ^{13}C NMR (100 MHZ, DMSO-d_6) δ 176.4, 173.1, 154.9, 148.2, 146.2, 136.8, 131.2, 126.6, 123.8, 122.1, 120.6, 119.1, 118.4, 106.6, 39.5 (CH_2 is under DMSO peak). HRMS (EI): Exact mass calculated for $C_{15}H_{11}NO_4[M]^+$: 269.0688. Found: 269.0694.

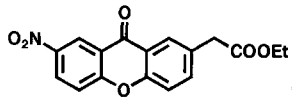

(12)

ethyl (7-nitro-9-oxo-9H-xanthen-2-yl)acetate

To a solution of 99% ethanol (200 mL) and concentrated sulphuric acid (2 mL) in a 300 mL round bottom flask was added **6** (1.74 g, 5.8 mmol). The solution was refluxed for 2 hours and cooled to room temperature. The solution was then cooled in an ice-water bath, causing the product to crash out. Suction filtration followed by cold ethanol washes, to remove any residual H_2SO_4, afforded the fluffy pale yellow solid **12** (1.43 g, 4.4 mmol, 75%). R_f = 0.71 in 1:1 v/v EtOAc:hexanes. ^{1}H NMR (400 MHz, DMSO d_6) δ 8.86 (d, 1H, J = 2.8 Hz), 8.63 (dd, 1H, J_1 = 2.8 Hz, J_2 = 9.4 Hz), 8.12 (d, 1H, J

= 2.0 Hz), 7.90 (d, 1H, J = 9.3 Hz), 7.84 (dd, 1H, J_1 = 2.2 Hz, J_2 = 8.6 Hz) 7.71 (d, 1H, J = 8.6 Hz), 4.12 (q, 2H, J = 7.1 Hz), 3.91 (s, 2H), 1.21 (t, 3H, J = 7.1 Hz). ^{13}C NMR (100 MHZ, DMSO d_6) δ 175.1, 170.8, 158.8, 154.4, 143.3, 137.7, 131.9, 129.4, 126.4, 122.0, 120.9, 120.4, 120.3, 118.4, 60.4, 39.5 (CH_2 is under DMSO peak), 14.0. HRMS (EI): Exact mass calculated for $C_{17}H_{13}NO_6[M]^+$: 327.0743. Found: 327.07249.

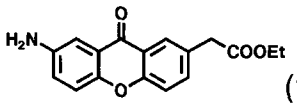

(**14**)

ethyl (7-amino-9-oxo-9H-xanthen-2-yl)acetate

In a clean dry 500 mL round bottom flask, **12** (0.50 g, 1.5 mmol) was dissolved in 300 mL ethyl acetate. 10% Pd/C (0.10 g, catalytic) was added and the solution was nitrogen purged while stirring for 15 minutes. Using hydrogen filled balloons, the solution was then purged for 20 minutes and left stirring under hydrogen atmosphere. After 2 hours of stirring, celite was added to aid filtration of the Pd/C, after suction filtration, the organic solution was dried over $MgSO_4$ and the solvent was removed by rotary evaporation, yielding a yellow solid (**14**) (0.44 g, 99%). R_f = 0.38 in 1:1 v/v EtOAc:hexanes. ^{1}H NMR (400 MHz, DMSO d_6) δ 8.06 (d, 1H, J = 2.1 Hz), 7.70 (dd, 1H, J_1 = 2.5 Hz, J_2 = 8.8 Hz), 7.56 (d, 1H, J = 8.6 Hz), 7.41 (d, 1H, J = 8.9 Hz), 7.27 (d, 1H, J = 2.8 Hz), 7.15 (dd, 1H, J_1 = 3.0 Hz, J_2 = 8.8 Hz), 5.45 (s, 2H), 4.06 (q, 2H, J = 7.1 Hz), 3.84 (s, 2H), 1.20 (t, 3H, J = 7.1 Hz). ^{13}C NMR (100 MHZ, DMSO d_6) δ 175.8, 171.0, 154.4, 147.6, 145.6, 136.0, 129.8, 126.2, 123.3, 121.6, 120.1, 118.5, 118.0, 105.9, 60.4, 39.5 (CH_2 is under DMSO peak),

14.0. HRMS (EI): Exact mass calculated for $C_{17}H_{15}NO_4[M]^+$: 297.1001. Found: 297.09863.

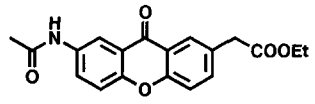

(**16**)

ethyl [7-(acetylamino)-9-oxo-9H-xanthen-2-yl]acetate

To a flame-dried 300 mL round-bottomed flask was added **14** (0.50 g, 1.7 mmol) and dissolved in extra dry dichloromethane (100 mL). To this mixture was added excess acetic anhydride (1.8 mL, 19 mmol) and excess pyridine (1.6 mL, 20 mmol). This reaction mixture was stirred under nitrogen for 2.5 hrs. This was then transferred into a separatory funnel and washed with 3 x 100 mL 1% HCl. The organics were then dried on $MgSO_4$, filtered, and the solvent was removed by rotary evaporation, yielding a pale yellow solid. The product was then recrystallized from boiling ethanol, giving the pure product (**16**) (0.43 g, 75%). R_f = 0.27 in 1:1 v/v EtOAc:hexanes. ^1H NMR (400 MHz, DMSO d_6) δ 10.3 (s, 1H), 8.49 (s, 1H), 8.10 (d, 1H, J = 2.2 Hz), 8.00 (dd, 1H, J_1 = 3.0 Hz, J_2 = 9.4 Hz), 7.78 (dd, 1H, J_1 = 2.5 Hz, J_2 = 8.6 Hz), 7.64 (2 ds, 2H, J = 9.4 Hz, 8.6 Hz), 4.11 (q, 2H, J = 7.2 Hz), 3.87 (s, 2H), 2.10 (s, 3H), 1.20 (t, 3H, J = 6.9 Hz). ^{13}C NMR (100 MHZ, DMSO d_6) δ 175.7, 170.9, 168.4, 154.4, 151.3, 136.6, 135.6, 130.5, 126.9, 126.2, 120.9, 120.3, 118.5, 118.0, 114.1, 60.3, 39.5 (CH_2 is under DMSO peak), 23.9, 14.0. HRMS (EI): Exact mass calculated for $C_{19}H_{17}NO_5[M]^+$: 339.1107. Found: 339.1116.

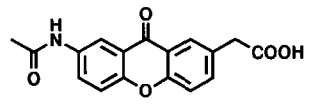

(**10**)

ethyl [7-(acetylamino)-9-oxo-9H-xanthen-2-yl]acetic acid

To a 1:1 (v/v) solution of 0.1 M sodium hydroxide and acetonitrile (200 mL) in a 250 mL round bottom flask was added **16** (0.43 g, 1.3 mmol) and stirred under air for 18 hrs. The mixture was then acidified using 10% HCl, producing a precipitate. The resulting solid was suction filtered, washing with 1% HCl, water, and ethyl acetate, giving the product **10** (0.38 g, 96%). R_f = 0.03 in 1:1 v/v EtOAc:hexanes. ^{1}H NMR (400 MHz, DMSO d_6) δ 12.5 (s broad, COOH), 10.3 (s, 1H), 8.49 (d, 1H, J = 2.8 Hz), 8.09 (d, 1H, J = 2.5 Hz), 8.00 (dd, 1H, J_1 = 2.8 Hz, J_2 = 9.4 Hz), 7.76 (dd, 1H, J_1 = 2.8 Hz, J_2 = 8.6 Hz), 7.65 (d, 1H, J = 8.8 Hz), 7.61 (d, 1H, J = 8.6 Hz), 3.78 (s, 2H), 2.10 (s, 3H). ^{13}C NMR (100 MHZ, DMSO d6) δ 175.8, 172.4, 168.4, 154.4, 151.3, 136.8, 135.7, 131.2, 126.9, 120.9, 120.3, 118.6, 117.9, 114.2, 39.5 (CH_2 is under DMSO peak), 23.9. HRMS (EI): Exact mass calculated for $C_{17}H_{13}NO_5[M]^+$: 311.0794. Found: 311.07908.

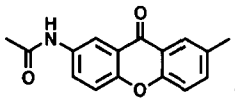

(**18**)

N-(7-methyl-9-oxo-9H-xanthen-2-yl)acetamide

10 (30 mg) was dissolved in 25 mL of 80:20 v/v PBS:ACN in a 50 mL Pyrex round bottomed flask. The sample was then irradiated with 6 UVB lamps (3 per side) in a Luzchem photoreactor for 3 hours. Following irradiation, the pale yellow solid precipitate (**18**) was removed by suction filtration. ^{1}H NMR

(400 MHz, DMSO d_6) δ 10.29 (s, 1H), 8.47 (d, 1H, J = 2.8 Hz), 7.97 (d, 2H, J = 2.5 Hz), 7.68 (d, 1H, J = 2.8 Hz), 7.63 (d, 1H, J = 8.8 Hz), 7.54 (d, 1H, J = 8.6 Hz), 2.44 (s, 3H), 2.10 (s, 3H). ^{13}C NMR (100 MHZ, DMSO d_6) δ 176.3, 169.0, 154.2, 151.9, 137.0, 136.1, 134.1, 127.4, 125.6, 121.5, 120.8, 119.1, 118.4, 114.7, 24.4, 20.8. HRMS (EI): Exact mass calculated for $C_{16}H_{13}NO_3[M]^+$: 267.0895. Found: 267.08925.

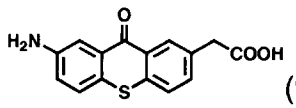

(9)

(7-amino-9-oxo-9H-thioxanthen-2-yl)acetic acid

In a clean dry 500 mL round bottom flask, **7** (0.10 g, 0.30 mmol) was dissolved in 400 mL ethyl acetate. 10% Pd/C (0.03 g) was added and the solution was nitrogen purged while stirring for 25 minutes. Using hydrogen filled balloons, the solution was then purged for 20 minutes and left stirring under hydrogen atmosphere. After 2 hours of stirring, celite was added to aid filtration of the Pd/C, after suction filtration, the solvent was removed by rotary evaporation. Following recrystallization from boiling ethanol, the pure solid yellow product **9** was obtained (0.070 g, 0.25 mmol, 82%). R_f = 0.26 in 1:1:0.02 v/v/v DCM:diethyl ether:acetic acid. ^1H NMR (400 MHz, DMSO d_6) δ 8.33 (d, 1H, J = 2.0 Hz), 7.71 (d, 1H, J = 8.2 Hz), 7.66 (d, 1H, J = 2.6 Hz), 7.61 (dd, 1H, J_1 = 2.0 Hz, J_2 = 8.3 Hz), 7.50 (d, 1H, J = 8.7 Hz), 7.08 (dd, 1H, J_1 = 2.6 Hz, J_2 = 8.7 Hz), 5.66 (s, 2H), 3.73 (s, 2H). ^{13}C NMR (100 MHZ, DMSO d_6) δ 178.6, 172.5, 148.1, 135.4, 133.7, 133.1, 129.6, 127.7, 126.4,

122.0, 121.2, 110.9, 39.5 (CH_2 is under DMSO). HRMS (EI): Exact mass calculated for $C_{15}H_{11}NO_3S[M]^+$: 285.0460. Found: 285.04387.

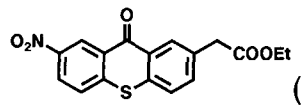

(13)

ethyl (7-nitro-9-oxo-9H-thioxanthen-2-yl)acetate

To a solution of 95% ethanol (200 mL) and concentrated sulphuric acid (2 mL) in a 250 mL round bottom flask was added **7** (0.30 g, 0.95 mmol). The solution was refluxed for 2 hours then cooled to room temperature. The volume was reduced to ~50 mL by rotary evaporation then was cooled in an ice water bath, causing the yellow solid crash out. The solid was removed by suction filtration, followed by washing with cold ethanol, giving **13** as a yellow solid (0.28 g, 0.82 mmol, 86%). R_f = 0.70 in 1:1 v/v EtOAc:hexanes. ^{1}H NMR (400 MHz, DMSO d_6) δ 9.08 (d, 1H, J = 2.3 Hz), 8.48 (dd, 1H, J_1 = 2.6 Hz, J_2 = 8.9 Hz), 8.39 (d, 1H, J = 1.6 Hz), 8.13 (d, 1H, J = 8.7 Hz), 7.88 (d, 1H, J = 8.3 Hz), 7.75 (dd, 1H, J_1 = 2.0 Hz, J_2 = 8.3 Hz), 4.12 (q, 2H, J = 7.1 Hz), 3.91 (s, 2H), 1.21 (t, 3H, J = 7.1 Hz). ^{13}C NMR (100 MHZ, DMSO d_6) δ 177.8, 170.8, 145.6, 143.8, 135.1, 134.5, 134.1, 129.8, 128.6, 128.4, 127.5, 126.9, 126.1, 123.9, 60.5, 39.5 (CH_2 is under DMSO), 14.0. HRMS (EI): Exact mass calculated for $C_{17}H_{13}NO_5S[M]^+$: 343.0514. Found: 343.05004.

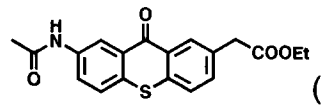

(**17**)

ethyl [7-(acetylamino)-9-oxo-9H-thioxanthen-2-yl]acetate

In a clean dry 250 mL round bottom flask, **13** (0.28 g, 0.82 mmol) was dissolved in 200 mL ethyl acetate. 10% Pd/C (0.08 g) was added and the solution was nitrogen purged while stirring for 25 minutes. Using hydrogen filled balloons, the solution was then purged for 20 minutes and left stirring under hydrogen atmosphere. After 3 hours of stirring the Pd/C catalyst was filtered using suction filtration, using celite to aid the filtration. Following filtration the solvent was removed by rotary evaporation, yielding a yellow solid. The solid was then directly added to a flame-dried 250 mL round-bottomed flask and dissolved in anhydrous dichloromethane (150 mL). To this mixture was added acetic anhydride (1.0 mL, 11 mmol, excess) and anhydrous pyridine (0.90 mL, 11 mmol, excess). The reaction mixture was stirred under nitrogen for 3.5 hrs. The contents of the flask were then transferred into a separatory funnel and extracted with dichloromethane, washing with 3 x 50 mL 1% HCl. The organics were then dried on $MgSO_4$, filtered, and the solvent was removed by rotary evaporation. Normal phase column chromatography using 1:1 v/v ethyl acetate:hexanes as the eluent yielded the pure yellow solid **17** (0.09 g, 0.25 mmol, 30% isolated yield). R_f = 0.26 in 1:1 v/v EtOAc:hexanes. ^{1}H NMR (400 MHz, DMSO-d_6) δ 10.36 (s, 1H), 8.71 (d, 1H, J = 2.4 Hz), 8.38 (d, 1H, J = 1.8 Hz), 8.03 (dd, 1H, J_1 = 2.4 Hz, J_2 = 9.1 Hz), 7.80 (m, 2H), 7.67 (dd, 1H, J_1 = 2.1 Hz, J_2 = 8.3 Hz), 4.01 (q, 2H, J = 7.1 Hz), 3.88 (s, 2H), 2.10 (s, 3H), 1.20 (t, 3H, J = 7.1 Hz). ^{13}C

NMR (100 MHZ, DMSO-d_6) δ 178.5, 170.9, 168.7, 138.2, 135.1, 134.2, 133.2, 130.2, 129.7, 128.7, 127.8, 127.0, 126.6, 124.4, 117.8, 60.4, 39.5 (CH_2 under DMSO), 24.0, 14.1. HRMS (EI): Exact mass calculated for $C_{19}H_{17}NO_4S[M]^+$: 355.0878. Found: 355.08825.

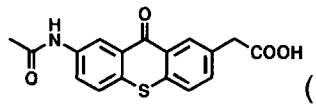

(**11**)

[7-(acetylamino)-9-oxo-9H-thioxanthen-2-yl]acetic acid

To a 1:1 (v/v) solution of 0.1 M sodium hydroxide and ACN (40 mL) in a 50 mL Erlenmeyer flask was added **17** (0.090 g, 0.25 mmol) and stirred under air for 18 hrs. The mixture was then acidified using 10% HCl, producing a precipitate. Suction filtration followed by recrystallization from boiling ethanol yielded the pure yellow solid **11** (0.040 g, 0.13 mmol, 51%). R_f = 0.03 in 1:1 v/v EtOAc:hexanes. ^{1}H NMR (400 MHz, DMSO-d_6) δ 10.35 (s, 1H), 8.71 (d, 1H, J = 2.3 Hz), 8.37 (d, 1H, J = 1.5 Hz), 8.04 (dd, 1H, J_1 = 2.3 Hz, J_2 = 8.7 Hz), 7.80 (d, 2H, J = 9.0 Hz), 7.67 (dd, 1H, J_1 = 1.6 Hz, J_2 = 8.4 Hz), 3.78 (s, 2H), 2.10 (s, 3H). ^{13}C NMR (100 MHZ, DMSO-d_6) δ 178.6, 172.4, 168.8, 138.2, 134.9, 134.4, 130.3, 129.7, 128.8, 127.8, 127.2, 126.5, 126.4, 124.6, 117.9, 39.5 (CH_2 under DMSO), 24.0. HRMS (EI): Exact mass calculated for $C_{17}H_{13}NO_4S[M]^+$: 327.0565. Found: 327.05726.

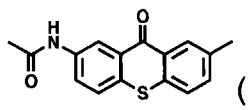
(**19**)

N-(7-methyl-9-oxo-9H-thioxanthen-2-yl)acetamide

To 10 mL of 1:1 v/v 0.1 M NaOH:ACN was added 20 mg of **11** and placed into quartz test tubes. The samples were irradiated with 8 UVB lamps (4 per side) under air for 48 hours in a merry-go-round apparatus. Following irradiation, the samples were acidified with 10% HCl and extracted with 3 x 20 mL EtOAc. The combined organics were then washed with 3 x 20 mL 1% HCl, dried with $MgSO_4$, filtered, and the solvent was removed by rotary evaporation, giving a yellow solid mixture of starting material (**11**) and photoproduct (**19**). ^{1}H NMR (400 MHz, DMSO-d_6) δ 10.66 (s, 1H), 8.49 (d, 1H, J = 2.0 Hz), 8.29 (d, 1H, J = 1.7 Hz), 8.18 (d, 1H, J = 2.0 Hz), 8.02 (dd, 1H, J_1 = 2.6 Hz, J_2 = 8.9 Hz), 7.80 (d, 1H, J = 9.1 Hz), 7.61 (dd, 1H, J_1 = 2.0 Hz, J_2 = 8.6 Hz), 2.46 (s, 3H), 2.14 (s, 3H). ^{13}C NMR (100 MHZ, DMSO-d_6) δ 167.0, 163.3, 144.4, 137.7, 135.8, 134.1, 131.5, 131.1, 128.7, 128.6, 126.4, 124.5, 123.3, 117.6, 29.0, 22.3. HRMS (EI): Exact mass calculated for $C_{16}H_{13}NO_2S[M]^+$: 283.0667. Found: 283.06701.

2.8.2. Photodecarboxylation Quantum Yield

For quantum yield measurements, 3 mM solutions of one of **10** or **11** in 0.1 M phosphate buffer (PBS) adjusted to pH 7.4 was irradiated under 8 UVB lamps in a Luzchem photoreactor simultaneously with solutions of **Kp**.

All solutions absorbed greater than 3 in the excitation region, ensuring that essentially all photons were absorbed. Following irradiation, all samples were diluted with acetonitrile (ACN) to match the HPLC eluent (80:20 v/v water:ACN). Comparing peak areas recorded by HPLC-UV at an isospestic points for each sample gave the percent photoconversion, which was used to calculate the number of moles converted. Using Equation 1, the quantum yield of decarboxylation was calculated. Φ_X and Φ_{ST} are the quantum yields of conversion, respectively. X_X and X_{ST} are the number of moles converted of the sample and the actinometer. Errors are reported as one standard deviation.

$$\Phi_X = \Phi_{ST}\left(\frac{X_X}{X_{ST}}\right)$$

Equation 1

2.8.2. Fluorescence

All spectra were recorded on a luminescence spectrometer from Photon Technology International. All samples were measured under air, and adjusted such that absorbance was 0.1 or less at the excitation wavelength of 350 nm. All spectrometer slits were opened to 2 nm.

Quantum yields of fluorescence were determined by comparison to an actinometer, quinine bisulfate (Φ_F = 0.58 in 0.05 M H_2SO_4).[20] By comparison

of the slopes obtained by plotting emission peak area versus absorbance for 5 samples of each according to Equation 2, the fluorescent quantum yields can be obtained. In Equation 2, the symbols Φ_X and Φ_{ST} represent the quantum yields of fluorescence of the sample and the actinometer, respectively. $Slope_X$ and $Slope_{ST}$ are the slopes of peak area vs absorption at the excitation wavelength for the sample and the actinometer, respectively. It should be noted here that an additional correction must be made when the actinometer and sample are measured in solvents with different refractive indices.

$$\Phi_X = \Phi_{ST}\left(\frac{Slope_X}{Slope_{ST}}\right)$$

Equation 2

2.8.2. Nanosecond Laser Flash Photolysis

The laser flash setup used in all experiments is a custom system using Luzchem software. Kinetics and spectra were recorded using the third harmonic of an Nd/YAG laser, generating pulses at 355 nm of 8 ns in duration and at an average power of 10 mJ/shot. All experiments were done under nitrogen atmosphere unless otherwise specified. Experiments were performed in 7 x 7 mm^2 quartz cuvettes in static or flowed cells. When using flow cells, nitrogen was bubbling through the system at a high rate, and the sample was flowing at an approximate rate of 1 drop/s.

2.9. References

1. Martinez, L. J.; Scaiano, J. C., Transient Intermediates in the Laser Flash Photolysis of Ketoprofen in Aqueous Solutions: Unusual Photochemistry for the Benzophenone Chromophore. *J. Am. Chem. Soc.* **1997,** *119* (45), 11066-11070.

2. Blake, J. A.; Gagnon, E.; Lukeman, M.; Scaiano, J. C., Photodecarboxylation of Xanthone Acetic Acids: C-C Bond Heterolysis from the Singlet Excited State. *Org. Lett.* **2006,** *8*, 1057-1060.

3. Pelliccioli, A. P.; Wirz, J., Photoremovable Protecting Groups: Reaction Mechanisms and Applications. *Photochem. Photobiol. Sci* **2002,** *1*, 441-458.

4. Majjigapu, J. R. R.; Kurchan, A. N.; Kottani, R.; Gustafson, T. P.; Kutateladze, A. G., Release and Report: A New Photolabile Caging System with a Two-Photon Fluorescence Reporting Function. *J. Am. Chem. Soc.* **2005,** *127*, 12458-12459.

5. Dalton, J. C.; Montgomery, F. C., Solvent Effects on Thioxanthone Fluorescence. *J. Am. Chem. Soc.* **1974,** *96*, 6230-6232.

6. Blake, J. A. Ph.D. Thesis. University of Ottawa, Ottawa, 2010.

7. Rewcastle, G. W.; Atwell, G. J.; Baguley, B. C.; Calveley, S. B.; Denny, W. A., Potential Antitumor Agents. 58. Synthesis and Structure-Activity Relationships of Substituted Xanthenone-4-Acetic Acids Active Against the Colon 38 Tumor in Vivo. *J. Med. Chem.* **1989,** *32*, 793-799.

8. Goldberg, A. A.; Walker, H. A., Synthesis of Diaminoxanthones. *J. Chem. Soc.* **1953**, 1348-1357.

9. Pace, T. C. S.; Monahan, S. L.; MacRae, A. I.; Kaila, M.; Bohne, C., Photophysics of Aminoxanthone Derivatives and Their Application as Binding Probes for DNA. *Photochem. Photobiol.* **2006,** *82*, 78-87.

10. Rarick, M. J.; Brewster, R. Q.; Dains, F. B., The Formation of Aromatic Ethers from p-Nitrofluorobenzene. *J. Am. Chem. Soc.* **1933,** *55*, 1289-1290.

11. Mann, F. G.; Turnbull, J. H., Xanthones and Thioxanthones. Part I. The Synthesis of 2- and 3-Dialkylaminoalkylamino-derivatives. *J. Chem. Soc.* **1951**, 747-756.

12. Carey, F. A., Preparation of Amines by Reduction. In *Organic Chemistry*, Fifth ed.; McGraw-Hill: New York, 2003; pp 931-932.

13. Clayden, J.; Greeves, N.; Warren, S.; Wothers, P., *Organic Chemistry*. Oxford: New York, 2001.

14. Carey, F. A., Reactions of Carboxylic Acid Anhydrides. In *Organic Chemistry*, Fifth ed.; McGraw-Hill: New York, 2003; pp 842-843.

15. Carey, F. A., Ester Hydrolysis in Base. In *Organic Chemistry*, Fifth ed.; McGraw-Hill: New York, 2003; pp 852-853.

16. Margerum, J. D.; Petrusis, C. T., Photodecarboxylation of Nitrophenylacetate Ions. *J. Am. Chem. Soc.* **1969,** *91*, 2467-2472.

17. Cohen, S. G.; Parola, A.; Parsons, G. H. J., Photoreduction of Amines. *Chem. Rev.* **1973,** *73*, 141-161.

18. Santhanam, M.; Ramakrishnan, V., Photochemical Study of Energy Transfer from Benzophenone Triplet to Aniline. *Chem. Comm.* **1970**, 344-345.

19. Van, S.-P.; Hammond, G. S., Amine Quenching of Aromatic Fluorescence and Fluorescent Exciplexes. *J. Am. Chem. Soc.* **1978,** *100*, 3895-3902.

20. Lakowicz, J. R., In *Principles of Fluorescence Spectroscopy*, Second ed.; Kluwer Academic/Plenum: New York, 1999; p 698.

21. Turro, N. J.; Ramamurthy, V.; Scaiano, J. C., *Modern Molecular Photochemistry of Organic Molecules*. University Science Books: Sausalito, California, 2010.

22. Costanzo, L. L.; Guidi, G. D.; Condorelli, G.; Cambria, A.; Fama, M., Molecular Mechanism of Drug Photosensitization-II. Photohemolysis Sensitized by Ketoprofen. *Photochem. Photobiol.* **1989,** *50*, 359-365.

23. Burns, M. D.; Lukeman, M., Efficient Photodecarboxylation of Trifluoromethyl-Substituted Phenylacetic and Mandelic Acids. *Photochem. Photobiol.* **2010**. DOI: 10.1111/j.1751-1097.2010.00737.x

24. Neumann, M. G.; Gehlen, M. H.; Encinas, M. V.; Allen, N. S.; Corrales, T.; Peinado, C.; Catalina, F., Photophysics and Photoreactivity of Substituted Thioxanthones. *J. Chem. Soc., Faraday Trans.* **1997,** *93*, 1517-1521.

25. Garner, A.; Wilkinson, F., Laser Photolysis Studies of the Triplet State of Xanthone and its Ketyl Radical in Fluid Solution. *J. Chem. Soc., Faraday Trans. 2* **1976,** *72*, 1010-1020.

26. Scaiano, J. C., Solvent Effects in the Photochemistry of Xanthone. *J. Am. Chem. Soc.* **1980,** *102* (26), 7747-7753.

27. Shizuka, H., Photophysics and Photochemistry of Triplet Exciplexes Between Triplet Naphthalene Derivatives and Benzophenone. *Pure & Appl. Chem.* **1997,** *69* (4), 825-830.

28. Yamaji, M.; Tanaka, T.; Shizuka, H., Solvent Dependence of Triplet Energy Transfer Reaction Competing with Hydrogen Atom Abstraction Between Triplet Benzophenone and 1-Naphthol Studied by Laser Flash Photolysis. *Chem. Phys. Lett* **1993,** *202*, 191-195.

3. Toward Photorelease from Surface Tethered Xanthonate Photocages

3.1. Introduction 81
3.2. Release from Acetamide Functionalized Xanthonate Photocages 82
3.2.1. Synthesis of 20 83
3.2.2. Photochemistry of 20 86
3.2.3. Synthesis of 21 88
3.2.4. Photochemistry of 21 90
3.3. Toward Tethered Photorelease 92
3.3.1. Attempted Coupling *via* Amine Linker 92
3.3.2. A New Direction for Polymer Tethering 93
3.4. Summary 97
3.5. Experimental Details 98
3.4.1. Synthetic Procedures 98
3.5. References 113

3.1. Introduction

After having demonstrated that **10** undergoes clean photodecarboxylation upon UV irradiation, the capability of the acetamide functionalized xanthonate photocages to release biologically relevant molecules will be tested. To do this, photocages will be synthesized with leaving groups attached β to the carboxylic acid group. Following synthesis their basic photochemistry will be assessed with respect to their ability to release leaving groups. Once the capability of photorelease is confirmed, polymer tethering through amide coupling chemistry will be attempted through the amine linker.

This chapter describes the progress made toward polymer-tethered photorelease from xanthonate photocages. Firstly, the synthesis and photochemistry of acetamide functionalized xanthonate photocages will be studied. Next, attempts made at coupling to carboxylic acid terminated polymers through the amine will be described, followed by the proposal of a new alternative route to polymer tethering through a short chain linker.

3.2. Release from Acetamide Functionalized Xanthonate Photocages

Prior to integration of xanthonate photocages into polymers *via* amide coupling, it was important to assess the photochemical behavior of the acetamide derivatives equipped with relatively simple leaving groups, chosen as representative models for more complex systems. Using **12**, the synthesis of which has been described earlier (Section 2.2.3.), as a starting precursor, acetamide xanthonate photocages equipped with a variety of leaving groups can be prepared with relative ease. This section describes the synthesis and basic photochemistry of acetamide functionalized xanthonate photocages containing acetate and phenylalanine leaving groups (**20** and **21**, respectively).

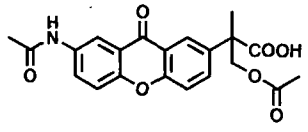

20

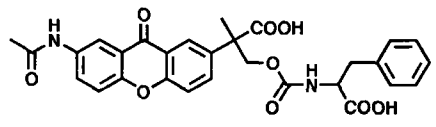

21

The model leaving groups were chosen to demonstrate the versatility of acetamide functionalized xanthonate photocages. Acetate was chosen to represent direct photorelease of a carboxylate *via* elimination of the carbanion. The phenylalanine leaving group, on the other hand, was chosen as a representative example for release of an amino acid from the amine

through a carbamate linkage *via* elimination of the leaving group followed by thermal elimination of a second molecule of carbon dioxide.

3.2.1. Synthesis of 20

The synthesis of **20** was carried out starting with **12**. Firstly, the benzyl position was methylated using lithium diisopropylamine (LDA) and iodomethane in dry tetrahydrofuran (THF) at -78°C in a dry ice/acetone bath (Scheme 3 - 1, i). The product was isolated by organic extraction followed by column chromatography. The product, **22**, was easily characterized using ^{1}H NMR in DMSO-d_6 by the loss of the methylene singlet at 3.91 ppm, along with the appearance of the methyl doublet at 1.47 ppm and methine quartet at 4.09 ppm. The product was further verified by ^{13}C NMR and HR-MS.

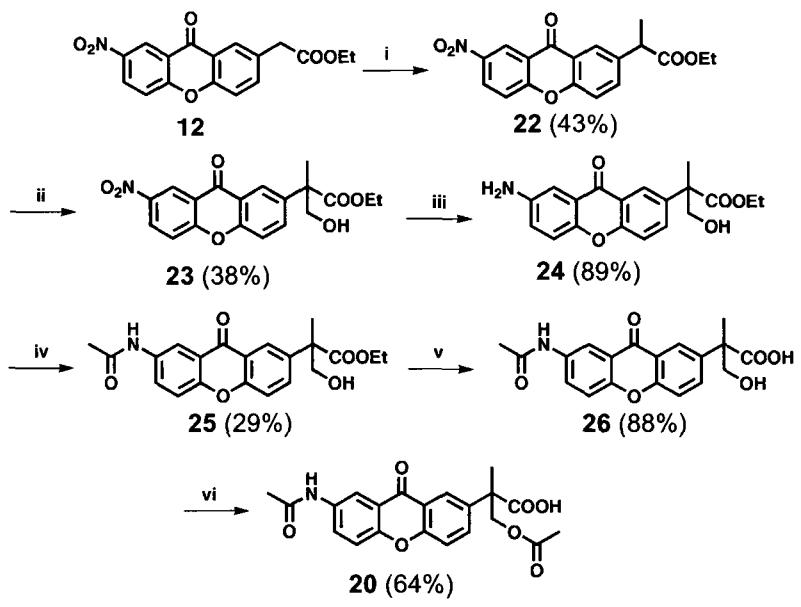

Scheme 3 - 1: Synthetic route for 20: i) LDA, CH_3I, THF, -78°C; ii) K_2CO_3, $(CH_2O)_n$, DMSO; iii) Pd/C, H_2, EtOAc; iv) Ac_2O, pyridine, DCM, v) 0.1 M NaOH, ACN; vi) Ac_2O, pyridine, DCM.

Following methylation, the terminal alcohol was added using paraformaldehyde under basic conditions in DMSO (Scheme 3 - 1, *ii*). The product, **23**, was verified by ^1H NMR in DMSO-d_6, with the disappearance of the benzylic methine proton at 4.09 ppm and with the appearance of two doublets of doublets (dd) at 3.76 and 3.91 ppm, shown in Figure 3 - 1. These diastereotopic protons, adjacent to the chiral centre, are not magnetically equivalent and thus are observed as two separate signals,[1] each of which is split by the geminal proton and then split once again by the geminal alcohol. The identity of **23** was further verified by ^{13}C NMR and HR-MS. It should be noted that the reaction conditions used for formaldehyde addition provided significant improvement in the ease of reaction setup over that utilized to

make ketoprofenate analogs, as well as an increase in percent yield (38% for **23** compared to 27% for the ketoprofenate analogue).[2]

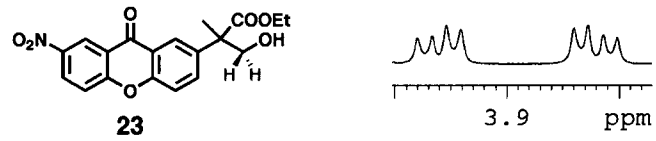

23

Figure 3 - 1: ^{1}H NMR splitting pattern of diastereotopic protons (indicated in red) for 23. The signal for each proton is observed as a doublet of doublets split first by the geminal proton (J_2 = 10.6 Hz) and again by the geminal alcohol (J_1 = 5.2 Hz).

The next step, reduction of the nitro to an amine, was carried out as before using palladium catalyzed hydrogenation (Scheme 3 - 1, iii).[3] The pure product, **24**, was obtained after 4 hours, as easily verified by ^{1}H NMR (in DMSO-d_6) with the appearance of the amino singlet at 5.46 ppm, along with a greater shielding effect in the aromatic protons due to the presence of the electron rich amine moiety.[1] The identity of the product was further confirmed by ^{13}C NMR and HR-MS.

Following reduction, the produced amine was converted to acetamide derivative **25** through reaction with acetic anhydride (Ac_2O) in dry dichloromethane (DCM), using pyridine as a base (Scheme 3 - 1, iv).[4] The reaction was complete after stirring for 24 hours under nitrogen, as observed by TLC. ^{1}H NMR showed the disappearance of the amino singlet at 5.46 ppm, along with appearance of amide singlet at 10.29 ppm, confirming

successful conversion to **25**. The product was further identified by ^{13}C NMR and HR-MS.

The ethyl ester was then hydrolyzed by stirring overnight in 1:1 v/v 0.1 M NaOH:ACN (Scheme 3 - 1, v).[5] The product was isolated by acidification and extraction with ethyl acetate. The loss of the ethyl ester peaks at 4.12 and 1.59 ppm in the ^{1}H NMR spectrum confirmed the identity of **26**. The product was further characterized by ^{13}C NMR and HR-MS.

Finally, the acetate leaving group was added by reaction of the benzyl alcohol of **26** with acetic anhydride in dry dichloromethane (Scheme 3 - 1, vi). Stirring overnight under nitrogen gave **20**, which was isolated by organic extraction. The product was then purified by reverse phase column chromatography using 1:1 v/v EtOAc:hexanes as the eluent. ^{1}H NMR spectroscopy confirmed the product, showing the appearance of the acetate singlet at 2.10 ppm. The identity of **20** was further confirmed by ^{13}C NMR and HR-MS.

3.2.2. Photochemistry of 20

Following the synthesis of **20**, the basic photochemistry was probed to assess the ability of the acetamide functionalized xanthonate photocages to photorelease leaving groups in the same manner as the parent xanthonate photocage.[6]

20 (1.6 mM in 80:20 v/v PBS:ACN) was irradiated for 30 minutes in a quartz test tube under air in a Luzchem photoreactor using 8 UVB lamps. Following acidification and organic extraction, the contents of the test tube were analyzed by ^{1}H NMR. It should be noted that the sample was acidified to ensure that both starting material and photoproduct were analyzed. The ^{1}H NMR spectrum showed the appearance of two new singlet peaks at 5.23 and 5.59 ppm, arising from the formation of the alkene photoproduct, **27** (30% by NMR). The production of **27** is consistent with the photorelease mechanism of **2**,[6] whereby photodecarboxylation of **20** generates a benzylic carbanion which subsequently undergoes elimination of the acetate leaving group, forming the alkene photoproduct (**27**), as shown in Scheme 3 - 2. The identity of the photoproduct, **27**, was further confirmed by ^{13}C NMR and HR-MS. The successful release of acetate from **20** demonstrated the ability of acetamide functionalized xanthonate photocage derivatives to release leaving groups.

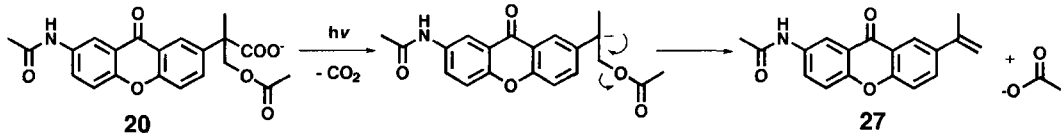

Scheme 3 - 2: Photorelease of acetate leaving group from 20 in basic aqueous media *via* photodecarboxylation followed by elimination of the generated carbanion.

3.2.3. Synthesis of 21

The synthesis of **21** was carried out beginning with **23**, whose synthesis has been described previously (Section 3.2.1.). The first step was to form a chloroformate group from the primary alcohol of **23** using triphosgene and pyridine in dry DCM (Scheme 3 - 3, i).[7] The formation of the chloroformate (**28**) was easily observed by ^{1}H NMR in $CDCl_3$, showing a shift in the diastereotopic proton signals from 3.80 and 4.03 ppm in **23** to 4.65 and 4.84 ppm in **28**, owing to a stronger deshielding of the methylene protons by the electron withdrawing chloroformate.[1] The carbamate was formed by reaction of the produced chloroformate, **28**, with phenylalanine methyl ester hydrochloride in anhydrous pyridine (Scheme 3 - 3, ii).[8] Stirring overnight under nitrogen atmosphere lead to complete conversion, as observed by TLC. Column chromatography afforded the pure product, **29**. The product was identified by ^{1}H NMR in DMSO-d_6 with the appearance of the phenylalanine methyl ester peaks, along with an additional carbamate proton signal at 4.22 ppm. ^{13}C NMR and ESI-MS further confirmed the identity of the product, **29**.

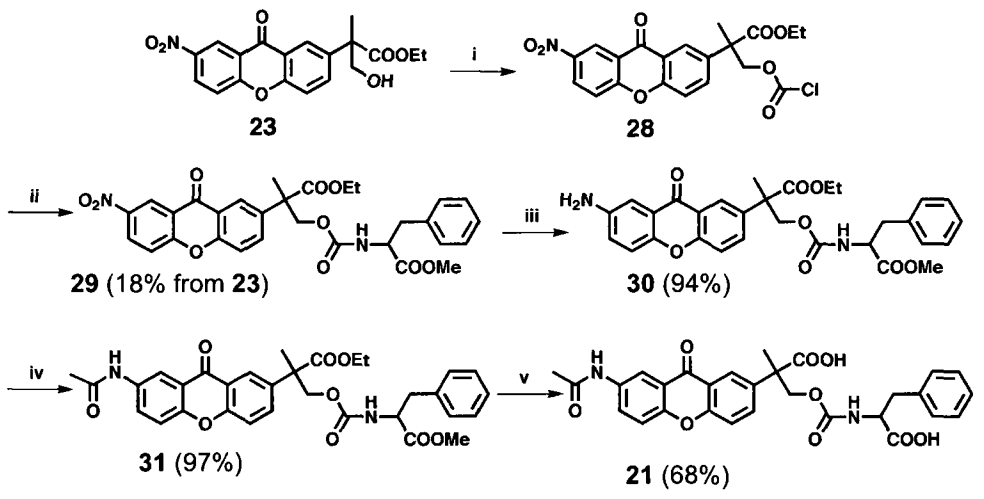

Scheme 3 - 3: Synthetic route for 21: i) triphosgene, pyridine, DCM; ii) Phe-Me, pyridine, iii) Pd/C, H_2, EtOAc, iv) Ac_2O, pyridine, DCM; v) 0.1 M NaOH, ACN.

Following carbamate formation, the nitro was reduced to an amine using palladium catalyzed hydrogenation under one atmosphere of hydrogen in ethyl acetate (Scheme 3 - 3, iii). Removal of the catalyst by filtration through celite followed by removal of the solvent by rotary evaporation afforded the yellow solid **30**. The product was identified by ^{1}H NMR in DMSO-d_6 with the appearance of the amino singlet at 5.48 ppm. ^{13}C NMR and ESI-MS further confirmed the identity of the product.

The acetamide was formed by reaction of **30** with excess acetic anhydride and pyridine in anhydrous DCM (Scheme 3 - 3, iv). The reaction was complete following stirring under nitrogen overnight, as observed by TLC. Organic extraction with multiple acidic water washes afforded the pure yellow solid **31** upon removal of the solvent by rotary evaporation. The loss of the amino singlet at 5.48 ppm in the ^{1}H NMR spectrum (in DMSO-d_6), along

with the appearance of the acetamide singlet peaks at 10.32 and 2.10 ppm confirmed the identity of the product. **31** was further characterized by ^{13}C NMR and ESI-MS.

Finally, the esters were hydrolyzed by stirring for 48 hours in 2:1 v/v 0.1 M NaOH:ACN (Scheme 3 - 3, v). Organic extraction following acidification afforded the solid product, **21**, following removal of the solvent by rotary evaporation. The product was identified by the loss of the ester peaks in the ^{1}H NMR spectrum in DMSO-d_6. The product was further confirmed by ^{13}C NMR and ESI-MS.

3.2.4. Photochemistry of 21

To identify the photoproducts, a solution of **21** was prepared (1.6 mM in 80:20 v/v PBS:ACN) and placed in a quartz test tube. The solution was irradiated for 30 minutes under air using 8 UVB lamps in a Luzchem photoreactor. During this time, the white solid product (**27**) was observed as a precipitate crashing out of solution, owing to its low solubility in aqueous media. Upon acidification and organic extraction, the contents were analyzed by NMR spectroscopy. ^{1}H NMR in DMSO-d_6 showed the disappearance of phenylalanine and diastereotopic methylene peaks, along with the appearance of the alkene singlets at 5.59 and 5.23 ppm, confirming the identity of **27** as the only photoproduct (78% yield by NMR). The product was further characterized by ^{13}C NMR and HR-MS. It should be noted that the

photoreleased phenylalanine was removed by repeated aqueous washings, therefore was not observed in the NMR spectra.

The appearance of product **27** arising from the photolysis of **21** is consistent with the mechanism whereby photodecarboxylation affords a benzylic carbanion, which then undergoes elimination of the phenylalanine leaving group, as shown in Scheme 3 - 4. The successful photorelease of phenylalanine showed the versatility of acetamide functionalized xanthonate photocages, demonstrating the capability to release amine-containing compounds such as amino acids or drugs through a carbamate.

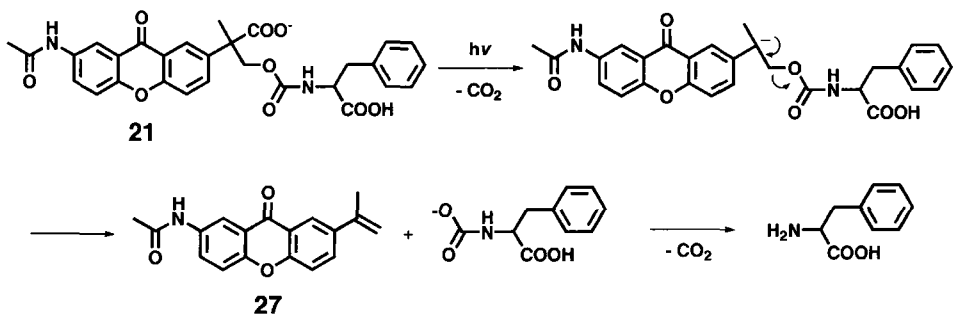

Scheme 3 - 4: Photorelease of phenylalanine leaving group from 21 in basic aqueous media *via* photodecarboxylation followed by elimination of the generated carbanion to produce the photoproduct 27. Thermal decarboxylation from the released carbamate then affords phenylalanine.

3.3. Toward Tethered Photorelease

3.3.1. Attempted Coupling *via* Amine Linker

Once demonstrated that acetamide functionalized xanthonate photocages (**20** and **21**) undergo the same photodecarboxylation and elimination of leaving groups as parent xanthonate photocages, attention was turned toward tethering amino functionalized photocage precursors to carboxylic acid terminated polymers.

Several attempts were made using conventional coupling chemistry of amine terminated precursors (**14** or **30**) with acrylic acid containing polymers, poly(acrylic acid) and poly(ethylene-co-acrylic acid). These polymers were chosen as general models for carboxylic acid containing scaffolds to be tested prior to coupling to the collagen-MPC interpenetrating network described in Section 1.2.2. Following literature procedures[9] routinely carried out for peptide synthesis and amide coupling chemistry using either dicyclohexylcarbodiimide (DCC) or 1-ethyl-3-(3-dimethylaminopropyl) carbodiimide (EDC) as coupling agents, no reaction was observed. Several modifications were made to the procedure, varying temperature, solvent and base, all to no avail. Other methods were attempted to perform amide coupling using 2-ethoxy-1-ethoxycarbonyl-1,2-dihydroquinoline (EEDQ) as a coupling reagent,[10, 11] or using acyl chloride formation.[12] All conditions tried gave no reaction, as observed by TLC, thus were not pursued further.

Attachment through the amine proved very difficult by conventional amide coupling chemistry, likely owing to a combined effect of steric hindrance within the polymer matrix along with the weak nucleophilicity of the aromatic amine.

3.3.2. A New Direction for Polymer Tethering

After several failed attempts at direct attachment of the amino functionalized photocage precursors to polymers *via* common amide coupling methods, attention was turned toward using a short chain linker to remove the point of attachment from the aromatic amine.

It is important to note that the collagen-MPC interpenetrating network[13] described in Section 1.2.2. contains both carboxylic acid and amine moieties, which could be used to tether *via* amide coupling amines or carboxylic acids, respectively. Taking advantage of the variety of terminal moieties present in the collagen-MPC IPN, a short chain linker could be easily synthesized such that the site of attachment is removed from the aromatic ring, as in **33** in Scheme 3 - 5. This added linker would provide a new route to polymer tethering through amide coupling chemistry while maintaining the same photochemistry demonstrated for **21**.

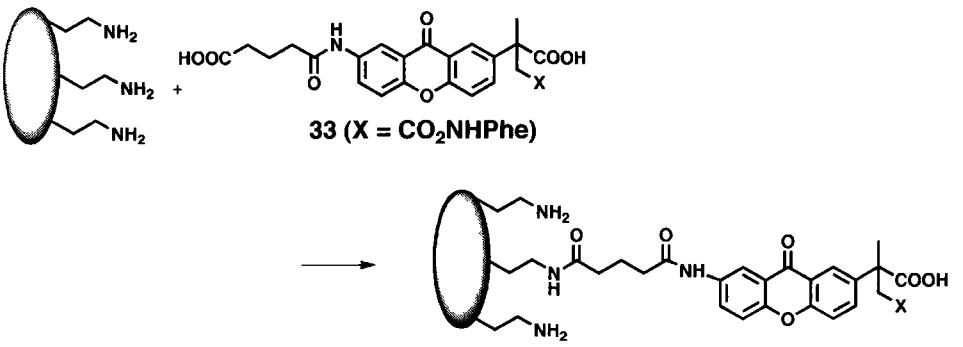

Scheme 3 - 5: Proposed alternative coupling strategy through a short chain alkyl linker (Phe = phenylalanine).

Following literature procedure,[14] **32** was obtained by refluxing **30** with glutaric anhydride in DMF overnight, followed by organic extraction and column chromatography (Scheme 3 - 6, i). The identity of **32** was confirmed by ^{1}H NMR in DMSO-d_6 by the disappearance of the amino singlet at 5.48 ppm, along with the appearance of the amide singlet (at 10.28 ppm) and new alkyl peaks (at 2.30, 2.40 and 1.84 ppm). The product was further characterized by ^{13}C NMR and ESI-MS.

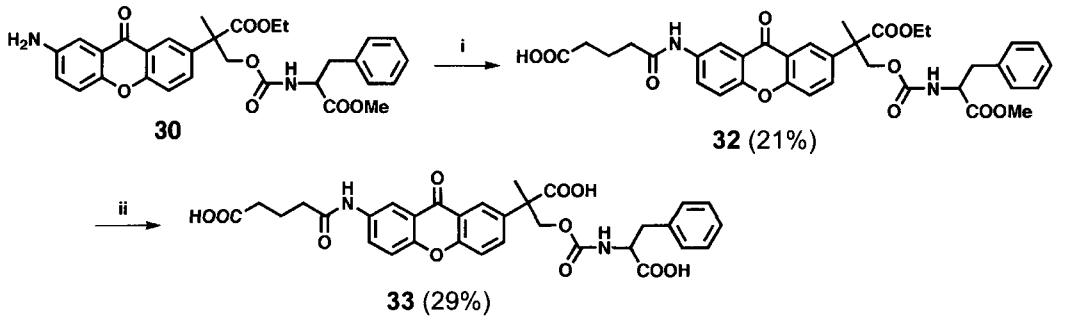

Scheme 3 - 6: Synthetic route for the preparation of 33. i) glutaric anhydride, DMF, Δ; ii) NaOH, ACN.

The esters of **32** were then hydrolyzed by refluxing for 48 hours in 2:1 v/v 0.1 M NaOH:ACN (Scheme 3 - 6, ii). Following acidification and organic extraction using EtOAc, the hydrolysis product (**33**) was obtained as a pale yellow solid. ^{1}H NMR in DMSO-d_6 confirmed the identity of **33** by the loss of ester peaks. The product was further characterized by ^{13}C NMR and ESI-MS.

To identify photoproducts resulting from UVB irradiation, **33** (1.6 mM in 80:20 v/v PBS:ACN) was irradiated under air using 8 UVB lamps in a quartz test tube. Following irradiation, the sample was acidified, extracted with EtOAc, and analyzed by ^{1}H NMR in DMSO-d_6. The ^{1}H NMR spectrum showed the appearance of two new singlet peaks at 5.23 and 5.59 ppm, arising from the formation of the alkene photoproduct, **34** (71% by NMR). The product was further characterized HR-MS.

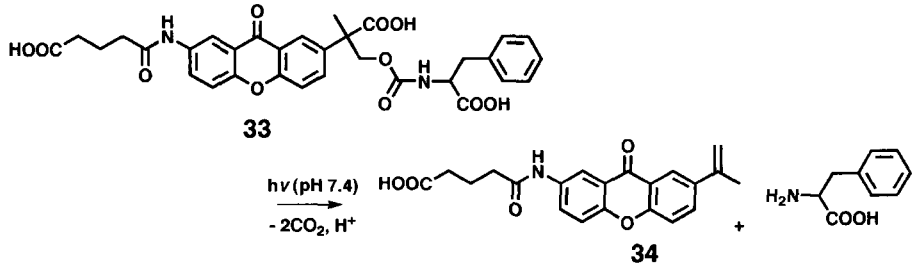

Scheme 3 - 7: Photorelease of phenylalanine leaving group from 33 in basic aqueous media to form the photoproduct 34. The reaction proceeds by a mechanism analogous to that shown Scheme 3 - 4.

This added linker demonstrated a new potential route for polymer tethering by amide coupling chemistry. The formation of **34** from UVB

irradiation of **33** showed that the photochemistry is consistent with that of **21**, thus is not affected by the added linking moiety.

3.4. Summary

The photochemistry of **20** and **21** successfully demonstrated the capability of acetamide functionalized xanthonate photocages to release biologically relevant leaving groups. These encouraging results showed that the same photorelease as reported for parent xanthonate photocages[6] still occurs with the amide moiety in place, albeit with a lower photodecarboxylation quantum yield as was discussed in Chapter 2. The release of acetate and phenylalanine were representative of a broader variety of carboxylate or amine containing leaving groups such as other amino acids or drugs.

Due to the low reactivity of the aromatic amine, polymer tethering of photocages proved very difficult by the methods initially proposed. Considering this, a short chain linker (as in **33**) was utilized that has no effect on the photochemistry. This added linker should assist with amide coupling, as well as reduce steric hindrance within polymer matrices. This reduced steric hindrance will be advantageous both for tethering applications as well as photorelease from polymers.

3.5. Experimental Details

All chemicals and solvents were purchased from Aldrich unless otherwise specified. Phenylalanine methyl ester hydrochloride was purchased from Nova Biochem and used directly without prior purification. Water was purified through a Millipore MilliQ system. ^{1}H and ^{13}C NMR spectra were recorded on a Bruker-Avance-400 at 400 and 100 MHz, respectively. All NMR shifts are reported relative to internal TMS. HR-MS (EI) spectra were recorded on a Kratos Concept 1S. HR-MS (ESI) spectra were recorded on a Micromass Q-Tof. All normal phase column chromatography was carried out using Merck silica gel 230-400 mesh. All reverse phase column chromatography was carried out using Merck silica gel 60 RP-18 200-400 mesh.

3.4.1. Synthetic Procedures

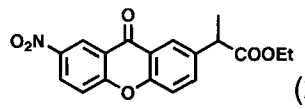

(22)

ethyl 2-(7-nitro-9-oxo-9H-xanthen-2-yl)propanoate

To a clean, flame dried 2-neck 250 mL round bottom flask was added **12** (1.51 g, 4.6 mmol). The starting material was dissolved in 200 mL dry THF under nitrogen and the solution was cooled to -78°C in a dry ice/acetone bath. After 20 minutes of stirring, LDA was added (3 mL of 1.8 M solution, 5.4

mmol) and the solution was stirred an additional 20 minutes before adding CH_3I (2 mL, excess). The solution was stirred for 20 hours under nitrogen during which time the temperature was raised to 20°C. The solution was acidified with 10 % HCl and extracted with 3 x 50 mL EtOAc. The combined organics were washed with 3 x 100 mL 1% HCl, dried with $MgSO_4$, filtered, and the solvent removed by rotary evaporation. The product was isolated by column chromatography using 1:4 v/v EtOAc:hexanes. Recrystallization from hot ethanol gave the pure pale yellow solid, **22** (0.70 g, 2.0 mmol, 43%). R_f = 0.40 in 1:3 v/v EtOAc:hexanes. ^1H NMR (400 MHz, DMSO-d_6) δ 8.88 (d, 1H, J = 2.6 Hz), 8.63 (dd, 1H, J = 2.9 Hz, J = 9.2 Hz), 8.13 (d, 1H, J = 2.6 Hz), 7.92 (d, 1H, J = 9.5 Hz), 7.89 (dd, 1H, J = 2.3 Hz, J = 8.9 Hz), 7.75 (d, 1H, J = 8.6 Hz), 4.09 (m, 3H), 1.47 (d, 3H, J = 7.5 Hz), 1.16 (t, 3H, J = 7.2 Hz). 13C NMR (100 MHZ, DMSO-d6) δ 175.2, 173.4, 158.9, 154.6, 143.5, 138.1, 135.9, 129.5, 126.5, 124.4, 122.1, 121.1, 120.4, 118.8, 60.5, 43.7, 18.5, 13.9. HR-MS (EI): Exact mass calculated for $C_{18}H_{15}NO_6$[M]+: 341.0899. Found: 341.08833.

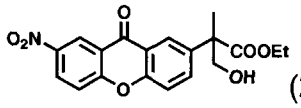

(**23**)

ethyl 3-hydroxy-2-methyl-2-(7-nitro-9-oxo-9H-xanthen-2-yl)propanoate

To a clean, dry 500 mL round bottom flask was added **22** (1.5 g, 4.5 mmol). The starting material was dissolved in 250 mL DMSO and purged with nitrogen for 20 minutes. To the solution was added K_2CO_3 (2 g, excess) and paraformaldehyde (2 g, excess), and the mixture was stirred under nitrogen

for 4 hours. Excess paraformaldehyde was removed by suction filtration, and the remaining liquid was acidified with 10% HCl and transferred into a separatory funnel. The mixture was extracted with 3 x 100 mL EtOAc, and the combined organics were washed thoroughly with 1% HCl to remove any remaining DMSO. The organic layer was dried with $MgSO_4$, filtered, and the solvent was removed by rotary evaporation. Isolation by column chromatography in 1:1 v/v EtOAc:hexanes afforded the pure pale yellow solid **23** (0.63 g, 1.7 mmol, 38 %). R_f = 0.56 in 2:1 v/v EtOAc:hexanes. ^{1}H NMR (400 MHz, $CDCl_3$) δ 9.23 (d, 1H, J = 2.6 Hz), 8.57 (dd, 1H, J_1 = 2.6 Hz, J_2 = 9.3 Hz), 8.31 (d, 1H, J = 2.4 Hz), 7.78 (dd, 1H, J_1 = 2.6 Hz, J_2 = 8.9 Hz), 7.65 (d, 1H, J = 9.1 Hz), 7.55 (d, 1H, J = 8.9 Hz), 4.24 (q, 2H, J = 7.1 Hz), 4.03 (dd, 1H, J_1 = 6.9 Hz, J_2 = 11.7 Hz), 3.80 (dd, 1H, J_1 = 6.9 Hz, J_2 = 11.7 Hz), 2.63 (t, 1H, J = 6.9 Hz), 1.74 (s, 3H), 1.25 (t, 3H, J = 7.5 Hz). ^{1}H NMR (400 MHz, DMSO-d_6) δ 8.88 (d, 1H, J = 2.9 Hz), 8.63 (dd, 1H, J = 2.9 Hz, J = 9.5 Hz), 8.11 (d, 1H, J = 2.6 Hz), 7.90 (m, 2H), 7.73 (d, 1H, J = 8.9 Hz), 5.15 (t, 1H, 5.0 Hz), 4.12 (m, 2H), 3.96 (dd, 1H, J = 5.2 Hz, J = 10.6 Hz), 3.82 (dd, 1H, J = 5.2 Hz, J = 10.6 Hz), 1.59 (s, 3H), 1.15 (t, 3H, J = 7.2 Hz). 13C NMR (100 MHZ, DMSO-d6) δ 175.2, 173.8, 158.8, 154.3, 143.4, 139.1, 134.9, 129.5, 123.3, 122.0, 121.0, 120.4, 120.2, 118.4, 66.9, 60.5, 52.0, 20.9, 13.9. HR-MS (EI): Exact mass calculated for $C_{19}H_{17}NO_7[M]^+$: 371.1005. Found: 371.09622.

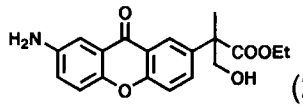

(**24**)

ethyl 2-(7-amino-9-oxo-9H-xanthen-2-yl)-3-hydroxy-2-methylpropanoate

To a clean, dry 250 mL round bottom flask was added **23** (0.10 g, 0.27 mmol) and dissolved in 50 mL EtOAc. To this was added the solid catalyst Pd/C (0.038 g, 5% Pd loading). The mixture was purged with nitrogen for 10 minutes, then with hydrogen gas for 20 minutes. The reaction was stirred under one atmosphere of hydrogen for 4 hours, at which point the reaction was complete, as verified by TLC. The heterogeneous catalyst was removed by suction filtration through celite and the solvent was removed by rotary evaporation, yielding the solid yellow product, **24** (0.083 g, 0.24 mmol, 89%). R_f = 0.32 in 1:1 v/v EtOAc:hexanes. ^{1}H NMR (400 MHz, DMSO-d_6) δ 8.06 (d, 1H, J = 2.8 Hz), 7.74 (dd, 1H, J = 2.6 Hz, J = 9.1 Hz), 7.57 (d, 1H, J = 8.8 Hz), 7.41 (d, 1H, J = 9.1 Hz), 7.28 (d, 1H, J = 3.1 Hz), 7.15 (dd, 1H, J = 2.8 Hz, J = 8.8 Hz), 5.46 (s, 2H), 5.10 (t, 1H, J = 5.1 Hz), 4.11 (m, 2H), 3.98 (dd, 1H, J = 3.4 Hz, J = 6.9 Hz), 3.78 (dd, 1H, J = 5.7 Hz, J = 10.1 Hz), 1.58 (s, 3H), 1.15 (t, 3H, J = 6.8 Hz). ^{13}C NMR (100 MHZ, DMSO-d_6) δ 175.9, 174.0, 154.3, 147.6, 145.6, 137.0, 133.2, 123.3, 121.6, 120.0, 118.5, 118.0, 106.0, 67.1, 60.5, 51.9, 20.9, 13.9. HR-MS (EI): Exact mass calculated for $C_{19}H_{19}NO_5[M]^+$: 341.1263. Found: 341.12829.

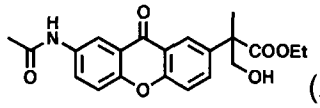

(**25**)

ethyl 2-[7-(acetylamino)-9-oxo-9H-xanthen-2-yl]-3-hydroxy-2-methyl propanoate

To a clean, dry 250 mL round bottom flask was added **24** (82.5 mg, 0.24 mmol) and dissolved in 100 mL dry DCM under nitrogen. To the mixture was added pyridine (0.7 mL, 8.7 mmol), and Ac_2O (0.7 mL, 7.4 mmol) and the solution was stirred under nitrogen for 24 hours. The reaction was worked up by acidification with 10% HCl and extracted using an additional 50 mL of DCM. The organics were washed with 3 x 50 mL of 1% HCl, dried over $MgSO_4$, and the solvent was removed by rotary evaporation. The product was isolated using column chromatography in 1:1 v/v EtOAc:hexanes, giving the pure pale yellow solid **25** (26.9 mg, 0.07 mmol, 29 %). ^{1}H NMR (400 MHz, DMSO-d_6) δ 10.29 (s, 1H), 8.47 (d, 1H, J = 2.9 Hz), 8.09 (d, 1H, J = 2.7 Hz), 8.02 (dd, 1H, J_1 = 2.9 Hz, J_2 = 9.3 Hz), 7.81 (dd, 1H, J_1 = 2.7 Hz, J_2 = 9.0 Hz), 7.66 (d, 1H, J = 3.5 Hz), 7.64 (d, 1H, J = 3.7 Hz), 5.12 (t, 1H, J = 5.1 Hz), 4.10-4.13 (m, 2H), 3.97 (dd, 1H, J_1 = 5.3 Hz, J_2 = 10.3 Hz), 3.79 (dd, 1H, J_1 = 5.1 Hz, J_2 = 10.3 Hz), 2.10 (s, 3H), 1.58 (s, 3H), 1.16 (t, 3H, J = 6.6 Hz). ^{13}C NMR (100 MHZ, DMSO-d_6) δ 175.9, 174.0, 168.5, 154.5, 151.5, 137.9, 135.8, 133.9, 127.1, 123.2, 121.1, 120.4, 118.7, 118.3, 114.4, 67.1, 60.6, 52.0, 24.0, 20.9, 14.0. HR-MS (EI): Exact mass calculated for $C_{21}H_{21}NO_6[M]^+$: 383.1369. Found: 383.13505.

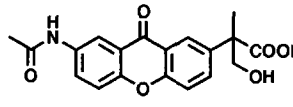

(**26**)

2-[7-(acetylamino)-9-oxo-9H-xanthen-2-yl]-3-hydroxy-2-methylpropanoic acid

To a clean 250 mL round bottom flask was added **25** (49 mg, 0.13 mmol). The starting material was then dissolved in 20 mL of 1:1 v/v ACN:0.1 M NaOH and allowed to stir under air for 22 hours. The reaction was then acidified with 10% HCl and extracted with 3 x 50 mL EtOAc. The combined organics were thoroughly washed with 3 x 50 mL of 1% HCl. The organics were then dried over $MgSO_4$, filtered, and the solvent was removed by rotary evaporation to afford the pale yellow solid, **26** (41 mg, 0.12 mmol, 88%). ^1H NMR (400 MHz, DMSO-d_6) δ 10.28 (s, 1H), 8.47 (d, 1H, J = 2.8 Hz), 8.13 (d, 1H, J = 2.5 Hz), 8.01 (dd, 1H, J_1 = 2.5 Hz, J_2 = 9.2 Hz), 7.85 (dd, 1H, J_1 = 2.5 Hz, J_2 = 9.1 Hz), 7.65 (d, 1H, J = 7.9 Hz), 7.63 (d, 1H, J = 7.6 Hz), 3.91 (d, 1H, J = 10.2 Hz), 3.76 (d, 1H, J = 10.2 Hz), 2.09 (s, 3H), 1.54 (s, 3H). ^{13}C NMR (100 MHZ, DMSO-d_6) δ 187.4, 175.9, 168.6, 154.4, 151.5, 138.6, 135.8, 134.2, 127.1, 123.4, 121.1, 120.2, 118.7, 118.0, 114.4, 67.4, 51.6, 24.0, 21.0. HR-MS (EI): Exact mass calculated for $C_{19}H_{17}NO_6[M]^+$: 355.1056. Found: 355.1075.

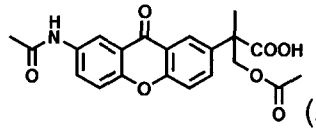

(**20**)

2-[7-(acetylamino)-9-oxo-9H-xanthen-2-yl]-3-(acetyloxy)-2-methylpropanoic acid

In a clean, dry 250 mL round bottom flask was dissolved **26** (0.10 g, 0.28 mmol) in 80 mL dry DCM under nitrogen. To this was added Ac_2O (1.0 mL,10.6 mmol), and anhydrous pyridine (1.0 mL, 12.4 mmol). The solution

was stirred under nitrogen for 20 hours, at which time 10 mL of water was added and the solution stirred for 15 minutes under air to hydrolyze unreacted acetic anhydride. The contents of the flask were the transferred into a separatory funnel, and extracted with 2 x 40 mL EtOAc. The combined organics were then washed with 3 x 50 mL dilute HCl washes. The organics were then dried with $MgSO_4$, filtered and the solvent removed by rotary evaporation, affording the pale yellow solid, **20** (0.07 g, 0.18 mmol, 64 %). ^1H NMR (400 MHz, DMSO-d_6) δ 10.29 (s, 1H), 8.47 (d, 1H, J = 2.3 Hz), 8.13 (d, 1H, J = 2.9 Hz), 8.02 (dd, 1H, J_1 = 2.6 Hz, J_2 = 9.0 Hz), 7.85 (dd, 1H, J_1 = 2.6 Hz, J_2 = 8.8 Hz), 7.63-7.66 (m, 2H), 3.93 (d, 1H, J = 10.2 Hz), 3.78 (d, 1H, J = 10.3 Hz), 2.10 (s, 3H), 1.56 (s, 3H), 1.23 (s, 3H). ^{13}C NMR (100 MHZ, DMSO-d_6) δ 175.9, 175.8, 169.9, 168.5, 154.4, 151.5, 138.3, 135.9, 134.2, 127.1, 123.3, 121.1, 120.2, 118.7, 118.0, 114.3, 67.2, 51.7, 24.0, 20.8, 20.5. HR-MS (EI): Exact mass calculated for $C_{21}H_{19}NO_7[M]^+$: 397.1162. Found: 397.1163.

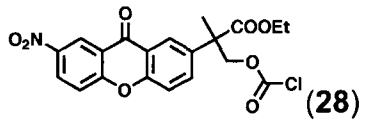

(28)

3-[(chlorocarbonyl)oxy]-2-methyl-2-(7-nitro-9-oxo-9H-xanthen-2-yl)propanoic acid

In a clean, flame dried 100 mL round bottom flask was dissolved **23** (0.20 g, 0.56 mmol) into dry DCM (40 mL). To this mixture was added triphosgene (0.11 g, 0.36 mmol) and the solution was cooled in an ice water bath for 20

minutes under nitrogen atmosphere. To this was added anhydrous pyridine (60 μL, 0.74 mmol) and the solution was stirred for 24 hours at which time the water bath temperature was raised to room temperature. To remove undesired pyridine salts and remaining triphosgene, hexanes were added, the volume reduced by rotary evaporation, and the resulting solid was filtered and discarded. The solvent from the remaining solution was removed by rotary evaporation, giving the product as a pale yellow solid. Due to its high reactivity, the chloroformate (**28**) was only characterized by ^{1}H NMR and used directly without further purification. R_f = 0.41 in 1:1 v/v EtOAc:hexanes. ^{1}H NMR (400 MHz, $CDCl_3$) δ 9.23 (d, 1H, J = 2.6 Hz), 8.58 (dd, 1H, J_1 = 2.9 Hz, J_2 = 9.1 Hz), 8.33 (d, 1H, J = 2.6 Hz), 7.79 (dd, 1H, J_1 = 2.9 Hz, J_2 = 9.0 Hz), 7.66 (dd, 1H, J = 9.0 Hz), 7.58 (d, 1H, J = 9.0 Hz), 4.84 (d, 1H, J = 10.7 Hz), 4.65 (d, 1H, J = 10.4 Hz), 4.25 (q, 2H, J = 7.0 Hz), 1.82 (s, 3H), 1.26 (t, 3H, J = 7.0 Hz).

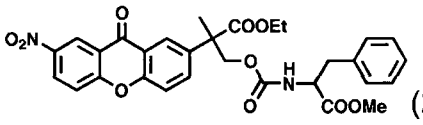

(**29**)

In a clean, dry, 50 mL round bottom flask was prepared a solution of phenylalanine methyl ester hydrochloride (0.14 g, 0.65 mmol) in anhydrous pyridine (2 mL) under nitrogen atmosphere. This mixture was stirred for one hour prior to injecting **28** (in 10 mL dry DCM) isolated above. The mixture was stirred under nitrogen atmosphere for 18 hours. The solvent was removed by rotary evaporation, and the product was separated by column

chromatography using 2:1 v/v hexanes:EtOAc as the eluent, giving the white solid **29** (0.06 g, 0.10 mmol, 18 % overall starting from **23**). R_f = 0.58 in 1:1 v/v EtOAc:hexanes. ^{1}H NMR (400 MHz, DMSO-d_6) δ 8.80 (d, 1H, J = 2.6 Hz), 8.57 (dd, 1H, J_1 = 2.8 Hz, J_2 = 9.1 Hz), 8.04 (s, 1H), 7.87 (s, 1H), 7.84 (s, 1H), 7.67 (d, 1H, J = 8.8 Hz), 7.12-7.23 (m, 5H), 4.32-4.54 (m, 2H), 4.22 (broad s, 1H), 4.08-4.16 (m, 2H), 3.60 (d, 3H, J = 10.1 Hz), 2.82-3.03 (m, 2H), 1.62 (s, 3H), 1.05-1.17 (m, 3H). ^{13}C NMR (100 MHZ, DMSO-d_6) δ 175.6, 173.2, 172.7, 159.3, 156.1, 155.0, 144.0, 137.9, 135.3, 135.2, 130.1, 129.5, 129.4, 128.7, 127.0, 123.7, 122.5, 121.6, 120.9, 119.3, 68.8, 61.6, 55.9, 52.4, 50.7, 36.8, 21.2, 14.3. ESI-MS: Exact mass calculated for $C_{30}H_{28}N_2O_{10}[M]^+$: 576.1744. Not Found. Exact mass calculated for $C_{30}H_{28}N_2O_{10}Na[M+Na]^+$: 599.1642. Found: 599.205.

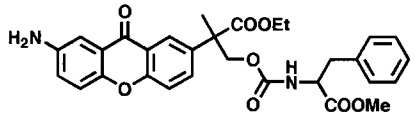

(**30**)

To a clean, dry 250 mL round bottom flask was dissolved **29** (0.27 g, 0.47 mmol) into 125 mL EtOAc. To this was added Pd/C (0.09 g, catalytic) and the mixture was purged for one hour with nitrogen gas. The mixture was then purged with hydrogen gas and allowed to stir under one atmosphere of hydrogen gas for 2 hours, at which point the reaction was complete by TLC. The heterogeneous catalyst was removed by filtration through celite and the solvent was removed by rotary evaporation, to afford the solid yellow product, **30** (0.24 g, 0.44 mmol, 94%). R_f = 0.28 in 1:1 v/v EtOAc:hexanes. ^{1}H NMR

(400 MHz, DMSO-d_6) δ 8.05 (s, 1H), 7.77 (s, 1H), 7.58 (d, 1H, J = 9.1 Hz), 7.42 (d, 1H, J = 9.1 Hz), 7.15-7.29 (m, 7H), 5.48 (s, 2H), 4.28-4.53 (m, 2H), 4.21 (broad s, 1H), 4.07-4.13 (m, 2H), 3.59 (d, 3H, J = 9.1 Hz), 2.83-3.02 (m, 2H), 1.59 (s, 3H), 1.07-1.19 (m, 4H). ^{13}C NMR (100 MHZ, DMSO-d_6) δ 175.6, 172.8, 172.0, 155.4, 154.4, 147.5, 145.8, 137.3, 137.2, 135.3, 132.8, 128.8, 126.3, 123.3, 122.9, 121.5, 120.0, 118.5, 118.3, 105.9, 68.2, 60.8, 55.4, 51.7, 50.0, 36.2, 20.5, 13.8. ESI-MS: Exact mass calculated for $C_{30}H_{30}N_2O_8[M]^+$: 546.2002. Not Found. Exact mass calculated for $C_{30}H_{30}N_2O_8Na[M+Na]^+$: 569.1900. Found: 569.251.

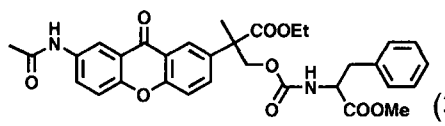

(**31**)

In a clean, dry 100 mL round bottom flask was dissolved **30** (0.12 g, 0.21 mmol) into dry DCM (75 mL) under nitrogen. To the solution was added anhydrous pyridine (0.17 mL, 2.1 mmol) and acetic anhydride (0.20 mL, 2.1 mmol) and the mixture was stirred under nitrogen for 23 hours. Water (10 mL) and ACN (10 mL) were added and the mixture was stirred for 30 minutes to hydrolyze the unreacted acetic anhydride. The contents of the flask were then transferred into a separatory funnel, acidified with 1% v/v HCl, and the organics extracted, washing with 6 x 50 mL dilute HCl. The organics were dried with $MgSO_4$, filtered, and the solvent was removed by rotary evaporation, affording **31** a pale yellow solid (0.12 g, 0.20 mmol, 97 %). R_f = 0.11 in 1:1 v/v EtOAc:hexanes. ^{1}H NMR (400 MHz, DMSO-d_6) δ 10.32 (s,

1H), 8.47 (d, 1H, J = 2.6 Hz), 8.07 (d, 1H, J = 2.6 Hz), 8.03 (dd, 1H, J_1 = 2.9 Hz, J_2 = 8.8 Hz), 7.81 (dd, 1H, J_1 = 2.9 Hz, J_2 = 8.8 Hz), 7.64-7.68 (m, 2H), 7.16-7.27 (m, 5H), 4.30-4.52 (m, 2H), 4.20 (broad s, 1H), 4.06-4.15 (m, 2H), 3.59 (d, 3H, J = 9.2 Hz), 2.81-3.02 (m, 2H), 2.10 (s, 3H), 1.60 (s, 3H), 1.08-1.16 (m, 4H). ^{13}C NMR (100 MHZ, DMSO-d_6) δ 175.7, 175.4, 172.8, 172.2, 168.4, 155.6, 154.6, 151.3, 137.4, 136.1, 135.9, 133.7, 129.0, 128.9, 128.2, 127.1, 126.4, 123.1, 121.0, 120.3, 118.7, 118.5, 114.2, 68.3, 60.9, 55.5, 51.9, 50.0, 36.2, 23.9, 20.6, 13.8. ESI-MS: Exact mass calculated for $C_{32}H_{33}N_2O_6[M+H]^+$: 589.2186. Found: 589.353. Exact mass calculated for $C_{32}H_{33}N_2O_6[M+Na]^+$: 611.2006. Found: 611.341.

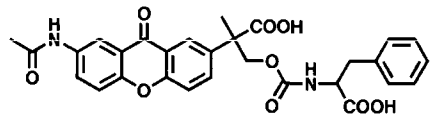

(**21**)

In a clean 100 mL round bottom flask was dissolved **31** (0.11 g, 0.19 mmol) into 20 mL of 2:1 v/v 0.1 M NaOH:ACN, and the solution was stirred under air for 48 hours. The contents of the flask were then acidified with 10 % HCl and transferred into a separatory funnel. The product was extracted with 2 x 40 EtOAc, and the organics were washed with 4 x 50 mL 1% HCl. The organics were then dried with $MgSO_4$, filtered, and the solvent was removed by rotary evaporation. The product was then purified by dissolving it in 0.1 M NaOH then crashing out the solid product by adding 10% HCl dropwise. The product was then collected by suction filtration, yielding the pale yellow solid product, **21** (0.07 g, 0.13 mmol, 68 %). R_f = 0.12 in 9:1 v/v EtOAc:MeOH. ^{1}H

NMR (400 MHz, DMSO-d_6) δ 10.29 (s, 1H), 8.48 (d, 1H, J = 2.6 Hz), 8.11 (t, 1H, J = 2.6 Hz), 8.02 (dd, 1H, J_1 = 2.9 Hz, J_2 = 9.1 Hz), 7.85 (dt, 1H, J_1 = 2.9 Hz, J_2 = 8.9 Hz), 7.67 (d, 1H, J = 9.1 Hz), 7.64 (d, 1H, J = 9.1 Hz), 7.13-7.28 (m, 5H), 4.29-4.43 (m, 2H), 4.10 (broad s, 1H), 2.77-3.04 (m, 2H), 2.09 (s, 3H), 1.56 (s, 3H), 1.06 (t, 1H, J = 6.6 Hz). ^{13}C NMR (100 MHZ, DMSO-d_6) δ 175.8, 174.7, 173.2, 168.5, 155.9, 154.5, 151.4, 135.9, 129.1, 129.0, 128.9, 128.2, 128.1, 127.1, 126.3, 126.2, 123.2, 121.1, 120.3, 118.7, 118.4, 114.3, 68.6, 55.9, 49.8, 23.9, 20.5, 18.6. ESI-MS: Exact mass calculated for $C_{29}H_{27}N_2O_9[M+H]^+$: 547.1717. Found: 547.267.

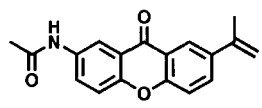

(**27**)

N-[9-oxo-7-(prop-1-en-2-yl)-9H-xanthen-2-yl]acetamide

In a quartz test tube was dissolved **21** (7 mg, 0.013 mmol) in 8 mL 80:20 v/v PBS:ACN. The solution was irradiated for 30 minutes under air using 8 UVB lamps in a Luzchem photoreactor. During the course of the photoreaction, a white precipitate was observed crashing out of the solution. The contents of the test tube were then acidified with 1% HCl and transferred into a separatory funnel, extracted with 2 x 20 mL EtOAc. The combined organics were then washed with 3 x 10 mL 1% HCl, dried using $MgSO_4$, and the solvent removed by rotary evaporation, giving **27** as a white solid product. (78% by NMR). ^{1}H NMR (400 MHz, DMSO-d_6) δ 10.29 (s, 1H), 8.48 (d, 1H, J = 2.6 Hz), 8.19 (d, 1H, J = 2.6 Hz), 8.08 (dd, 1H, J_1 = 2.6 Hz, J_2 = 9.0 Hz), 8.02 (dd, 1H, J_1 = 2.6 Hz, J_2 = 9.0 Hz), 7.64-7.67 (m, 2H), 5.59 (s, 1H), 5.23

(s, 1H), 2.21 (s, 3H), 2.10 (s, 3H). ^{13}C NMR (100 MHZ, DMSO-d_6) δ 175.9, 168.6, 155.0, 151.3, 140.9, 136.2, 135.9, 132.5, 127.0, 121.8, 121.0, 120.3, 118.7, 118.3, 114.2, 113.7, 24.0, 21.5. HR-MS (EI): Exact mass calculated for $C_{18}H_{15}NO_3[M]^+$: 293.1052. Found: 293.10400.

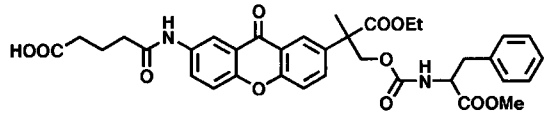

(32)

In a clean, dry 100 mL round bottom flask was dissolved **30** (0.15 g, 0.26 mmol) into anhydrous N,N'-dimethylformamide (DMF, 20 mL). To this mixture was added glutaric anhydride (0.033 g, 0.29 mmol) and the solution was refluxed under nitrogen for 19 hours. The solution was allowed to cool to room temperature and the contents of the flask were transferred into a separatory funnel. The mixture was acidified with 1% v/v HCl and extracted with 3 x 50 mL EtOAc. The combined organics were then washed with 6 x 25 mL. The organics were dried with $MgSO_4$, filtered, and the solvent was removed by rotary evaporation. The product was isolated by flash chromatography, using EtOAc as the initial eluent to remove the starting material, followed by 90:10 v/v EtOAc:MeOH to obtain the pale yellow solid product, **32** (36 mg, 0.055 mmol, 21%). ^1H NMR (400 MHz, DMSO-d_6) δ 10.28 (s, 1H), 8.50 (d, 1H, J = 2.6 Hz), 8.08 (d, 1H, J = 2.3 Hz), 8.04 (dd, 1H, J_1 = 2.8 Hz, J_2 = 9.1 Hz), 7.82 (dd, 1H, J_1 = 2.3 Hz, J_2 = 8.7 Hz), 7.66 (m, 2H), 7.16-7.28 (m, 5H), 4.30-4.52 (m, 2H), 4.20 (s, 1H), 4.08-4.13 (m, 2H), 3.59 (d, 3H, J = 9.2 Hz), 2.81-3.02 (m, 2H), 2.40 (t, 2H, J = 7.5 Hz), 2.30 (t,

2H, J = 7.0), 1.84 (p, 2H, 7.5 Hz), 1.60 (s, 3H), 1.08-1.19 (m, 4H). ^{13}C NMR (100 MHZ, DMSO-d_6) δ 175.8, 174.2, 172.9, 172.2, 171.0, 155.6, 154.6, 151.4, 137.5, 137.4, 136.2, 135.8, 129.0, 128.9, 128.2, 127.2, 126.5, 126.4, 123.1, 121.0, 120.3, 118.7, 118.6, 114.4, 68.4, 61.0, 55.5, 51.9, 50.1, 36.3, 35.4, 33.0, 20.7, 20.4, 13.9. ESI-MS: Exact mass calculated for $C_{35}H_{37}N_2O_{11}[M+H]^+$: 661.2397. Found: 661.362.

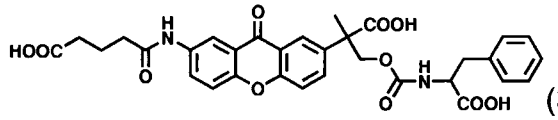

(33)

In a clean, dry, 100 mL round bottom flask was dissolved **32** (36 mg, 0.055 mmol) in 30 mL of 2:1 v/v 0.1 M NaOH:ACN. The solution was fit with a reflux condenser and refluxed under air for 48 hours. The solution was then acidified with 10% HCl and transferred into a separatory funnel. The organics were extracted with 2 x 40 mL EtOAc, and the combined organics were washed with 3 x 20 mL 1% HCl. The organics were then dried using MgSO4, filtered, and the solvent was removed by rotary evaporation, affording the pale yellow solid, **33** (10 mg, 0.016 mmol, 29%). ^{1}H NMR (400 MHz, DMSO-d_6) δ 12.46 (broad s, 3H), 10.26 (s, 1H), 8.51 (d, 1H, J = 2.6 Hz), 8.12 (t, 1H, J = 2.8 Hz), 8.03 (dd, 1H, J_1 = 2.6 Hz, J_2 = 9.3 Hz), 7.86 (dt, 1H, J_1 = 2.6 Hz, J_2 = 9.1 Hz), 7.63-7.68 (m, 2H), 7.17-7.29 (m, 5H), 4.29-4.44 (m, 2H), 4.11 (broad s, 1H), 2.78-3.04 (m, 2H), 2.41 (t, 1H, J = 7.5 Hz), 2.31 (t, 1H, J = 7.3 Hz), 1.85 (p, 1H, J = 7.5 Hz), 1.57 (s, 3H), 1.16-1.19 (m, 1H). ^{13}C NMR (100 MHZ, DMSO-d_6) δ 175.8, 174.7, 174.2, 173.3, 171.5, 171.0, 154.5, 152.8,

151.4, 137.9, 137.5, 136.7, 135.8, 129.0, 128.9, 128.2, 128.1, 126.4, 121.1, 120.3, 118.7, 118.5, 114.4, 111.2, 49.8, 35.5, 33.0, 29.2, 22.6, 22.1, 20.4, 14.1. ESI-MS: Exact mass calculated for $C_{32}H_{31}N_2O_{11}[M+H]^+$: 619.1928. Found: 619.199. Exact mass calculated for $C_{32}H_{30}N_2O_{11}Na[M+Na]^+$: 641.1747. Found: 641.158.

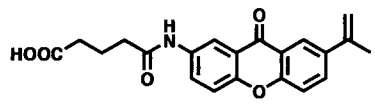

(**34**)

In a quartz test tube was dissolved **33** (5 mg, 0.008 mmol) in 5 mL 80:20 v/v PBS:ACN. The solution was irradiated for 30 minutes under air using 8 UVB lamps in a Luzchem photoreactor. The contents of the test tube were then acidified with 1% HCl, transferred into a separatory funnel, and extracted with 2 x 20 mL EtOAc. The combined organics were then washed with 3 x 10 mL 1% HCl, dried using $MgSO_4$, and the solvent removed by rotary evaporation, giving **34** as a white solid product (71% by NMR). ^{1}H NMR (400 MHz, DMSO-d_6) δ 10.26 (s, 1H), 8.51 (d, 1H, J = 2.6 Hz), 8.20 (d, 1H, J = 2.6 Hz), 8.08 (dd, 1H, J_1 = 2.6 Hz, J_2 = 9.1 Hz), 8.03 (dd, 1H, J_1 = 2.8 Hz, J_2 = 9.1 Hz), 7.67 (d, 1H, J = 2.4 Hz), 7.65 (d, 1H, J = 2.4 Hz), 5.59 (s, 1H), 5.23 (s, 1H), 2.41 (t, 2H, J = 7.3 Hz), 2.30 (t, 2H, J = 7.5 Hz), 2.21 (s, 3H), 1.84 (p, 2H, J = 7.2 Hz). HR-MS (EI): Exact mass calculated for $C_{21}H_{19}NO_5[M]^+$: 365.1263. Found: 365.12725.

3.5. References

1. Pavia, D.; Lampman, G.; Kriz, G., *Introduction to Spectroscopy*. Third ed.; Thomson Learning, Inc.: Toronto, 2001.

2. Lukeman, M.; Scaiano, J. C., Carbanion-Mediated Photocages: Rapid and Efficient Photorelease with Aqueous Compatibility. *J. Am. Chem. Soc.* **2005,** *127*, 7698-7699.

3. Clayden, J.; Greeves, N.; Warren, S.; Wothers, P., *Organic Chemistry*. Oxford: New York, 2001.

4. Carey, F. A., Reactions of Carboxylic Acid Anhydrides. In *Organic Chemistry*, Fifth ed.; McGraw-Hill: New York, 2003; pp 842-843.

5. Carey, F. A., Ester Hydrolysis in Base. In *Organic Chemistry*, Fifth ed.; McGraw-Hill: New York, 2003; pp 852-853.

6. Blake, J. A.; Lukeman, M.; Scaiano, J. C., Photolabile Protecting Groups Based on the Singlet State Photodecarboxylation of Xanthone Acetic Acid. *J. Am. Chem. Soc.* **2009,** *131*, 4127-4135.

7. Martyres, D. H.; Baldwin, J. E.; Adlington, R. M.; Lee, V.; Probert, M. R.; Watkin, D. J., Synthesis of a Novel Thiabicyclo[3.2.0]heptan-6-one Analogue of Penicillin. *Tetrahedron* **2001,** *57*, 4999-5007.

8. D'Addona, D.; Bochet, C. G., Preparation of Carbamates from Amines and Alcohols Under Mild Conditions. *Tetrahedron Lett.* **2001,** *42*, 5227-5229.

9. Valeur, E.; Bradley, M., Amide Bond Formation: Beyond the Myth of Coupling Reagents. *Chem. Rev. Soc.* **2009,** *38*, 606-631.

10. Belleau, B.; Malek, G., A New Convenient Reagent for Peptide Syntheses. *J. Am. Chem. Soc.* **1968,** *90*, 1651-1652.

11. Hyun, M. H.; Kang, M. H.; Han, S. C., Use of 2-Ethoxy-1-(ethoxycarbonyl)-1,2-dihydroquinoline as a Convenient Reagent for the Selective Protection or Derivatization of 2-Hydroxycarboxylic Acids. *Tetrahedron Lett.* **1999,** *40*, 3435-3438.

12. Montalbetti, C. A. G. N.; Falque, V., Amide Bond Formation and Peptide Coupling. *Tetrahedron* **2005,** *61*, 10827-10852.

13. Liu, W.; Deng, C.; McLaughlin, C. R.; Fagerholm, P.; Lagali, N. S.; Heyne, B.; Scaiano, J. C.; Watsky, M. A.; Kato, Y.; Munger, R.; Shinozaki, N.; Li, F.; Griffith, M., Collagen-Phosphorylcholine Interpenetrating Network Hydrogels as Corneal Substitutes. *Biomaterials* **2009,** *30*, 1551-1559.

14. Majjigapu, J. R. R.; Kurchan, A. N.; Kottani, R.; Gustafson, T. P.; Kutateladze, A. G., Release and Report: A New Photolabile Caging System with a Two-Photon Fluorescence Reporting Function. *J. Am. Chem. Soc.* **2005,** *127*, 12458-12459.

4. Conclusions and Future Directions

4.1. Final Comments **116**
4.2. Future Directions **119**
4.3. Claims to Original Research **120**

4.1. Final Comments

The results described in Chapter 2 indicate that xanthonate photocage precursors equipped with an amine moiety, as in **8** and **9**, are photochemically inactive in basic aqueous media. For tethering applications this property is useful, since amine photocage precursors to be used for attachment will not photodecarboxylate in their free form. It is only once the amine functionality is removed by formation of an amide that photochemistry is restored, as demonstrated by the photodecarboxylation of **10** and **11** in basic aqueous media. While solvent composition does affect the quantum yield of photodecarboxylation for acetamide derivatives, in complex natural systems (containing more than water) the quantum yield should be sufficient for the proposed application.

As discussed in Chapter 3, acetamide derivatives of xanthonate photocages are capable of photoreleasing leaving groups in the same manner as parent xanthonate photocages. In agreement with the photochemistry observed for **2**, the photochemical study of **20** showed that acetamide functionalized xanthonate photocages undergo photodecarboxylation upon UVB irradiation in basic aqueous media followed by elimination to form the alkene photoproduct (**27**) along with free acetate. The successful photorelease of phenylalanine from **21** expanded the scope of leaving groups to amine containing compounds such as amino acids or drugs, which can be readily attached *via* carbamate chemistry.

Recently, fellow graduate student J.A. Blake has further expanded the scope of leaving groups by demonstrating the photorelease of acyclovir from a xanthonate photocage in basic aqueous media. Due to the low reactivity of the alcohol and amine moieties of acyclovir, attachment was accomplished *via* carbonyl protection. Photorelease of the leaving group then restores the carbonyl of acyclovir as well as the antiviral activity of the drug.

The attempted coupling reactions discussed in Chapter 3 demonstrated the difficulty of amide formation by conventional methods, likely due to the low reactivity of a xanthonate amine combined with the steric hindrance of both the xanthonate precursor and polymer matrix. While this proved difficult in initial investigations, optimization and variation of coupling methods or reagents may still allow for such a coupling to take place.

The difficulty brought upon by coupling through the amine led to the modification of the amine with a short linking alkyl chain terminated by a carboxylic acid moiety. This modification is advantageous as the linking group is removed from the xanthonate chromophore, which eliminates the problem of coupling to an electron deficient nucleophile, as well it should alleviate steric hindrance about the xanthonate photocage.

With xanthonate photocage precursors containing amine and carboxylic acid linking groups having been successfully prepared, it is possible to couple these to the collagen-MPC interpenetrating network through either the carboxylic acid or amine, respectively. While all attempted coupling methods focused on the use of amide chemistry for ease of

synthesis, it should be noted that there are other methods that could be employed to tether to polymer scaffolds (for instance, click chemistry).

For the chemistry described in this thesis to be used for the proposed application, further synthesis is required to prepare photocage precursors equipped both with the acyclovir leaving group as well as a linking moiety (either an amine or carboxylic acid). Once these precursors are prepared, they can be integrated into the replacement corneal materials by amide coupling chemistry. Prior to their *in vivo* installation, *in vitro* testing will be required to ensure both that the same photorelease chemistry occurs and that the tethered photocage and resulting photoproduct are non-toxic to cells. Provided the tethered photocages are non-toxic, as expected, they could then be installed into living patients following corneal replacement surgery.

The unique strategy of using tethered xanthonate photocages equipped with acyclovir to combat corneal HSV-1 is a truly novel drug delivery method with a high degree of spatial and temporal control. While the application discussed is focused on tethered drug release, the underlying chemistry discussed can be applied in many ways beyond this particular field.

4.2. Future Directions

1 Attachment of xanthonate photocages to polymer scaffolds *via* amide coupling.

2 Photorelease of leaving groups (such as phenylalanine) from test polymer scaffold.

3 Synthesis of acyclovir loaded xanthonate photocage precursor with linking moiety.

4 Attachment of acyclovir equipped xanthonate photocage to collagen-MPC interpenetrating network *via* amide coupling chemistry.

5 *In vitro* testing of collagen-MPC tethered xanthonate photocage equipped with acyclovir.

6 Photorelease of acyclovir from corneal transplant materials using tethered xanthonate photocages.

4.3. Claims to Original Research

1 Synthetic procedures to prepare amine and acetamide derivatives of xanthonate acetic acid and thioxanthone acetic acid.

2 Photochemical study of amine derivatives **8** and **9** in basic aqueous media, confirming their photochemical inactivity.

3 Steady-state photochemical study of acetamide derivatives **10** and **11** in basic aqueous media using UVB irradiation.

4 Measurement of an unprecedented solvent composition effect on the quantum yield of photodecarboxylation for acetamide derivatives **10** and **11**.

5 Determination of quantum yields of fluorescence for **8-11**.

6 Laser flash photolysis study of **10** in basic aqueous media.

7 Synthetic procedures to prepare phenylalanine equipped xanthonate photocage precursors with amine linker.

8 Photorelease of phenylalanine from acetamide functionalized xanthonate photocage (**21**) in basic aqueous media.

9 Synthetic procedures to modify linking amine with alkyl chain and terminal carboxylic acid linker.

10 Photorelease of phenylalanine from xanthonate photocages equipped with carboxylic acid linker (**33**) in basic aqueous media.

APPENDIX 1 – ^{1}H and ^{13}C NMR Spectra

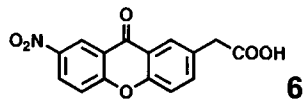

6

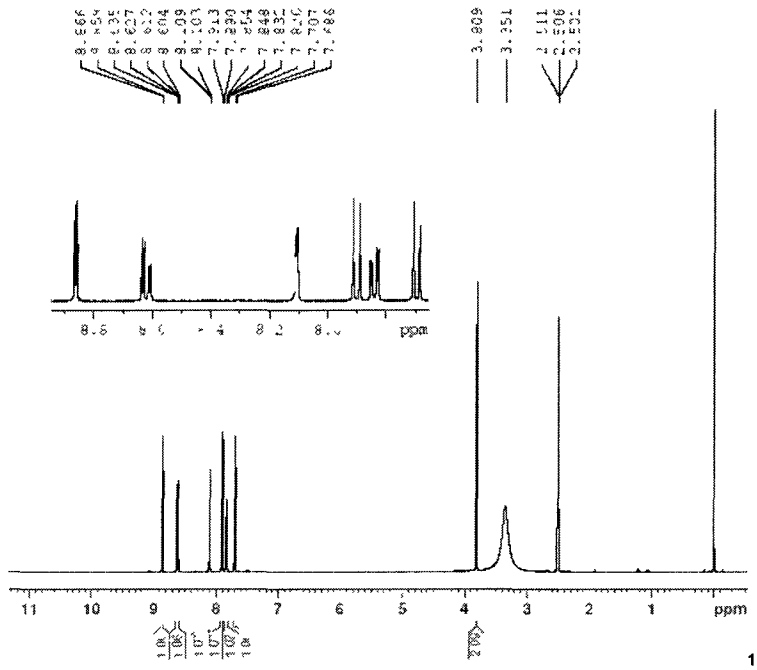

^{1}H, 400 MHz, DMSO-d_6

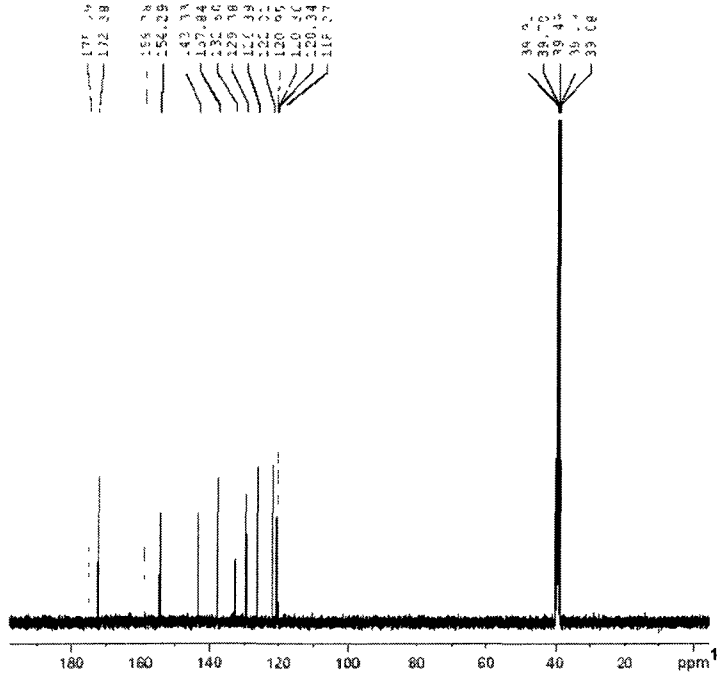

^{13}C, 100 MHz, DMSO-d_6

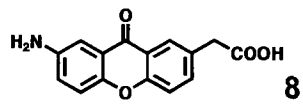

8

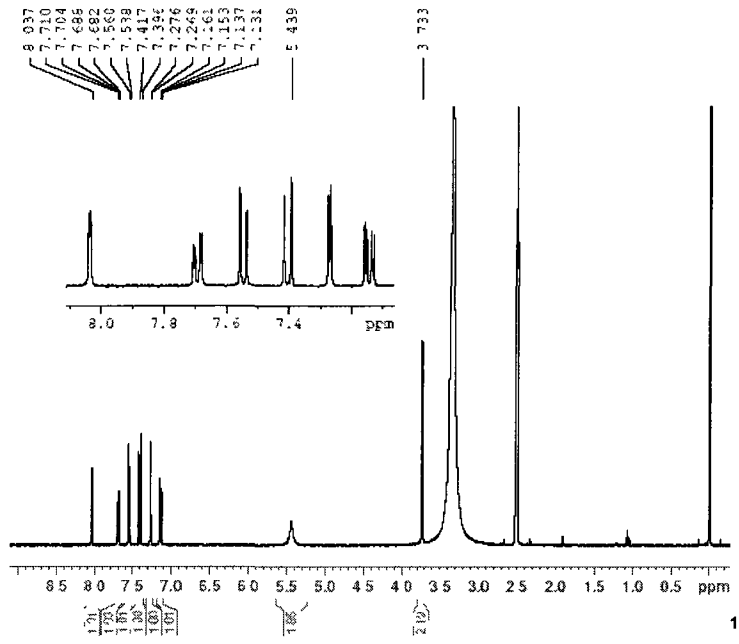

^{1}H, 400 MHz, DMSO-d_6

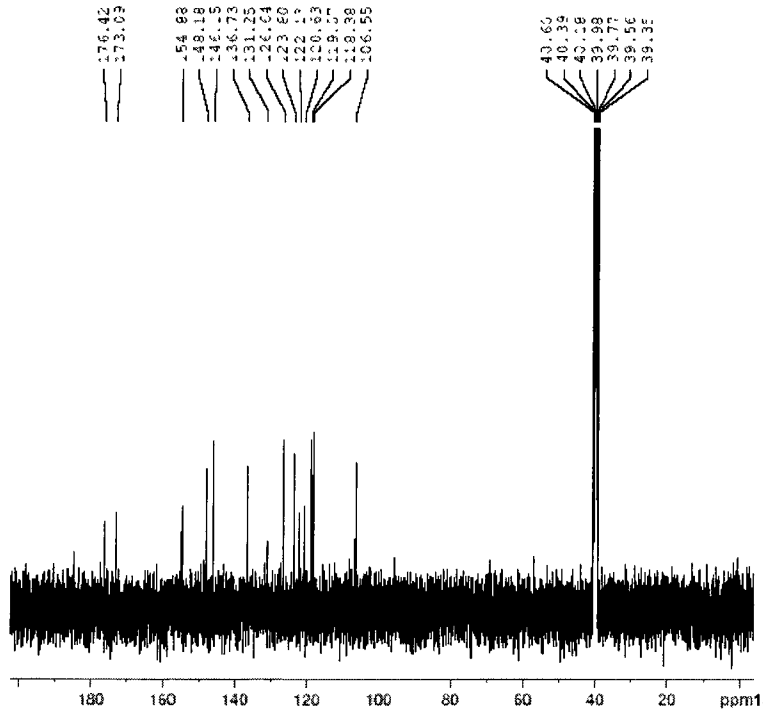

^{13}C, 100 MHz, DMSO-d_6

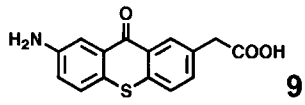

9

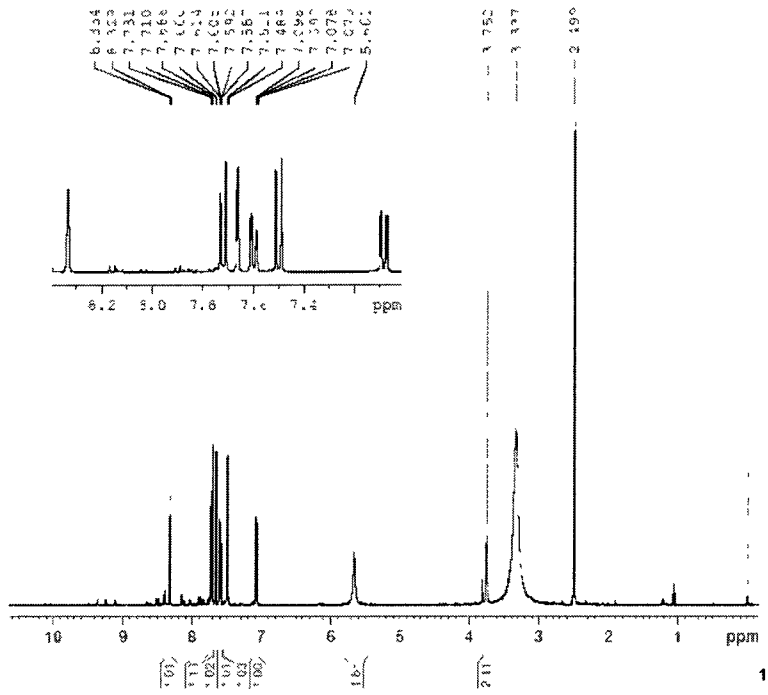

^{1}H, 400 MHz, DMSO-d_6

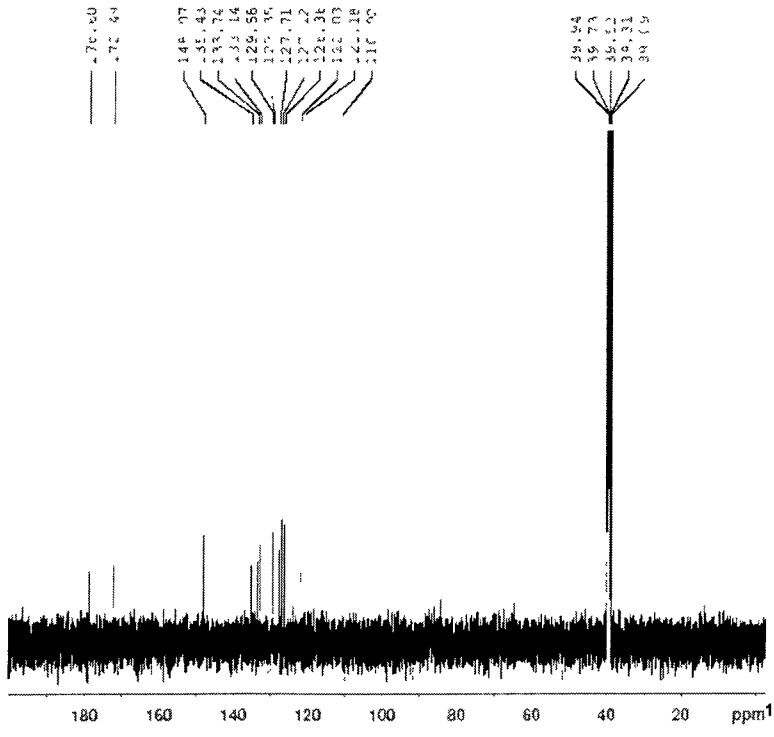

^{13}C, 100 MHz, DMSO-d_6

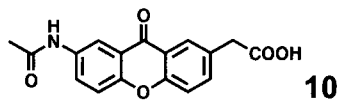

10

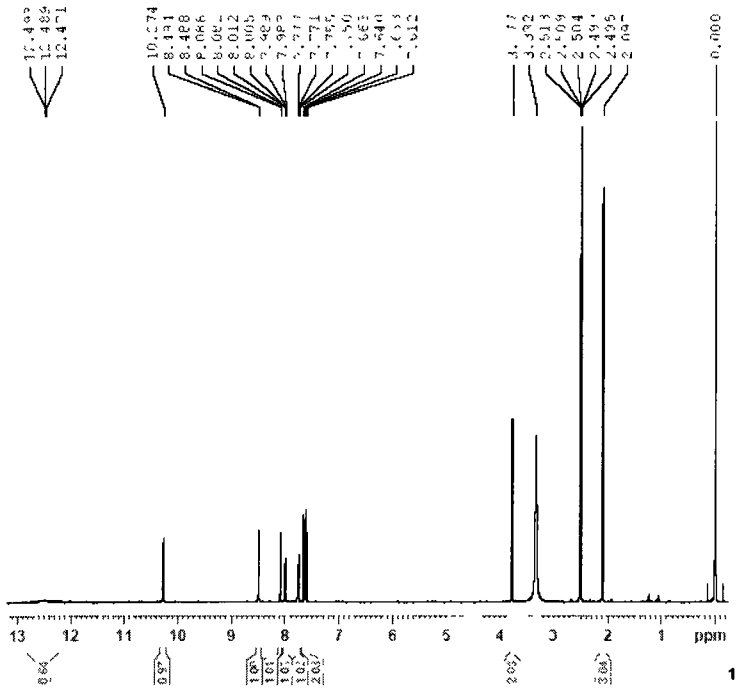

^{1}H, 400 MHz, DMSO-d_6

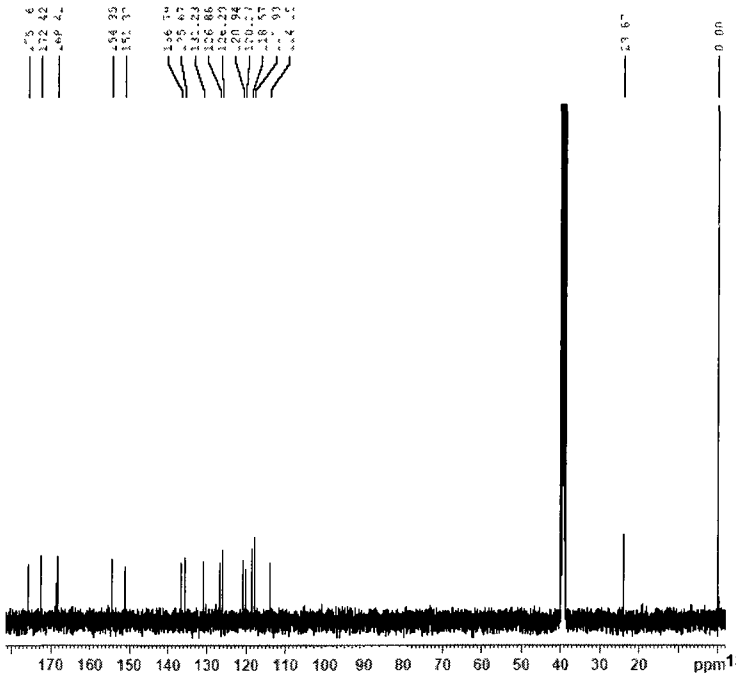

^{13}C, 100 MHz, DMSO-d_6

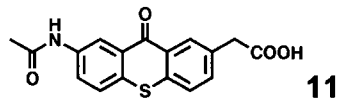

11

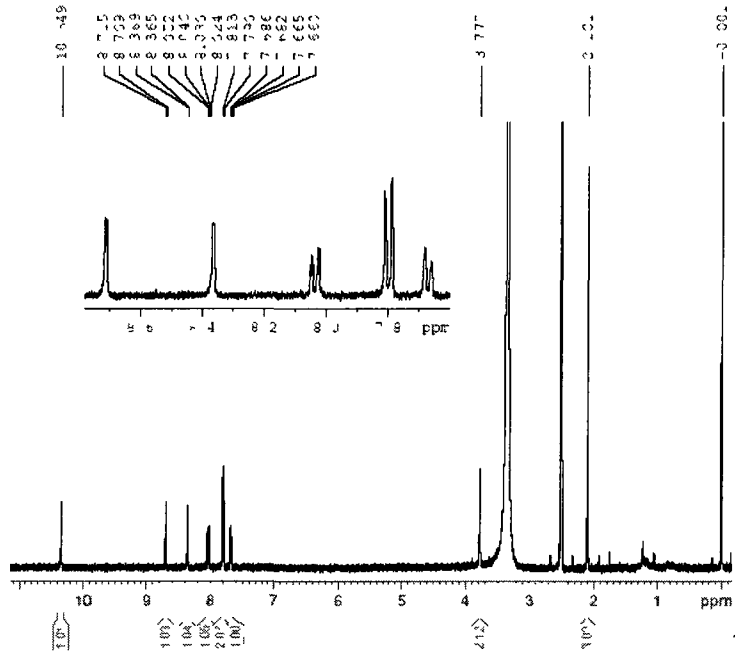

^{1}H, 400 MHz, DMSO-d_6

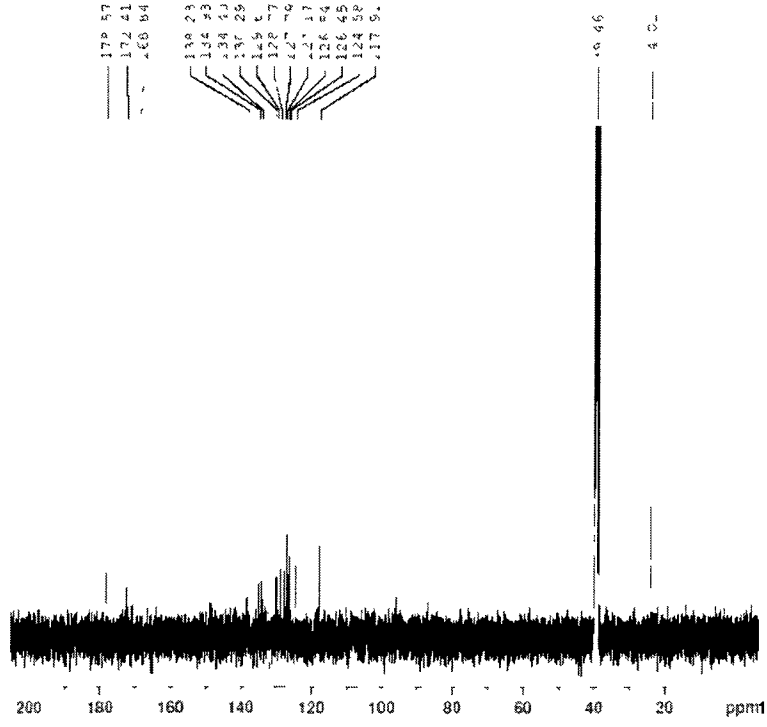

^{13}C, 100 MHz, DMSO-d_6

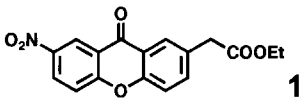

12

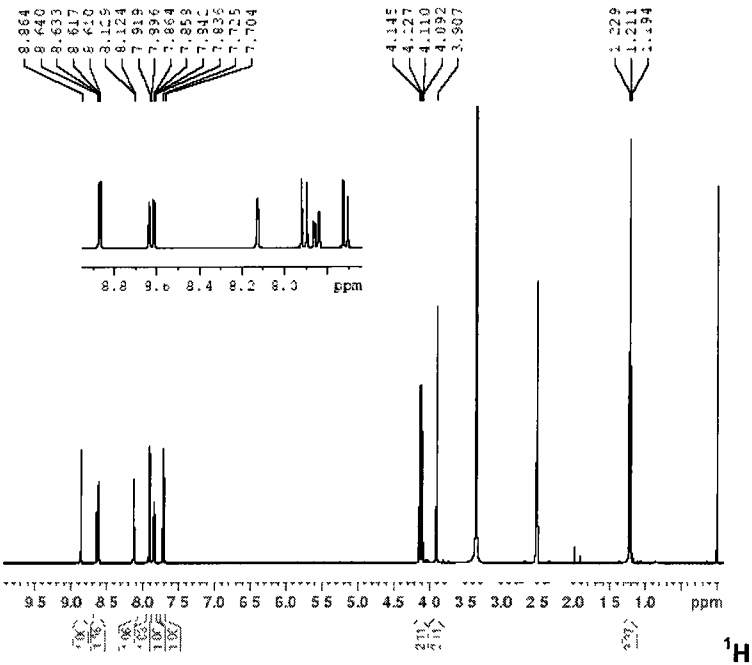

^{1}H, 400 MHz, DMSO-d_6

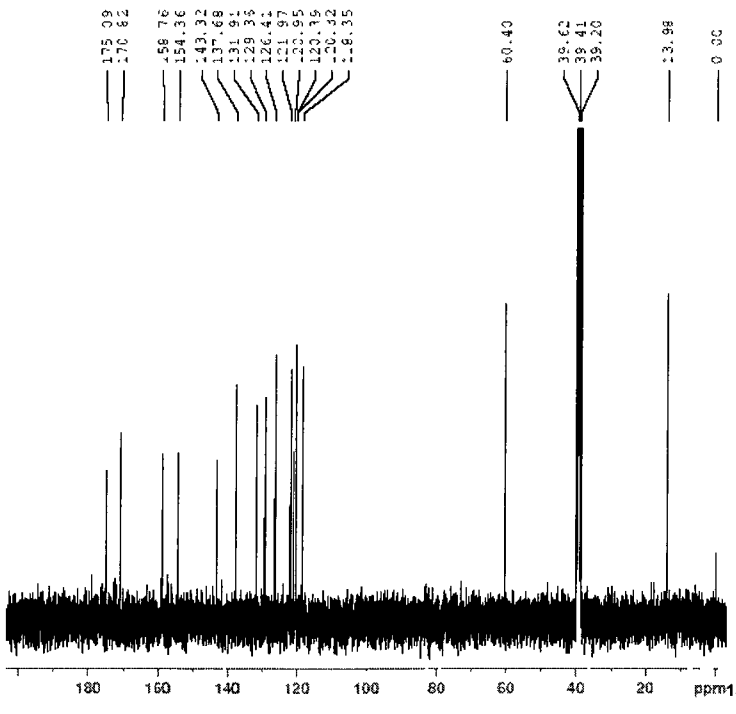

^{13}C, 100 MHz, DMSO-d_6

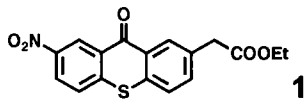

13

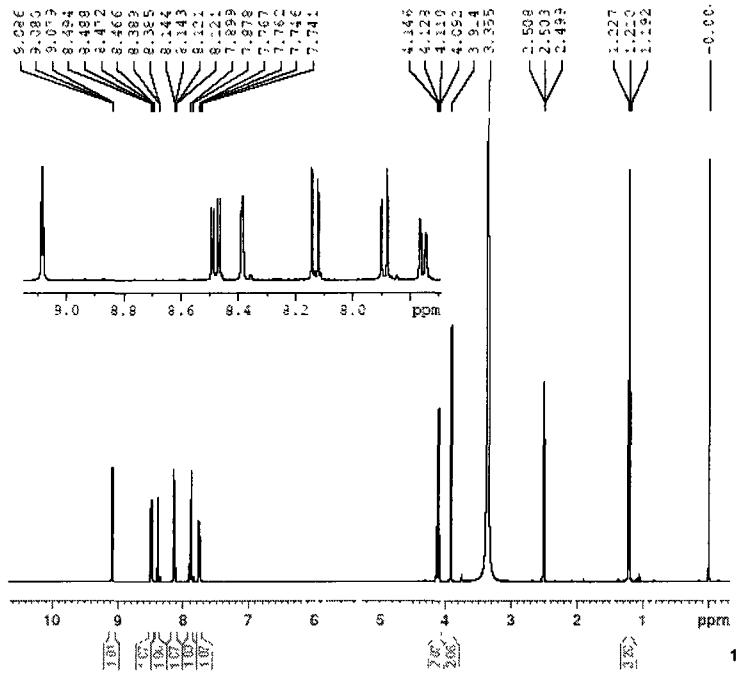

^{1}H, 400 MHz, DMSO-d_6

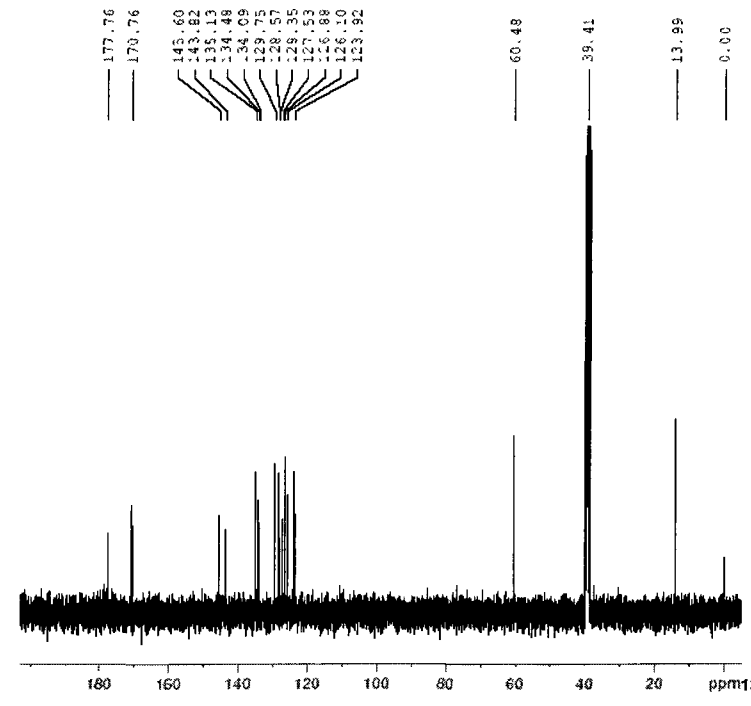

^{13}C, 100 MHz, DMSO-d_6

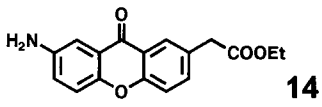

14

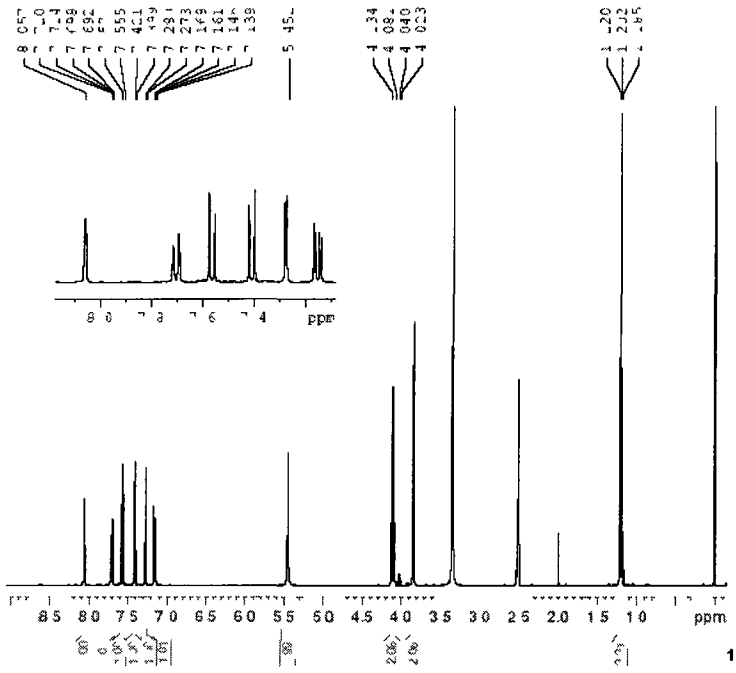

^{1}H, 400 MHz, DMSO-d_6

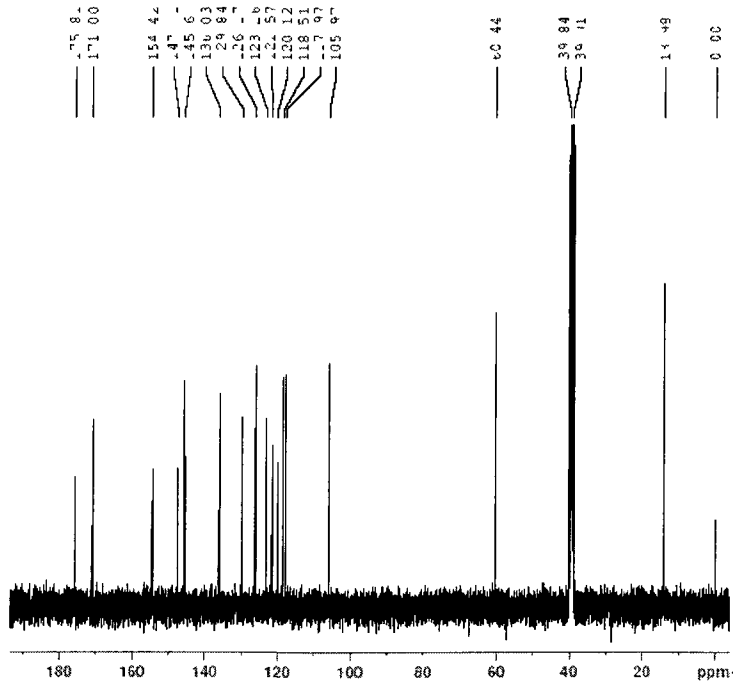

^{13}C, 100 MHz, DMSO-d_6

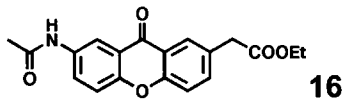

16

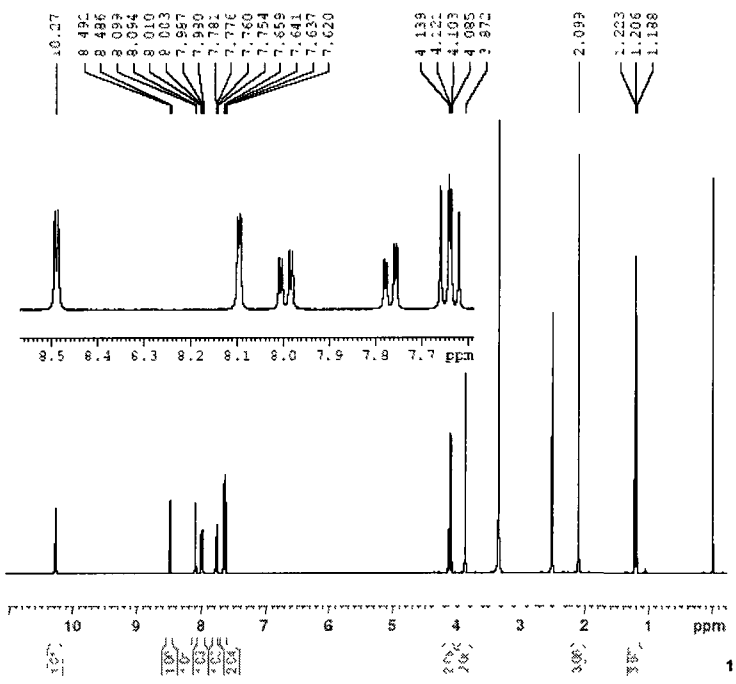

^{1}H, 400 MHz, DMSO-d_6

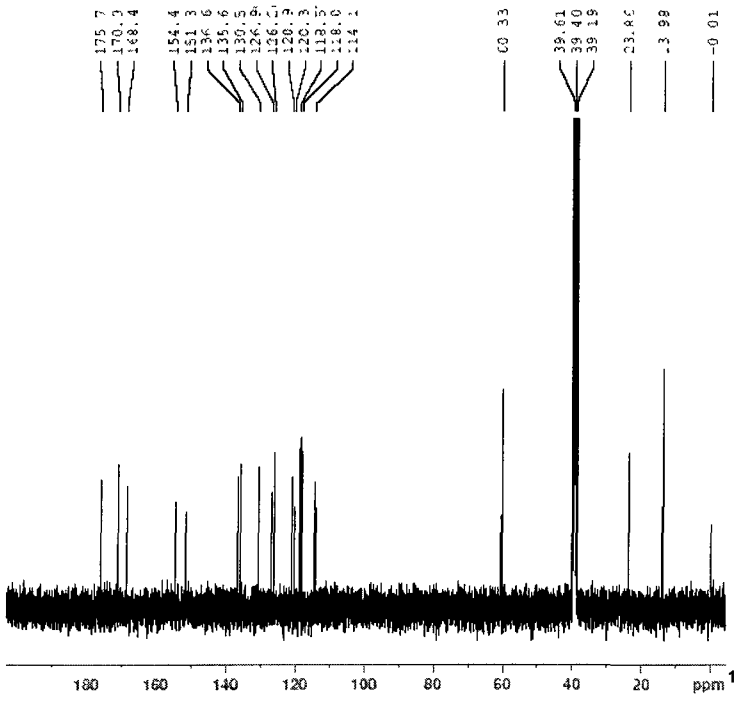

^{13}C, 100 MHz, DMSO-d_6

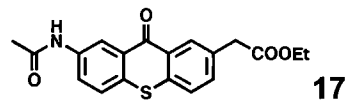

17

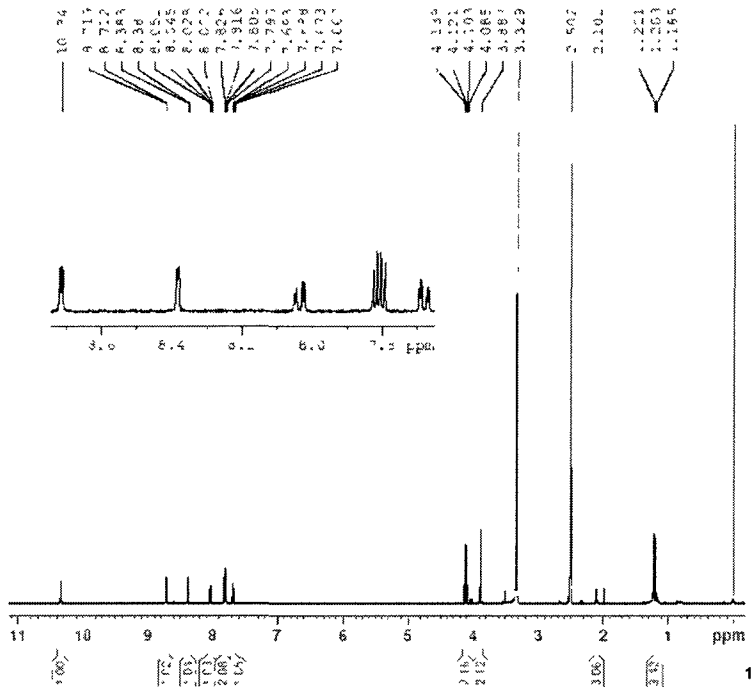

^{1}H, 400 MHz, DMSO-d_6

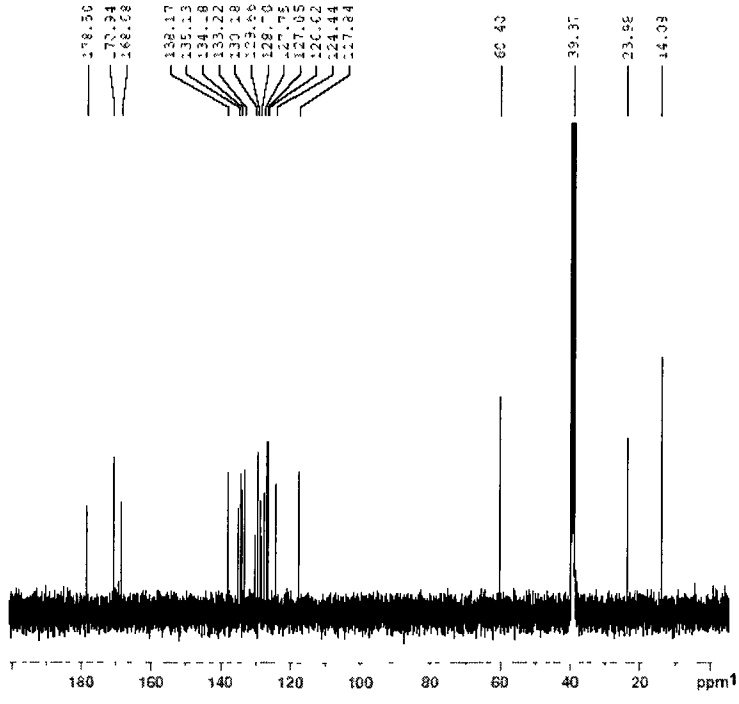

^{13}C, 100 MHz, DMSO-d_6

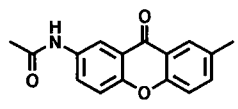

18

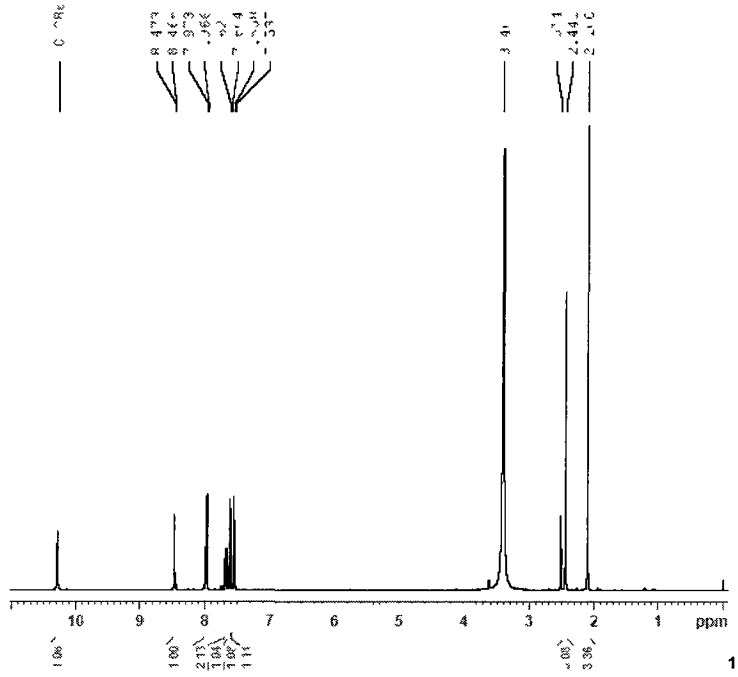

^{1}H, 400 MHz, DMSO-d_6

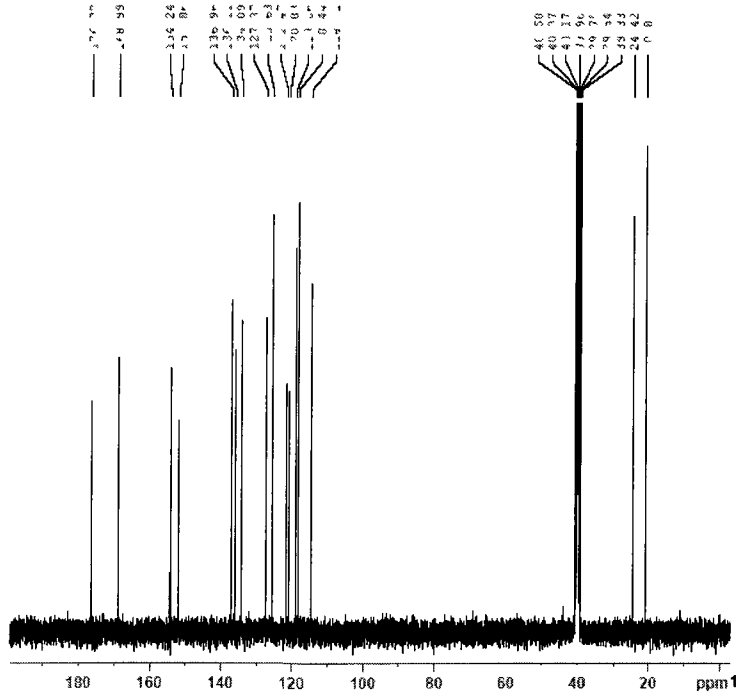

^{13}C, 100 MHz, DMSO-d_6

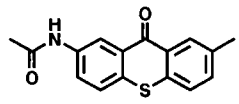

19

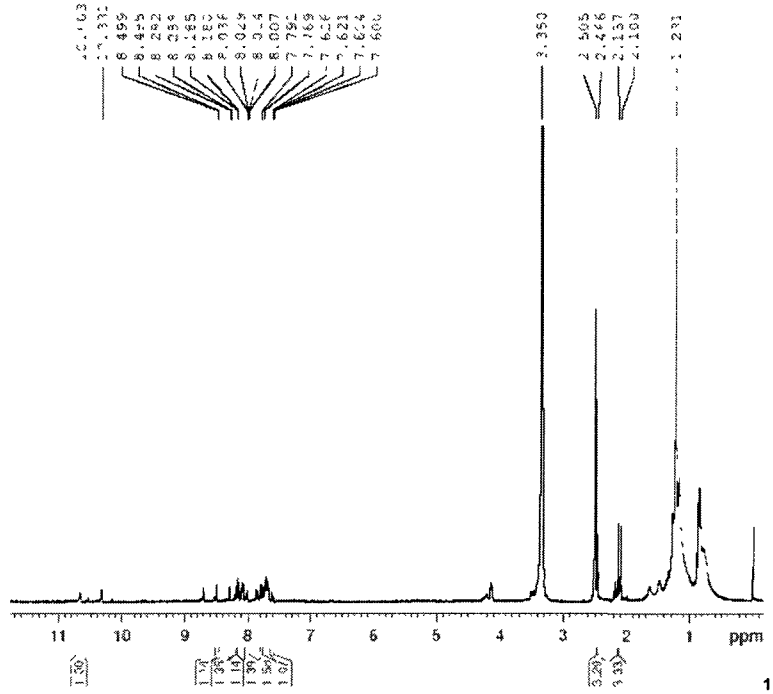

^{1}H, 400 MHz, DMSO-d_6

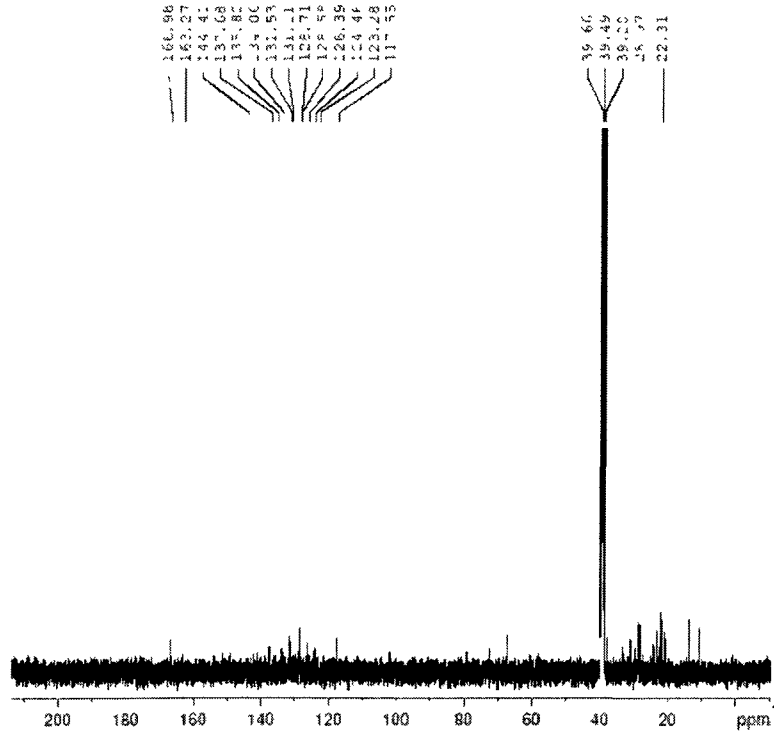

^{13}C, 100 MHz, DMSO-d_6

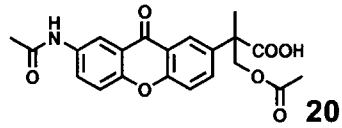

20

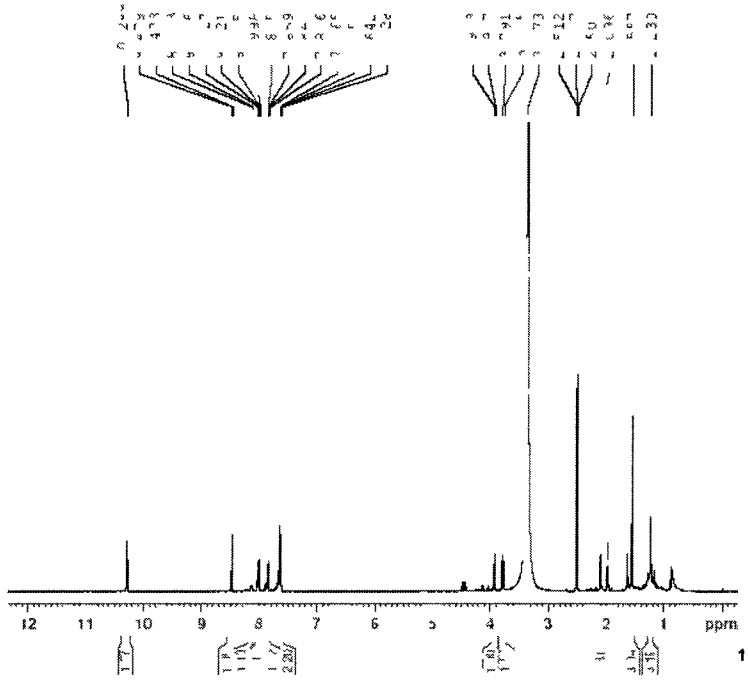

^{1}H, 400 MHz, DMSO-d_6

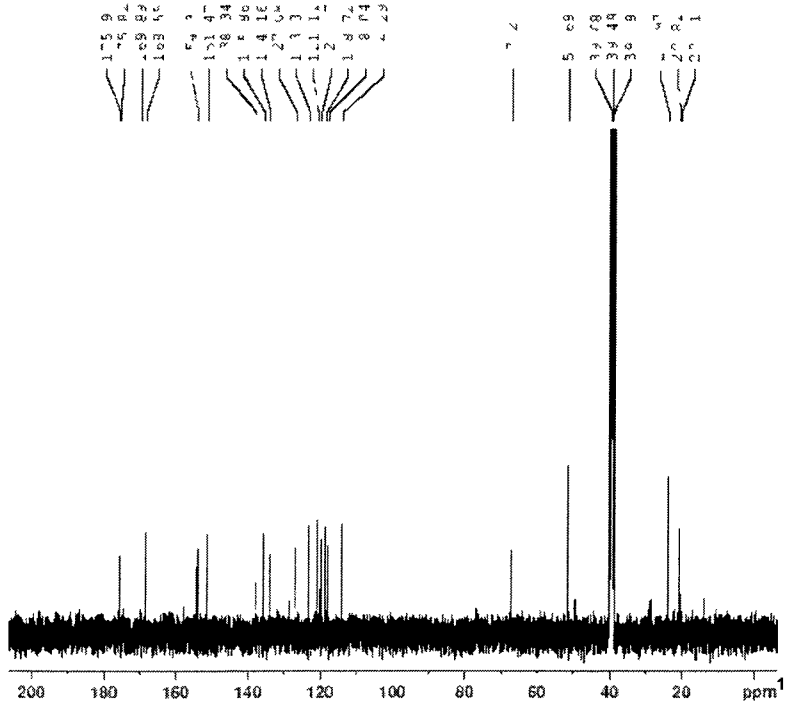

^{13}C, 100 MHz, DMSO-d_6

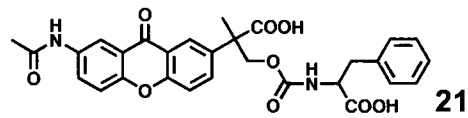

21

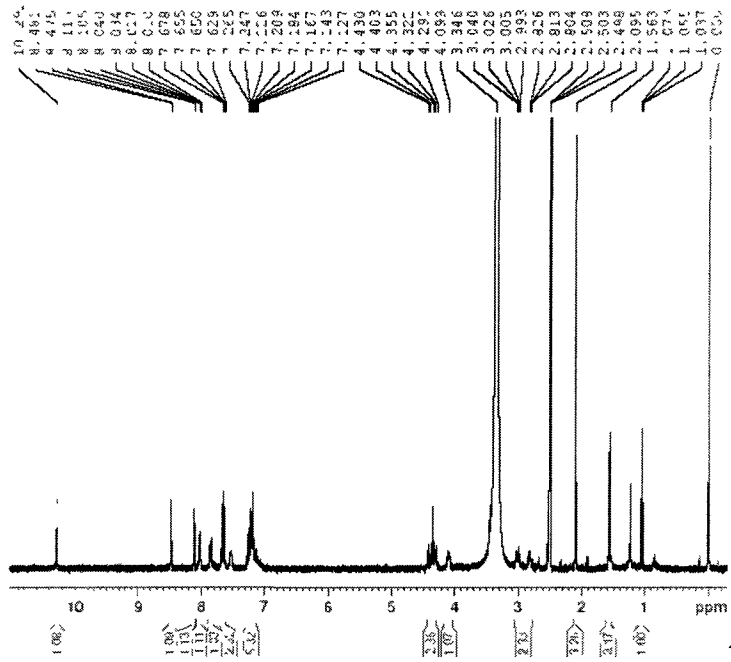

^{1}H, 400 MHz, DMSO-d_6

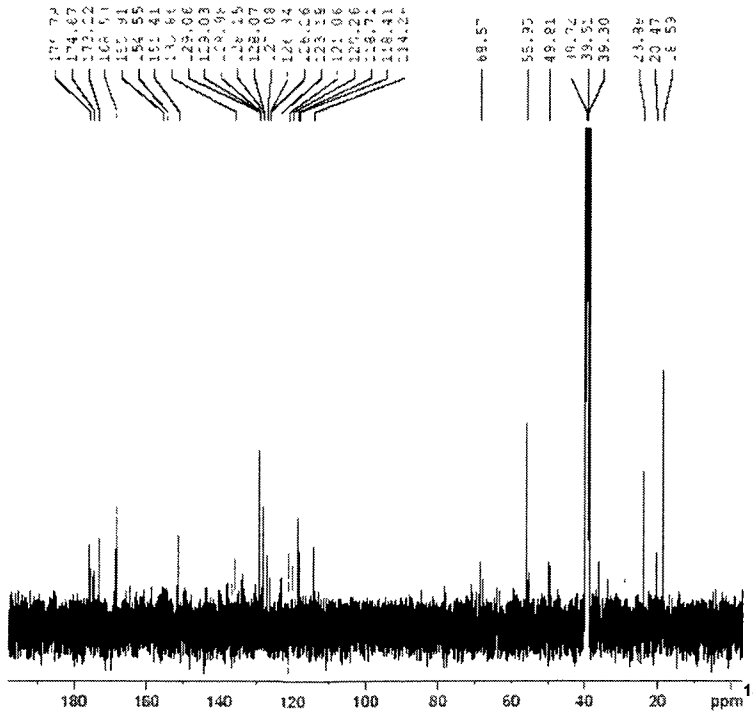

^{13}C, 100 MHz, DMSO-d_6

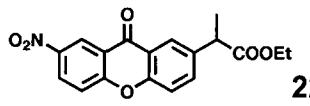

22

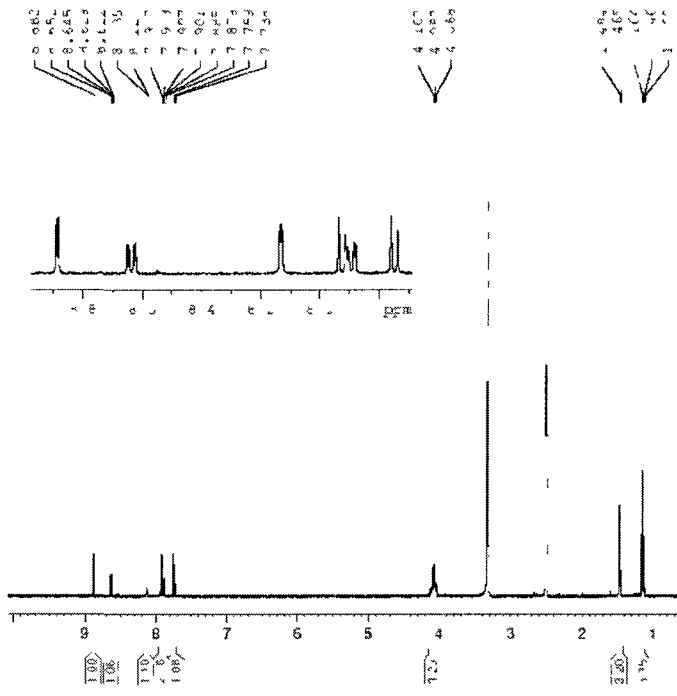

^{1}H, 400 MHz, DMSO-d_6

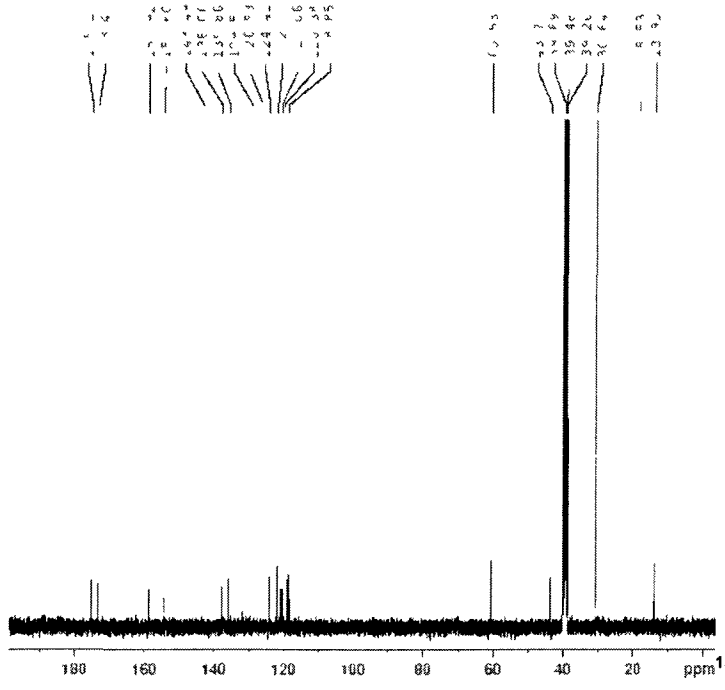

^{13}C, 100 MHz, DMSO-d_6

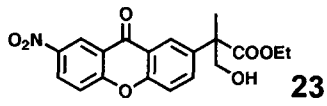

23

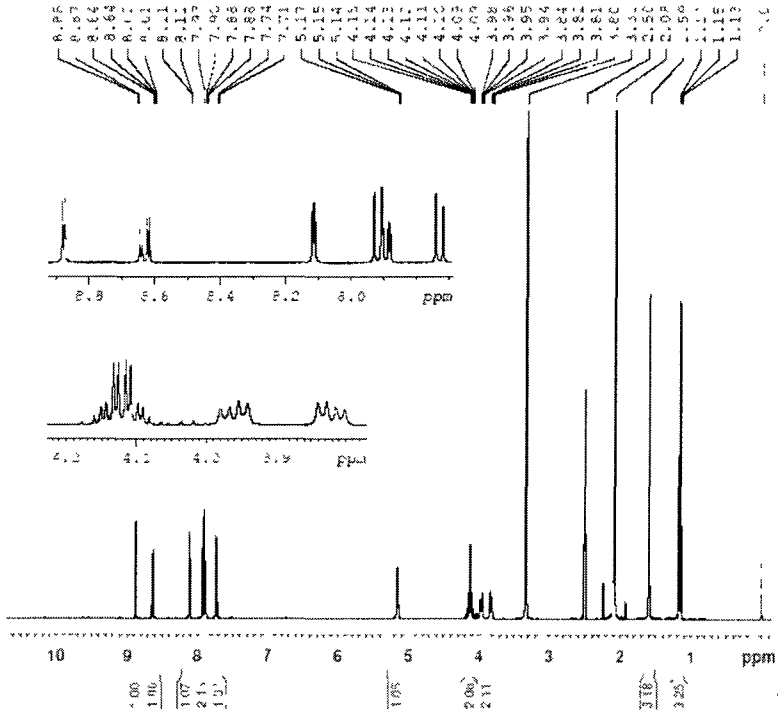

^{1}H, 400 MHz, DMSO-d_6

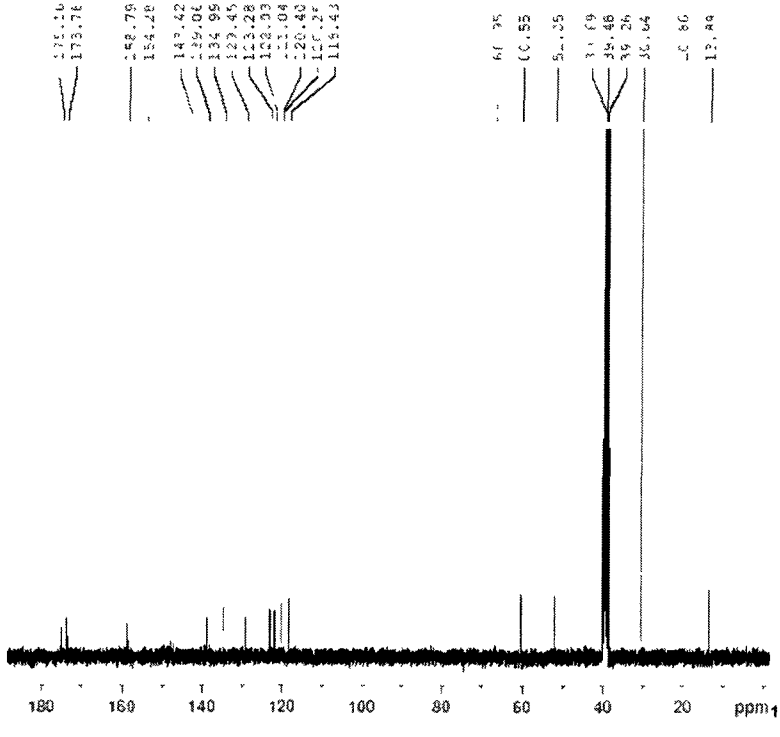

^{13}C, 100 MHz, DMSO-d_6

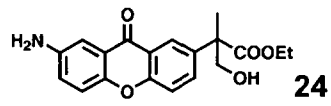

24

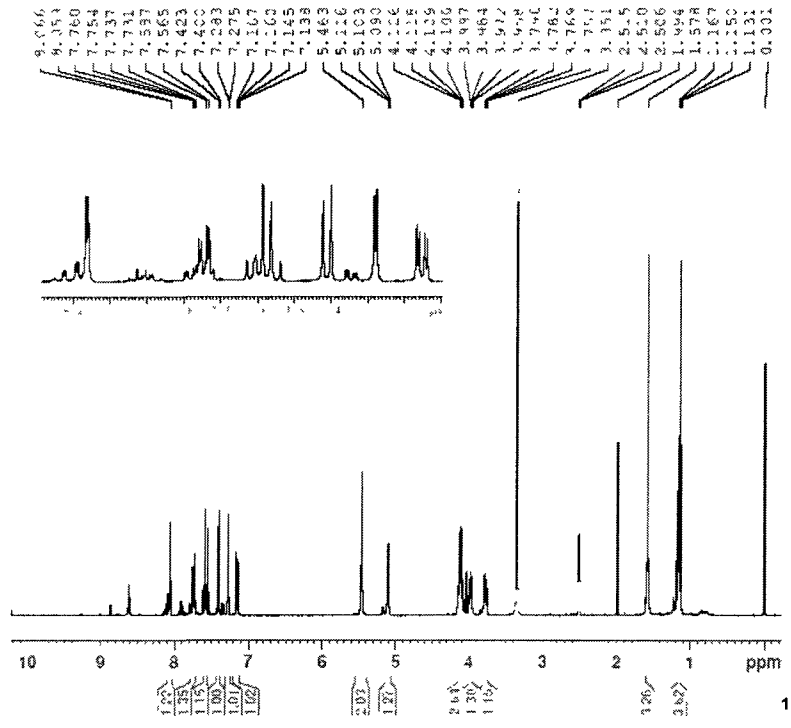

^{1}H, 400 MHz, DMSO-d_6

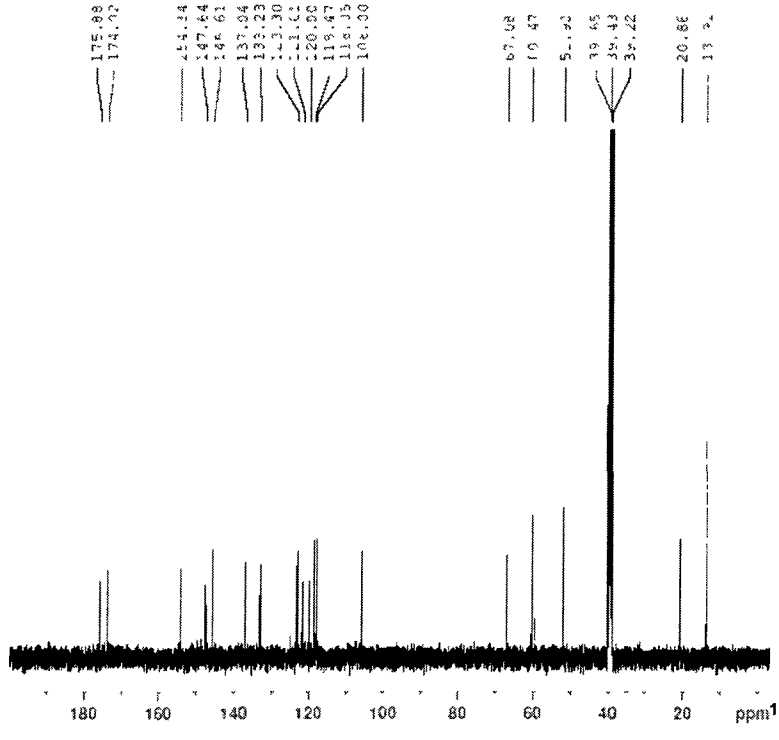

^{13}C, 100 MHz, DMSO-d_6

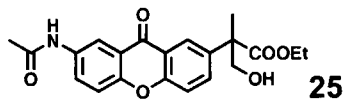

25

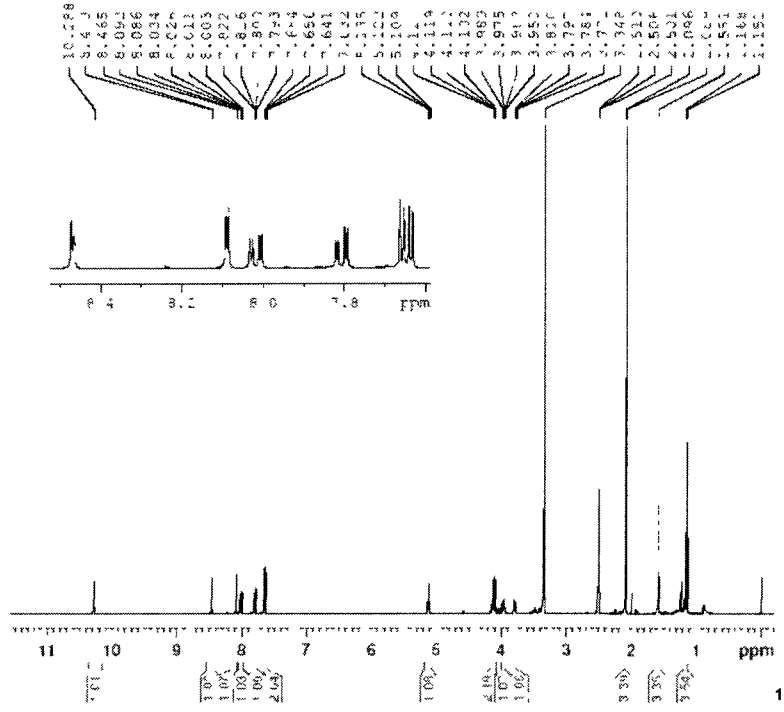

^{1}H, 400 MHz, DMSO-d_6

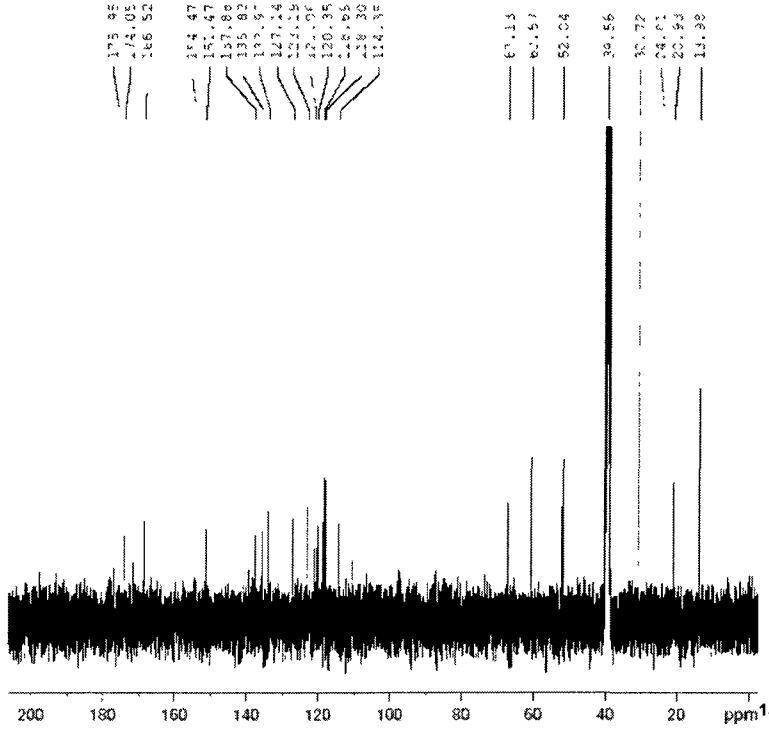

^{13}C, 100 MHz, DMSO-d_6

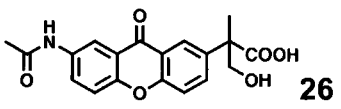

26

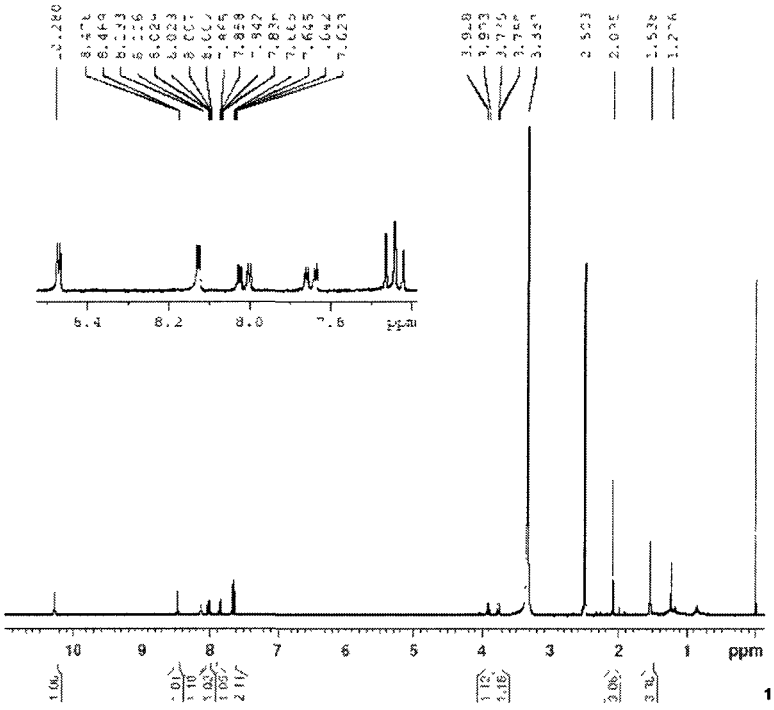

^{1}H, 400 MHz, DMSO-d_6

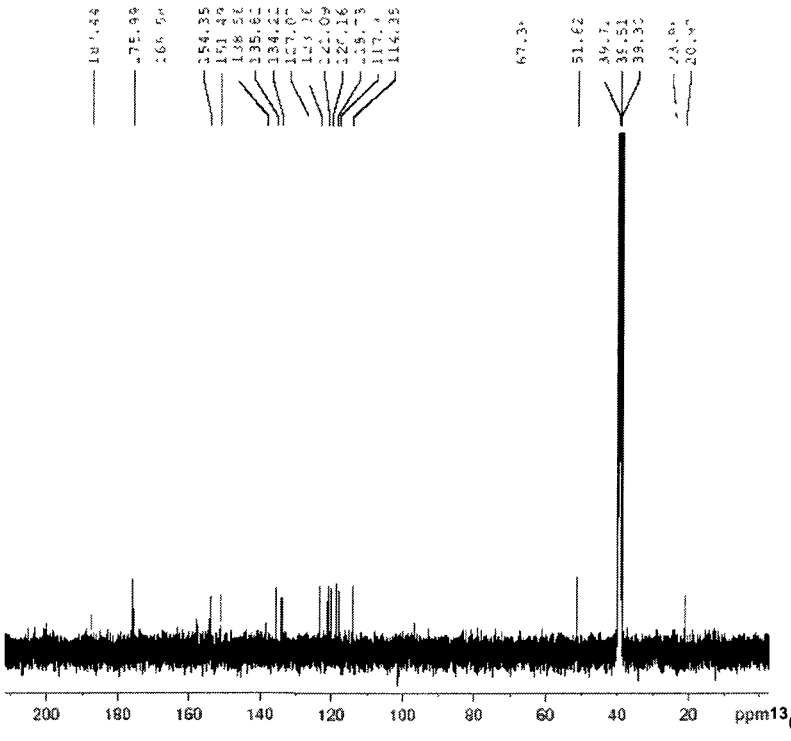

^{13}C, 100 MHz, DMSO-d_6

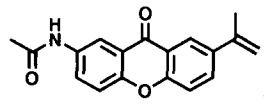

27

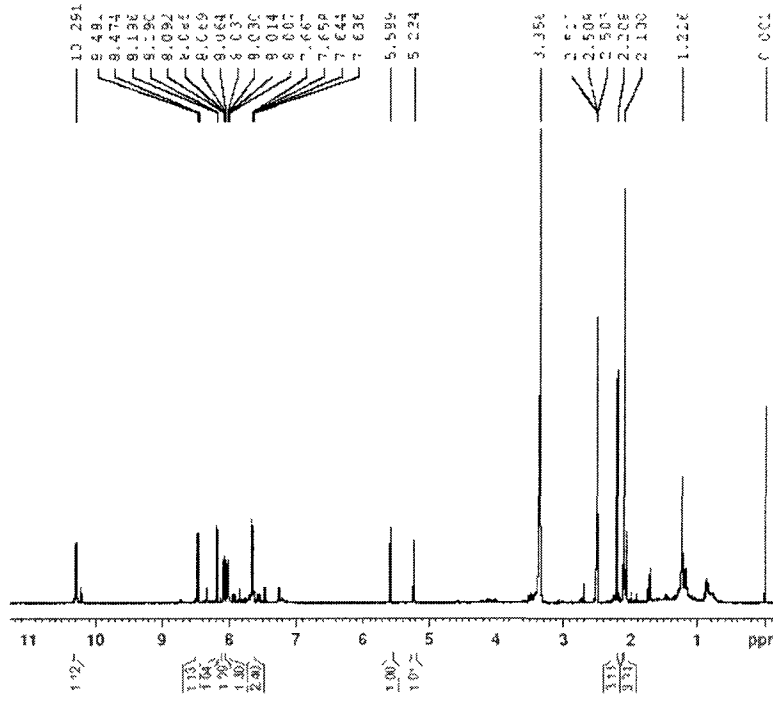

^{1}H, 400 MHz, DMSO-d_6

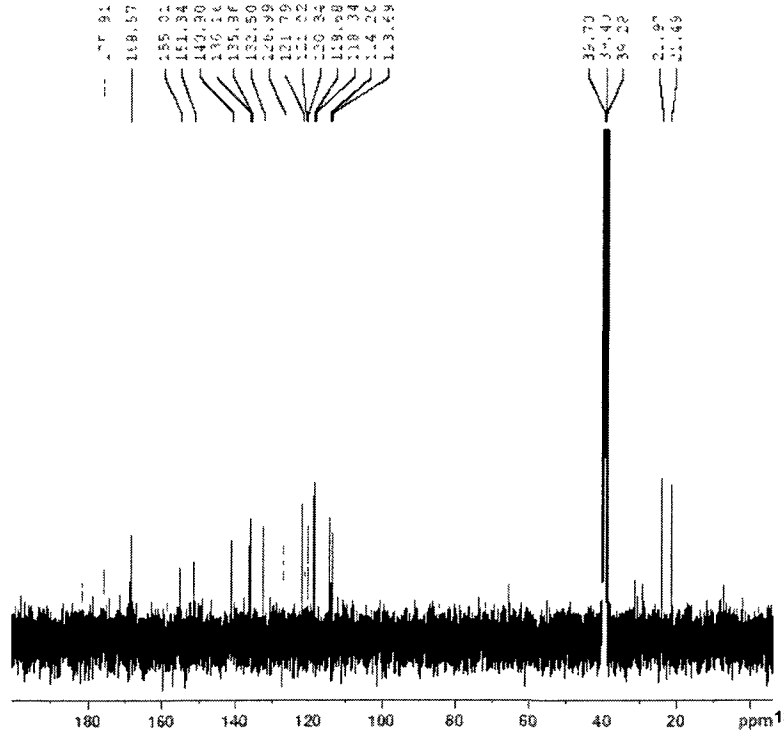

^{13}C, 100 MHz, DMSO-d_6

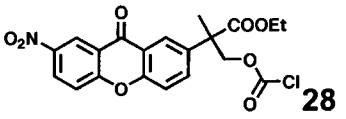

28

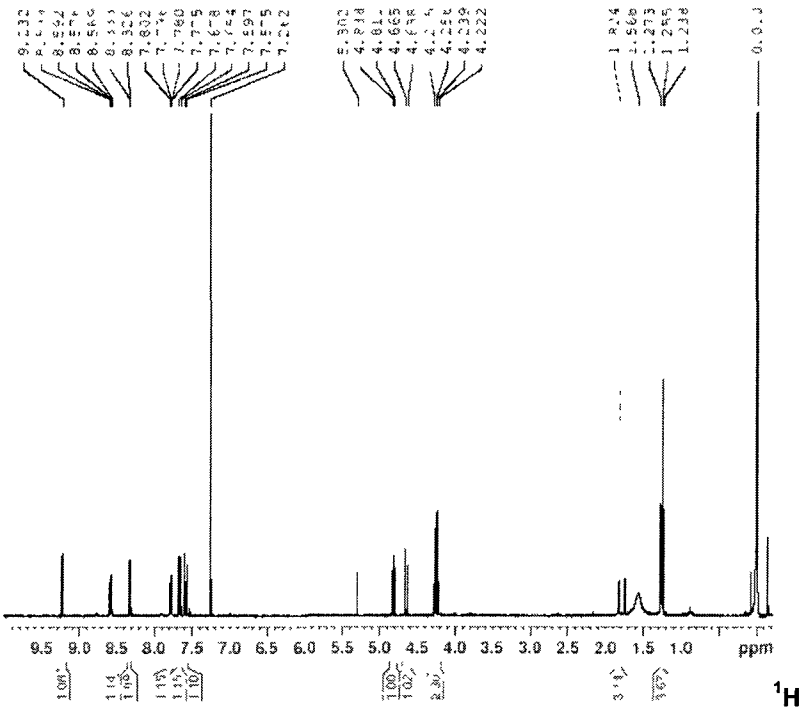

^{1}H, 400 MHz, $CDCl_3$

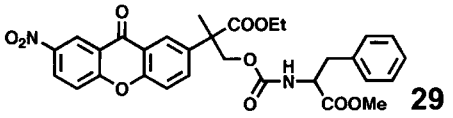

29

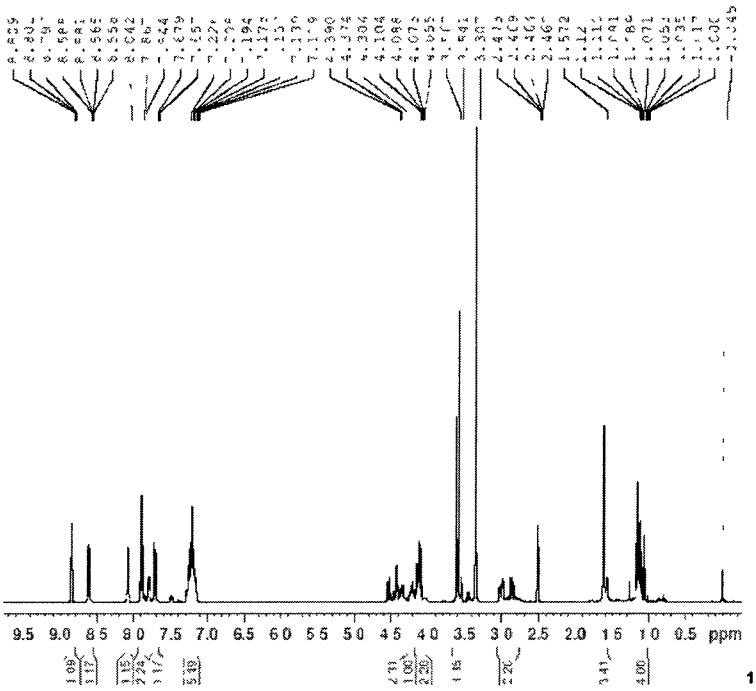

^{1}H, 400 MHz, DMSO-d_6

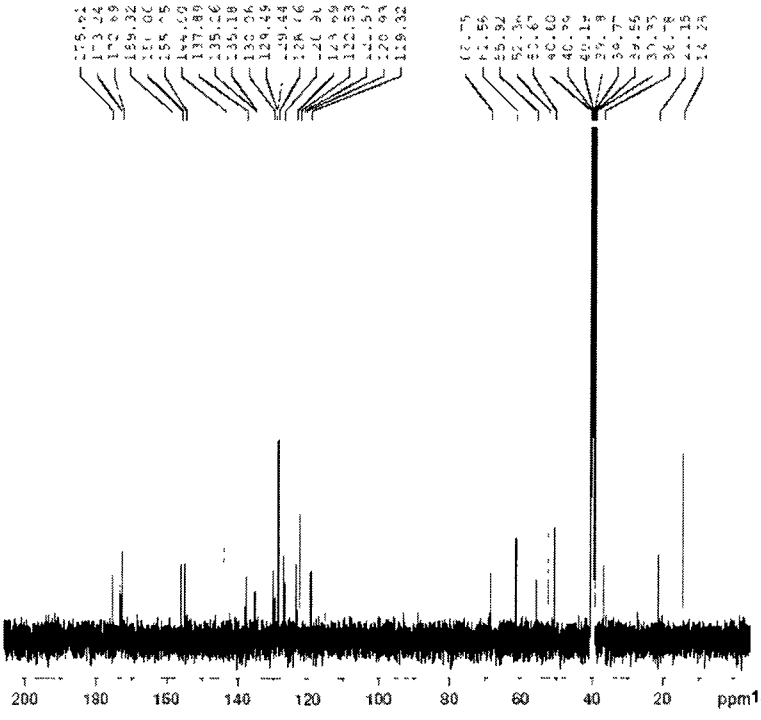

^{13}C, 100 MHz, DMSO-d_6

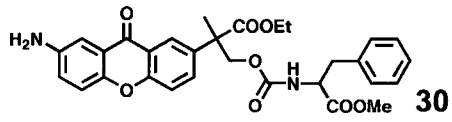

30

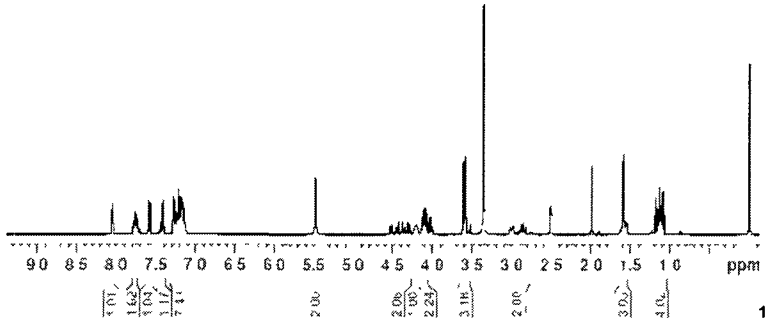

^{1}H, 400 MHz, DMSO-d_6

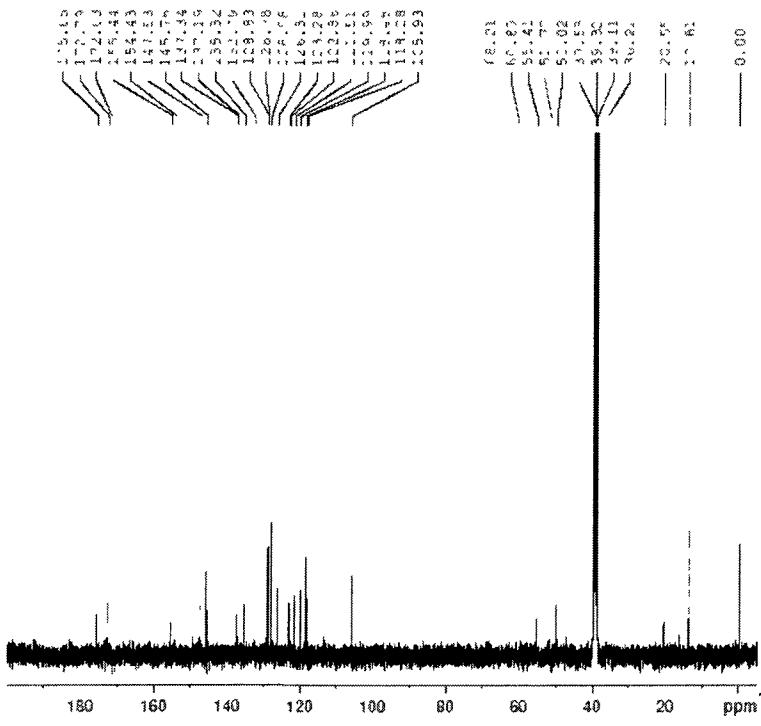

^{13}C, 100 MHz, DMSO-d_6

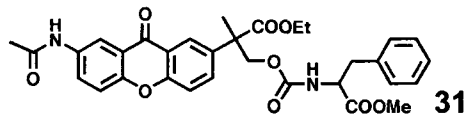

31

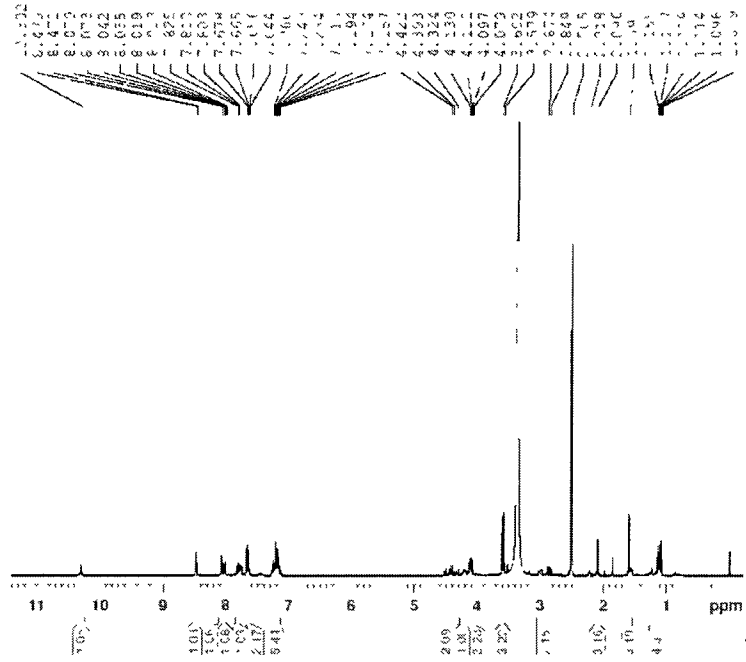

^{1}H, 400 MHz, DMSO-d_6

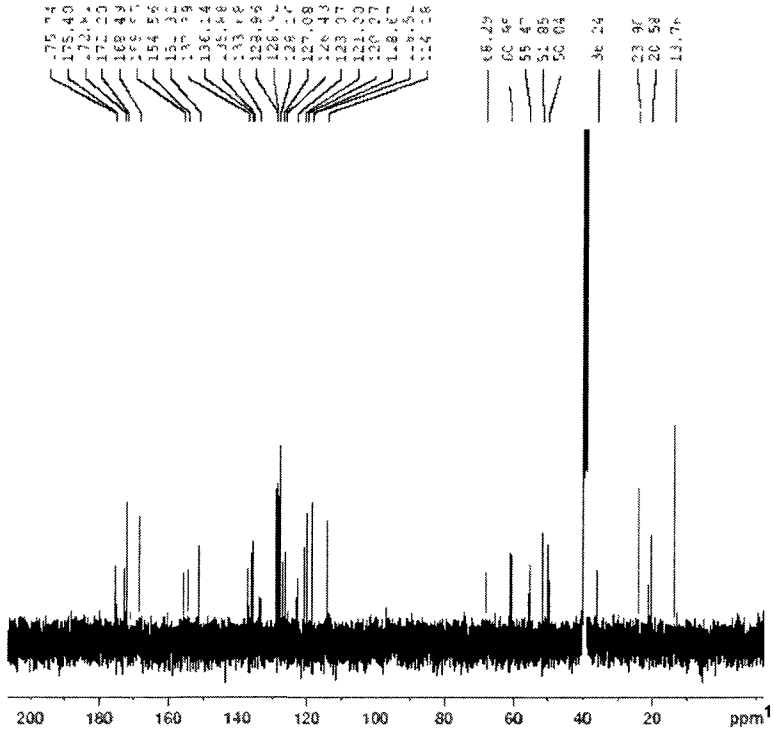

^{13}C, 100 MHz, DMSO-d_6

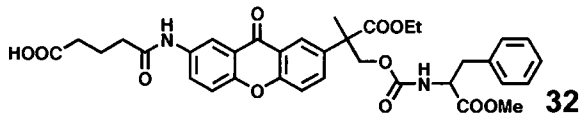

32

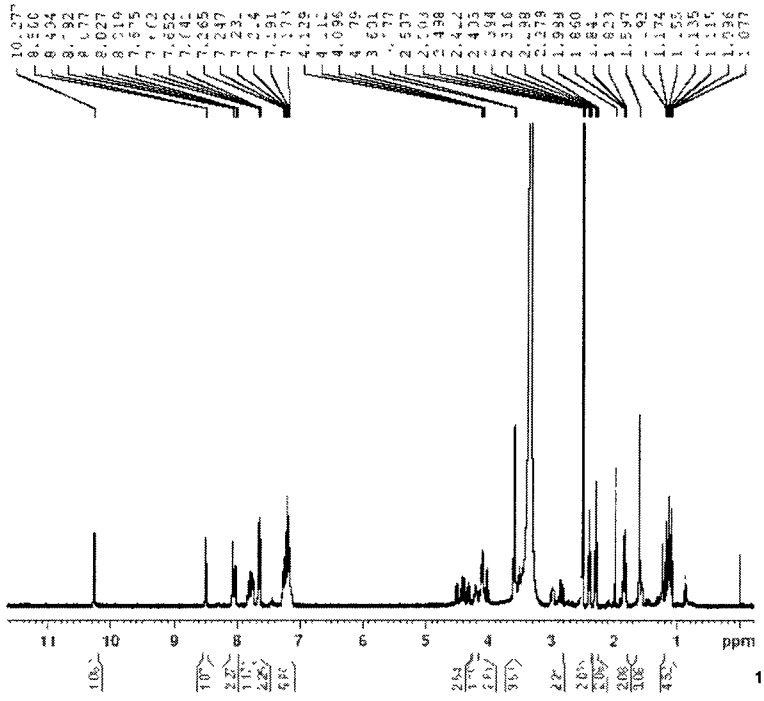

^{1}H, 400 MHz, DMSO-d_6

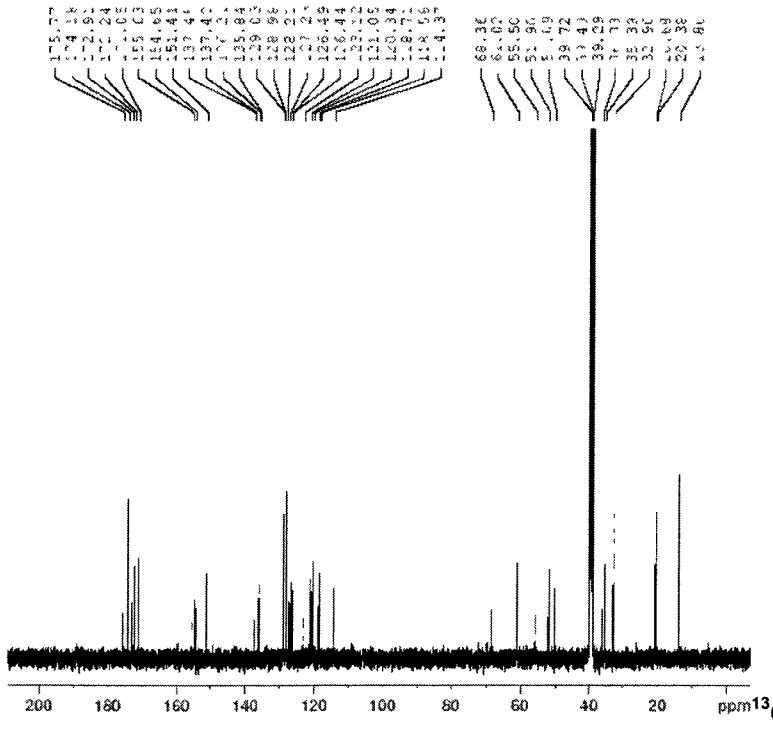

^{13}C, 100 MHz, DMSO-d_6

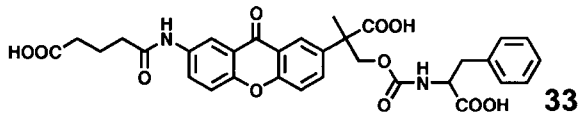

33

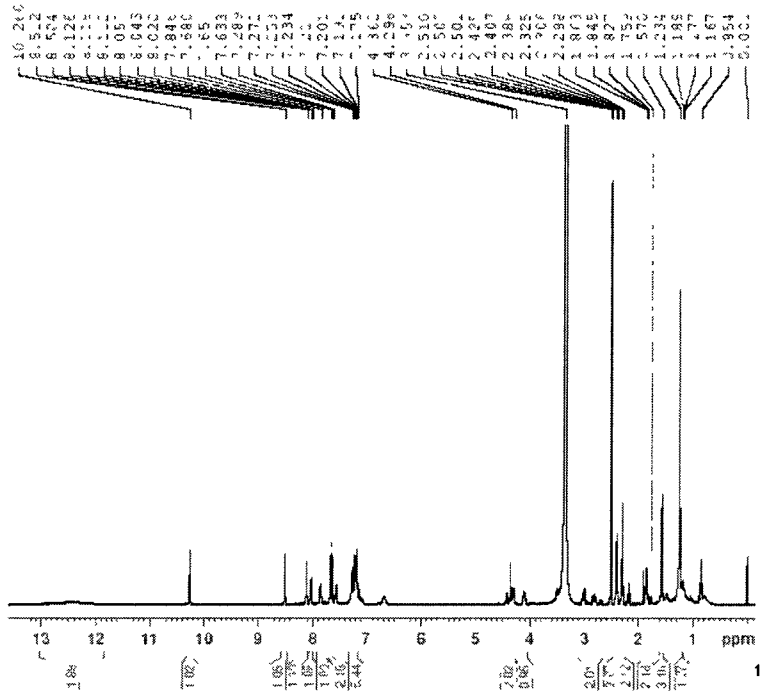

^{1}H, 400 MHz, DMSO-d_6

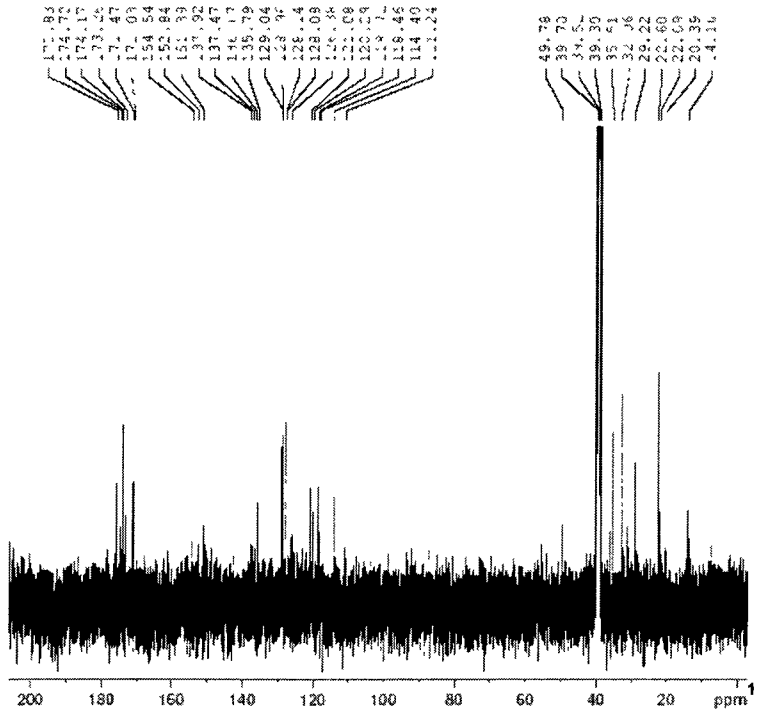

^{13}C, 100 MHz, DMSO-d_6

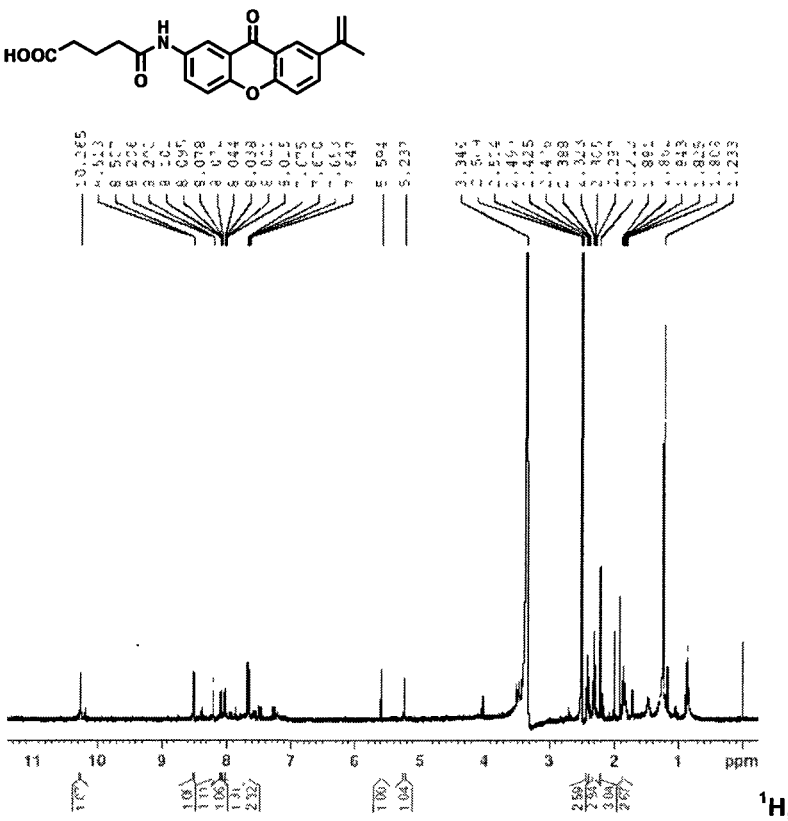

^{1}H, 400 MHz, DMSO-d_6